A study of the behaviour and interactions of the novel FERM protein Willin

By Lissa Rocha Herron, B.S.

A thesis submitted to the University of St. Andrews in partial fulfillment of the requirement of the degree of Doctor of Philosophy

School of Biology and School of Medicine

October 2007

CONTENTS

Declaration

I, Lissa Rocha Herron, hereby certify that this thesis, which is approximately 35,000 words in length, has been written by me, that it is the record of work carried out by me and that it has not been submitted in any previous application for a higher degree.

Date _____ _____

I was admitted as a research student in September, 2003 and as a candidate for the degree of Ph.D. in September, 2004; the higher study for which this is a record was carried out in the University of St Andrews between 2003 and 2007.

Date _____ _____

I hereby certify that the candidate has fulfilled the conditions of the Resolution and Regulations appropriate for the degree of Ph.D. in the University of St Andrews and that the candidate is qualified to submit this thesis in application for that degree.

Date _____ _____

Copyright declaration

In submitting this thesis to the University of St Andrews I understand that I am giving permission for it to be made available for use in accordance with the regulations of the University Library for the time being in force, subject to any copyright vested in the work not being affected thereby. I also understand that the title and abstract will be published, and that a copy of the work may be made and supplied to any bona fide library or research worker, that my thesis will be electronically accessible for personal or research use, and that the library has the right to migrate my thesis into new electronic forms as required to ensure continued access to the thesis. I have obtained any third-party copyright permissions that may be required in order to allow such access and migration.

Date _____ _____

Acknowledgements

I would like to express my immense gratitude to Dr. Frank Gunn-Moore, who has been a fantastic mentor and extremely supportive supervisor through what have been some very difficult times in my life. I could not have completed this Ph.D. without his help, kindness, generosity and understanding.

I would also like to thank:

My second supervisor, Prof. Simon Guild, especially for providing a friendly face at my talk at Life Sciences.

Dr. Fleur Davey, the font of all lab knowledge, who taught me just about everything I've learned in the last 4 years.

Dr. Maria Hill; without her thesis as a model, this one would have come on much more slowly!

Dr. Colin Sinclair, who first got me started in the Gunn-Moore group and has been a good friend and supporter ever since.

Yimin Ren, who could always be counted on for company in the lab on the weekends.

Dr. Dave Stevenson, for being a total dude.

The project students, Amy Cameron, Jessica Davis and Chris Cozens, for their help and data.

All the office mates and E floor chums, especially Carol Jolly, for support, friendship and long lunches.

My partner, Gary Stratton, for protecting me from the zombies.

Alex and Ian in stores for all their help with orders.

John Nicholson in the BMS for help with the Delta Vision and Brian Powell for technical assistance in the lab.

My family, especially my mother Carmo Herron, who has been endlessly supportive of all my educational endeavours throughout my life, even when they've taken me halfway across the world.

For my daddy, Tom Herron, who would have been so very proud.

Abbreviations used in this thesis

a	adenine
3AT	3-amino-1,2,4-triazole
A	alanine
Bis-Tris	Bis(2-hydroxyethyl)iminotris(hydroxymethyl)methane
bp	base pair
BSA	bovine serum albumin
c	cytosine
C	cysteine
Caspr	contactin-associated protein
CBB	calmodulin binding buffer
CD44	cluster of differentiation antigen 44
cDNA	complementary DNA
CEB	calmodulin elution buffer
CIAP	calf intestinal alkaline phosphatase
CNS	central nervous system
COS-7	african green monkey kidney cell line
C-terminus	carboxy terminus
D	aspartic acid/aspartate
DAPI	4',6-diamidino-2-phenylindole
Dbl	diffuse poorly differentiated B-cell lymphoma
DMEM	Dulbecco's modified eagle's medium
DMF	N,N-dimethylformamide
DNA	deoxyribonucleic acid
dNTP	deoxynucleoside triphosphate
DTT	dithiothreitol
E	glutamic acid/glutamate
E. coli	*Escherichia coli*
EDTA	ethylenediaminetetraacetic acid
EGF	epidermal growth factor
EGTA	ethyleneglycol-bis-(β-aminoethyl)-N,N'-tetraacetic acid
ERM	ezrin radixin moesin
ERK2	Extracellular signal-regulated kinase 2
EtBr	ethidium bromide
E3KARP	Na(+)/H(+) exchanger type 3 kinase A regulatory protein
F	phenylalanine
FCS	foetal calf serum
FERM	four-point-one ezrin radixin moesin
g	guanine
G	glycine
GDI	Guanosine nucleotide dissociation inhibitor
GFP	green fluorescent protein
Glut/Q	glutamine
GSH	reduced glutathione
GST	glutathione S-transferase
H/His	histidine
HEI10	Human enhancer of invasion, clone 10
HEK-293	human embryonic kidney cell line
HRP	horseradish peroxidase

I	isoleucine
ICAM	intracellular adhesion molecule
IPTG	isopropyl-β-D-thiogalactopyranoside
K	lysine
kb	kilobase pairs
L/Leu	leucine
LB	Luria broth
LiAc	lithium acetate
M	methionine
MEM	minimum essential medium Eagle
MOPS	3-morpholinopropanesulfonic acid
MQ	milli-Q purified water
N	asparagine
NBF	neutral buffered formalin
NEAA	non-essential amino acids
NGF	nerve growth factor
NP-40	nonidet P40
NrCAM	neuron-glia related cell adhesion molecule
N-terminus	amino terminus
Optiprep	60% (w/v) iodixanol in water
P	proline
PBS	phosphate buffered saline
PCR	polymerase chain reaction
PDGF	Platelet-derived growth factor
PDZ	Post Synaptic Density-95, discs-large, and zonula occludens-1
PEG	polyethylene glycol 3350
pen	penicillin
PFA	paraformaldehyde
PfuTURBO	DNA polymerase derived from *Pyrococcus furiosus*
PH	pleckstrin homology
PI	protease inhibitor cocktail
PIPES	piperazine-N,N'-bis(ethanesulfonic acid)
PIPK	phosphoinositol phosphate kinase
PMSF	phenylmethylsulfonyl fluoride
PNS	peripheral nervous system
PSB	protein sample buffer
PTPH1	Protein tyrosine phosphatase, non-receptor type 3
PTPMEG	Protein tyrosine phosphatase megakaryocyte
Pak1	p21-activating kinase 1
R	arginine
rpm	revolutions per minute
RIPA	radio-immunoprecipitation assay
S/Ser	serine
SAP102	synapse associated protein 102
SDS	sodium dodecyl sulfate
SDS-PAGE	sodium dodecyl sulfate polyacrylamide gel electrophoresis
SK-UT-1	human uterine leiomyosarcoma cell line
SOB	super optimal broth
SOC	super optimal catabolite repression broth
T/Thr	threonine

TAP	tandem affinity purification
TB	transformation buffer
TBE	tris-borate-EDTA buffer
TBS	tris buffered saline
TBS-T	tris buffered saline with Tween 20
TEV protease	tobacco etch virus protease
Tris	tris(hydroxymethyl) methylamine
Tris-HCl	tris(hydroxymethyl) aminomethane hydrochloride
Triton X-100	t-Octylphenoxypolyethoxyethanol
Tween 20	polyoxyethylenesorbitan monolaurate
UV	ultraviolet
V	valine
VASP	Vasodilator-stimulated Phosphoprotein
W/Trp	tryptophan
X-gal	5-bromo-4-chloro-3-indolyl-D-galactopyranoside
Y/Tyr	tyrosine
YPAD	Yeast Extract - Peptone - Dextrose plus Adenine medium

Abstract

Willin is a novel member of the Four-point-one Ezrin Radixin Moesin (FERM) protein superfamily, containing an N-terminal FERM domain most like the Ezrin-Radixin-Moesin (ERM) family but also the closely related protein Merlin. Willin was initially discovered as a yeast two-hybrid binding partner of neurofascin155, and this interaction has now been confirmed by both co-localisation studies and the use of two different biochemical methods. Like neurofascin155, Willin also localises to detergent resistant membranes, and like the ERM family, it is able to bind to phospholipids. The expression of Willin appears to be toxic as the production of cell-lines stably expressing Willin proved to be not possible and this appears to be because it induces apoptosis in cultured cells. This is a proliferation control function consistent with the suggestion that Willin is the human homologue of the *Drosophila* tumour suppressor 'Expanded'. Three antibodies to Willin were also characterised and a novel splice variant, Willin2, subcloned into a GFP-tagged plasmid for comparison with the original form.

Table of Contents

List of Figures

Figure **Page**

Chapter 3

Figure **Page**

Chapter 4

Figure **Page**

Chapter 6

List of Tables

CHAPTER 1: INTRODUCTION

Chapter 1: Introduction

1.1 The Band 4.1 Protein Superfamily

The Band 4.1 superfamily is a group of proteins characterised by a conserved domain known as the Four point one Ezrin Radixin Moesin (FERM) domain. Band 4.1, the prototype of the superfamily, is an erythrocyte membrane protein and a major component of the cortical cytoskeleton. Its N-terminal half was found to be well conserved throughout a variety of proteins, most of which have interactions with both the membrane and the cytoskeleton. This interesting ability has led to a high level of interest in these proteins, and a classification system for the band 4.1 proteins was proposed by Takeuchi (Takeuchi et al., 1994a) that divides them into five gene families based on sequence analysis (though more may exist): the band 4.1 family; the ERM family, into which fall ezrin, radixin, moesin and merlin, along with novel band 4.1-like proteins 6 and 7 (NBL6 and NBL7); the talin family; the PTPH1 family, which includes PTPH1, PTPMEG, NBL1, NBL2 and NBL3; and the NBL4 family, which also includes NBL5. This section will focus on Band 4.1, the ERM family, Merlin and Willin.

1.1.1. Band 4.1

Band 4.1 was originally identified as an 80kDa component of erythrocyte membrane, interacting with the actin and spectrin cytoskeletal network, and since then it has been identified in many cell types; larger isoforms of 135kDa and 145kDa have also been found in the nuclei of various cell types (Correas, 1991). The importance of 4.1 to red blood cell structural integrity is made clear by the misshapen erythrocytes found in patients with 4.1 deficiencies, known clinically as hereditary elliptocytosis

(Figure 1.1). Molecularly, the skeletal network and membrane structures become abnormally distributed (Yawata et al., 1997).

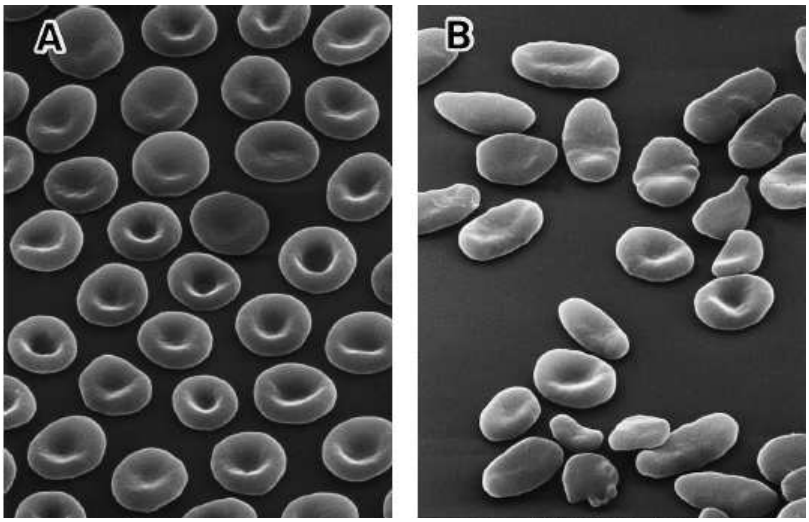

Figure 1.1. A) Scanning electron microscopy (EM) of normal red blood cells, with characteristic disc shape. B) Scanning EM of red blood cells from patient with homozygous hereditary elliptocytosis. The cytoskeleton is improperly formed. Taken from Yawata et al., 1997.

Interest in 4.1 increased when it was discovered that it was able to bind membrane, cytoskeletal and membrane proteins, which, combined with the clincial evidence, suggested an important linking function (Hemming et al., 1994; Pasternack et al., 1985; Walensky et al., 1998). Three distinct binding domains have been observed in protein 4.1: a C-terminal domain, a spectrin-actin binding domain, and a ~30kDa N-terminal domain that mediates binding with the membrane and membrane proteins (Sun et al., 2002; see Figure 1.2.)

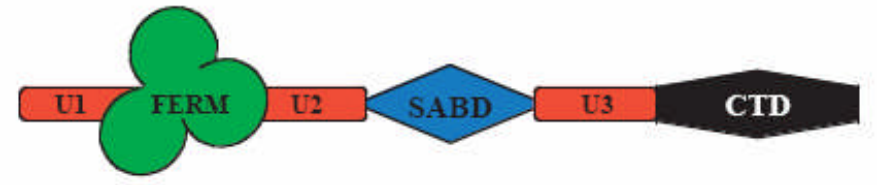

Figure 1.2. Overall structure of protein 4.1. The FERM domain is in the N-terminus, flanked by two regions of unique sequence, with a spectrin-actin binding domain located centrally and a C-terminal domain capable of binding further cytoplasmic and cytoskeletal proteins. Image taken from Sun et al., 2002.

It was recognised that the N-terminal domain of 4.1 was conserved in a rapidly growing list of other proteins, and was termed the Four point one Ezrin Radixin Moesin (FERM) domain after the proteins initially discovered to have this domain (Chishti et al., 1998).

1.1.2. The FERM domain

The FERM domain is usually found in the N-terminus of proteins, though in myosinVIIA it is in the C-terminus (Chishti et al., 1998), and in at least one novel FERM-containing family it is centrally located (Ussar et al., 2006). Around 300 amino acids in length, it is hydrophobic, cysteine-rich (Conboy, 1986) and globular (Chishti et al., 1998). Studies of crystal structures have shown that there are three subdomains, F1/A, F2/B and F3/C, forming a 'cloverleaf' structure (Hamada et al., 2000; Pearson et al., 2000). F1/A has a ubiquitin-like structure, F2/B an acyl-CoA binding protein-like structure, and F3/C resembles a fold found in phosphotyrosine binding (PTB), pleckstrin homology (PH), and Enabled/VASP Homology 1 (EVH1) domains (Hamada et al., 2000; Pearson et al., 2000). The FERM domain of various proteins has been shown to bind such a diverse range of molecules as phosphoinositols, glycophorins, CD44, ICAM-2 and the C-terminal domain of FERM-containing proteins (Chishti et al., 1998); there is also some evidence that it can bind actin (Martin et al., 1997; Roy et al., 1997). The crystal structures of Ezrin, Radixin and Moesin FERM domain is seen in Figure 1.3 (Smith et al., 2003).

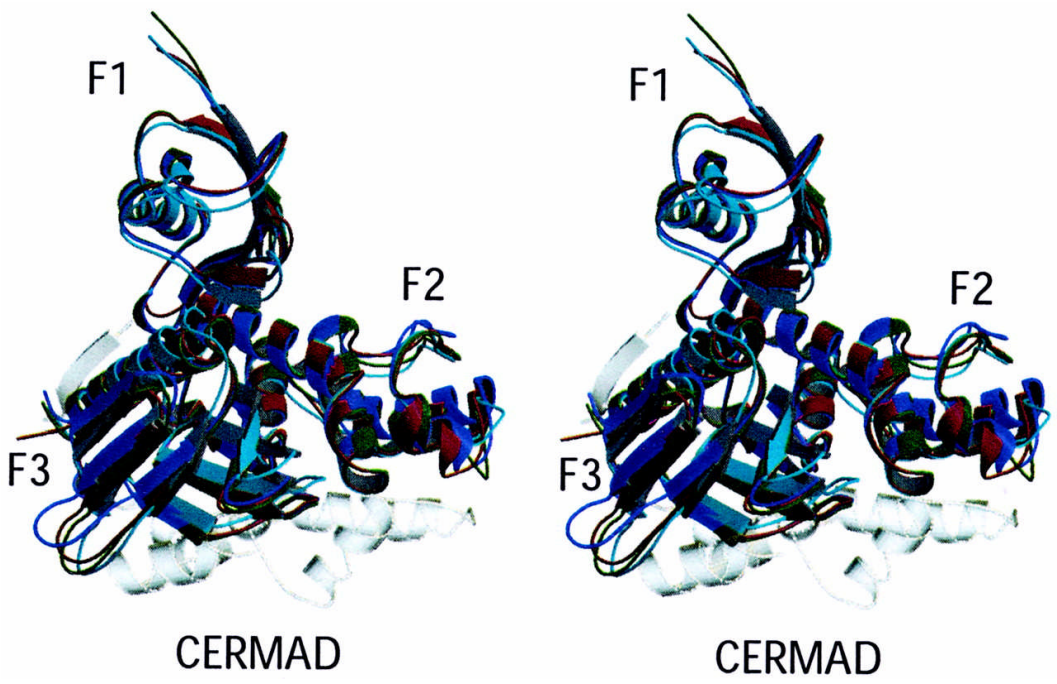

Figure 1.3. Overlaid FERM domains of Ezrin (red), Radixin (cyan), and Moesin (active: green; dormant: violet). The dormant Moesin FERM domain is shown bound to the C-terminal domain (white). Ribbon figures prepared with Bobscript and Raster3D structure programs. Image taken from Smith et al., 2003.

1.1.3. Ezrin, radixin and moesin

The ezrin/radixin/moesin (ERM) family consists of proteins that link the cell membrane with the actin cytoskeleton at the cell cortex (Bretscher et al., 2002). Regardless of the cell type in which they are found, the ERMs are generally localised at areas of rich actin activity, such as microvilli, filopodia, membrane ruffles and cell-cell contact sites (Turunen et al., 1998), where they are involved in the formation of those structures (Bonilha et al., 1999; Crepaldi et al., 1997; Martin et al., 1997; Takeuchi et al., 1994a; Yonemura and Tsukita, 1999); cell shape and motility (Lamb et al., 1997); cell-substrate and cell-cell adhesion (Kaul et al., 1996; Martin et al., 1995; Takeuchi et al., 1994a); and membrane trafficking (Cao et al., 1999; Defacque et al., 2000).

Ezrin, radixin and moesin share a FERM domain, a central alpha-helical domain and a C-terminal domain that contains an actin-binding motif (Figure 1.4).

This structure is highly conserved: ezrin shows about 97% identity amongst the mammalian forms, and 99% identity in the FERM domain between mouse and human forms; ezrin, radixin and moesin have 73-81% sequence identity (Turunen et al., 1998). The FERM domain connects to the cell membrane either directly through phosphoinositols, especially phosphatidylinositol-4,5-bisphosphate (Niggli et al., 1995), or by binding to membrane proteins such as CD44 (Tsukita et al., 1994) CD43 and ICAM-2 (Yonemura et al., 1998). The C-terminal domain has a highly-conserved actin binding site in the last 34 amino-acids (Turunen et al., 1994). Recently, the central coiled-coil domain has been shown to participate in masking of the FERM domain region and regulation of FERM binding (Li et al., 2007).

Figure 1.4. The ERM proteins share an overall structure consisting of an N-terminal FERM domain, a central coiled-coil domain and a C-terminal domain that includes a highly-conserved actin-binding motif in the final 34 amino acids. Image taken from Sun et al., 2002.

1.1.3.1. The ERM Association Domains regulate ERM protein activation

The ERM family members form intra- and intermolecular associations via N and C-terminal areas known as ERM Association Domains (ERMAD). The intramolecular association masks the membrane and actin binding sites, rendering the molecule inactive (Bretscher et al., 2000). Phosphorylation of a conserved threonine residue (Thr558 in Moesin, Thr567 in ezrin, and Thr564 in radixin) in the C-ERMAD seems to be responsible for the conversion to the active form (Pearson et al., 2000; Zhou et al., 2005), although two tyrosine residues (Tyr145 and Tyr353) in ezrin can be phosphorylated by the epidermal growth factor (EGF) receptor to produce an

active form (Krieg and Hunter, 1992). It has also been observed that EGF stimulation of A431 cells not only activates ERMs to break the intramolecular association, but also stimulates ERM oligomer formation, suggesting the oligomeric form could be a transition form in the activation pathway (Bretscher et al., 2000; Gautreau et al., 2002). Deactivation of the ERMs by dephosphorylation is also important for cell dynamics, and has been observed *in vivo* to correlate with breakdown of microvilli in such situations as anoxia and apoptosis (Chen and Mandel, 1997).

1.1.3.2. Expression of ERM proteins

In vivo, ERM proteins are found in most tissues, with each family member showing unique expression in different tissues. Ezrin was initially purified from intestinal microvilli, but is also present in the placenta, stomach, lung and kidney at high levels, and in lower levels in the spleen. Subcellularly, its distribution is largely in actin-rich surface projections, and in the tissues in which it can be found, ezrin is mainly associated with the apical surface of epithelial cells (Berryman et al., 1993). In Schwann cells, Ezrin has been found to localise at the paranodal microvilli that project into the Node of Ranvier (Gatto et al., 2003).

Moesin was first isolated from bovine uterine cells and originally thought to be an extracellular heparin-binding protein (Lankes et al., 1988), but was soon shown to be intracellular and very similar to ezrin (Lankes and Furthmayr, 1991; Sato et al., 1992). Berryman et al. (1993) found it to be most abundant in lung and spleen, and to a lesser extent in kidney, while others have observed it in macrophages, lymphocytes, fibroblastic, endothelial, epithelial and neuronal cell lines as well (Amieva and Furthmayr, 1995). Like ezrin, its subcellular localisation is specific to certain areas, chiefly filopodia, microvilli, microspikes and retraction fibres (Amieva and Furthmayr, 1995).

Radixin was initially purified from hepatic adherens junctions (Tsukita et al., 1989), but its subcellular localisation has been somewhat uncertain due to conflicting results with radixin antibody studies (Bretscher et al., 1997); different groups have shown it to localise to adherens junctions (Tsukita et al., 1989), microvilli (Amieva et al., 1994) contractile rings (Henry et al., 1995), focal contacts and cleavage furrows (Sato et al., 1991). Li and Crouch (2000) carried out experiments in chicken tissue and found high levels of radixin in kidney, liver, ovary and bone marrow; lower levels were detected in lung, thymus, colon and skin.

In contrast to the tissue-specific distribution *in vivo*, all three ERMs are usually co-expressed in cultured cells, perhaps due to the unique conditions of the *in vitro* environment (Franck et al., 1993; Sato et al., 1992). The tissue-specific distribution pattern of the ERMs implies functional differences amongst the family members, but there is redundancy to the extent that deleting one or even two of the proteins via antisense oligonucleotide inhibition (Takeuchi et al., 1994b) or in transgenic knockout mice (Doi et al., 1999) produces no observable changes in phenotype.

1.1.3.3. ERM proteins and disease

All members of the ERM family have been implicated in disease, particularly tumours. In *Drosophila*, which contains only Moesin and is thus an easier system in which to create complete knockout phenotypes, epithelial cells that lack Moesin lose epithelial morphological characteristics, such as apical-basal polarity, and adopt invasive migratory behaviour (Speck et al., 2003). Similar effects have been seen in prostate cancer cell lines interacting with endothelial cells; Harrison et al. (2002) found that ezrin co-localised and co-translocated with CD44, variants of which have been linked to metastasis and tumour progression, during tumour-endothelial cell

interactions in which healthy cells were captured by the tumour. This seems to imply that ezrin plays a key role in the cell motility and adhesion involved in metastasis. Further evidence of this is seen in glial cell tumours, known as gliomas, in the brain, where ezrin appears to be involved in a hepatocyte growth factor signalling cascade that promotes tumour migration (Wick et al., 2001). It is also likely that Ezrin is able to activate signalling pathways for cell survival, such as MAPK and Akt (see section 1.1.3.4), allowing metastatic cells to survive in what might have otherwise been a hostile environment (Curto and McClatchey, 2004). In addition, increased expression of Ezrin in some cancer types correlated with both metastatic potential and poor prognosis (Curto and McClatchey, 2004), while cytoplasmic ezrin in head and neck cancers correlates with poor outcome (Madan et al., 2006).

1.1.3.4. ERM proteins are involved in cell signalling

The ERMs appear to be involved in several signalling pathways- not a surprising observation given their essential linking position in the cell. Best studied have been their roles in Rho GTPase signalling pathways, implicated in cell survival and motility, again suggesting an important role for the ERM proteins in these cellular functions. RhoA has been shown to cause Rho kinase to phosphorylate ERM proteins and drive their localisation into apical membrane and actin rich structures (Shaw et al., 1998a), while in cortical neurons, Rho kinase is involved in ERM activation that leads to the formation of filopodia associated with neurite outgrowth (Haas et al., 2007). Another Rho GTPase, Rac1, can be activated by a constitutively active Ezrin, leading to E-cadherin dependent adherens junction assembly (Pujuguet et al., 2003); conversely, Auvinen et al. (2007) found that Ezrin localisation to N-cadherin-containing adherens junctions was regulated by Rac1 through PIPK activity. Recent studies suggest that Ras signalling can also be activated by the ERM proteins

(Morrison et al., 2007). Further regulation and activation of the Rho family by ERMs can also be accomplished through ERM binding of RhoGDI (Takahashi et al., 1997), which inhibits all Rho members, or Dbl, which stimulates all Rho members, and it appears that the interaction with these two regulators is mutually exclusive (Takahashi et al., 1998).

However, Rho-independent activation mechanisms also exist; it was observed that in the kidney-derived cell line MDCK ERM proteins appeared to be active in the absence of Rho, and that phosphatidylinositol-4,5-bisphosphate ($PI(4,5)P_2$), a membrane lipid, could regulate activation (Yonemura et al., 2002). The FERM domain of Ezrin is able to bind $PI(4,5)P_2$ (Niggli et al., 1995), which in turn has a great deal of influence on the intracellular localisation of Ezrin (Barret et al., 2000). $PI(4,5)P_2$ may in fact mediate the interaction of ERMs with adhesion molecules such as CD44 (Niggli et al., 1995).

ERM proteins have been implicated in additional pathways that may explain their potential role in cancer and tumour metastasis. They can activate cell survival signalling pathways through phosphatidylinositol 3-kinase (PI3K)/Akt signalling (Gautreau et al., 1999), such as in cases of apoptotic stress, where ERMs interact with NHE1 to mediate PI3K and Akt cell survival messages (Wu et al., 2004). Protein kinase C theta (PKCθ) and alpha (PCKα) forms are able to phosphorylate moesin (Pietromonaco et al., 1998) and ezrin (Ng et al., 2001) respectively, leading to formation of membrane protrusions and migratory cell behaviour.

Figure 1.5 shows a model for ERM activation in the context of the above signalling pathways (Mangeat et al., 1999). Active, phosphorylated ERM proteins are shown to interact with the membrane either through $PI(4,5)P_2$-mediated interaction with cell adhesion molecules such as CD44, or through multispanning transmembrane

proteins indirectly via PDZ domain-containing binding partners such as Ezrin binding protein 50 (EBP50) and E3KARP. ERMs can be phosphorylated by Rho, and when active ERMs are then able to recruit positive and negative regulators of Rho, Dbl and RhoGDI respectively, to maintain activation of the pathway. Also, PKC is another potential activator of the ERM proteins through ERMAD phosphorylation, perhaps under the influence of different extracellular signals than those that affect Rho.

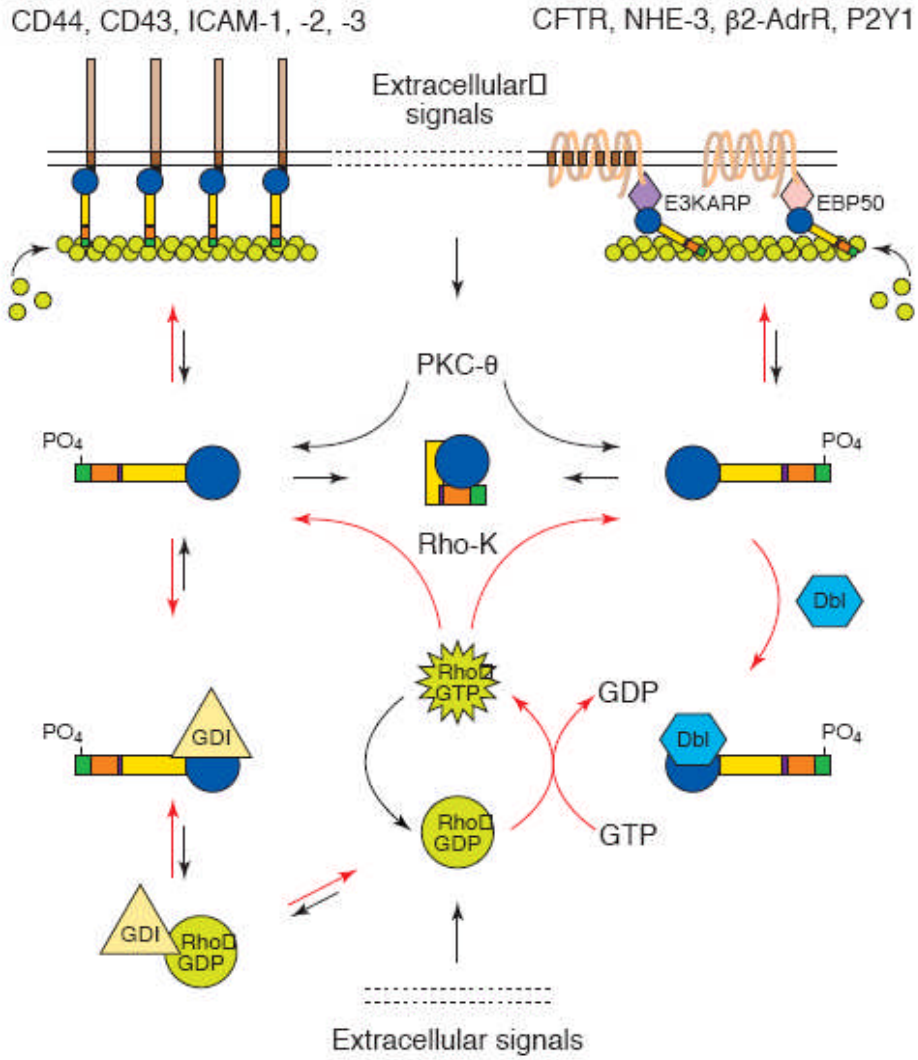

Figure 1.5. A model of ERM involvement in various signalling pathways. Extracellular signals lead to activation of ERM proteins through phosphorylating binding partners such as Rho kinase, PKC and PI(4,5)P2. This allows the ERMs to bind to actin, membrane and cytoplasmic binding partners, and regulators of Rho to keep the pathway active. Figure taken from Mangeat et al., 1998.

1.1.4. Merlin

It has long been known that mutations of merlin cause tumours in the nervous system. Merlin (moesin/ezrin/radixin-like protein), or schwannomin as it is also called, is the product of the brain tumour suppressor neurofibromatosis 2 (*NF2*) gene and shares 45% identity with the ERMs, including a FERM domain with over 60% idenitity between the human forms of merlin and ezrin (Turunen et al., 1998). Lallemand et al. (2003) observed that merlin appears to be required in the formation of adherens junctions and contact-dependent growth arrest.

1.1.4.1. Neurofibromatosis type 2 and the NF2 tumour suppressor gene

Neurofibromatosis type 2 (NF2) is an autosomal dominant syndrome characterised by first of all bilateral vestibular schwannomas, and usually also schwannomas of the cranial, spinal and cutaneous nerves; meningiomas and ependymomas are also commonly reported in NF2 patients (Ahronowitz et al., 2007; Evans et al., 1992). These tumours are slow-growing, making them resistant to chemotherapy and treatable only through repeated, often deforming and debilitating, surgical resections (McClatchey and Giovannini, 2005). The *NF2* gene is found on chromosome 22q12 (Trofatter et al., 1993), with 17 exons that can be alternatively spliced into isoform 1 (exons 1-17) or isoform 2 (exons 1-15 and 17), but only isoform 1 appears to have tumor suppressor function (Sherman et al., 1997).

Hundreds of mutations, both inherited and sporadic, and a range of disease severity have been observed in patients (Ahronowitz et al., 2007). Many of these mutations affect the interaction of Merlin with the cytoskeleton (Deguen et al., 1998), with abnormal cytoskeletal organisation often the result (Pelton et al., 1998). Merlin also plays a role in cell adhesion and contact inhibition. During development it guides the formation of junctional complexes, helping to create tissue fusion and determining

which cells will survive (McLaughlin et al., 2007). It also inhibits Rac (Okada et al., 2005) and Pak1 (Kissil et al., 2003), which allows for contact inhibition to occur. Lallemand et al. (2003) found that loss of NF2 destabilised adherens junctions, thus allowing tumourigenesis. Cell cycle control is also a potential function for Merlin, as it has been found to interact with the cell cycle regulator HEI10 and affect its targeting (Gronholm et al., 2006). Additionally, Merlin is shuttled to the nucleus in a cell cycle and density-dependent manner; once there it can inhibit activation of cell cycle promoter ERK2 (Muranen et al., 2005).

1.1.4.2. Merlin expression

Understandably, Merlin has mostly been studied within the context of its expression in Schwann cells of the peripheral nervous system, where it is developmentally regulated and a component of the paranode and Schmidt-Lanterman incisures (Scherer and Gutmann, 1996). It may play a role in Schwann cell differentiation from the pro-myelinating to the myelinating stage (Hung et al., 2002), and NF2 null mutants show abnormal myelination (Giovannini et al., 2000). However, Merlin has been found in other cell types, such as fibroblasts (Shaw et al., 2001); and in neurons of the central nervous system it is also a component of paranodes, though this time interacting with membrane glycoprotein Caspr on the axonal side (Denisenko-Nehrbass et al., 2003).

Subcellularly, Merlin shows strong cortical membrane localisation, particularly in actin-rich areas such as filopodia and membrane ruffles (Shaw et al., 1998b), and Stickney et al. (2004) showed that Merlin is constitutively localised to detergent-resistant membrane fractions known as lipid rafts. Raft localisation was not dependent on actin cytoskeleton or activation state, but activation did allow merlin to move from a less buoyant raft fraction with greater actin enrichment to a more

buoyant fraction (Figure 1.6), potentially containing different signalling molecules (Stickney et al., 2004); this is typical of raft-associated proteins, which are thought to have a dynamic relationship with rafts to allow for rapid adaptability to signals (Simons and Ehehalt, 2002). It is believed that this raft interaction is important in the function of Merlin, as many NF2 mutations make Merlin more soluble in Triton X-100 (Deguen et al., 1998; Stokowski and Cox, 2000), and as Schwann cells differentiate, Merlin goes from being a soluble cytoplasmic component to an insoluble interactant of β1 integrin (Obremski et al., 1998).

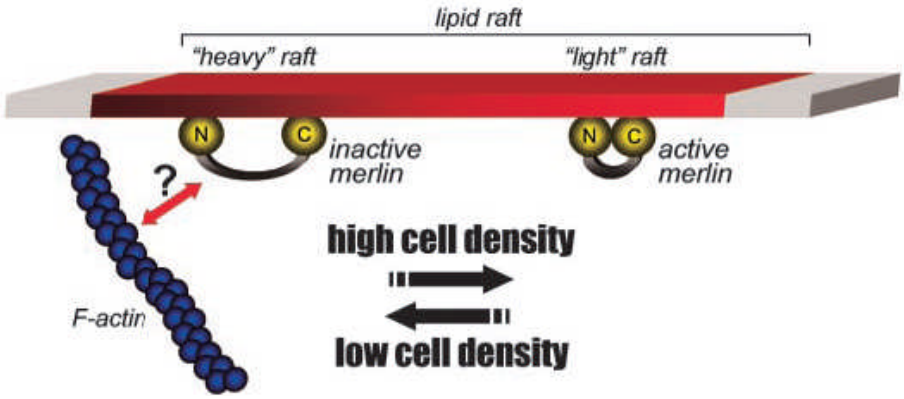

Figure 1.6. A model of how Merlin buoyancy within lipid rafts is affected by cell density-dependent activation. High cell density is associated with active Merlin and light raft localisation. Image taken from Stickney et al., 2004.

Like the ERMs, Merlin also shows a close association with the cytoskeleton, but *in vivo* this interaction may occur indirectly through the association of Merlin and βII-spectrin (Gutmann, 2001). Certainly any interaction with actin is different in Merlin, as it lacks the C-terminal actin-binding motif, but does contain several putative actin-binding sites in the N-terminal half (Brault et al., 2001; Xu and Gutmann, 1998). NF2 tumors often show cytoskeletal defects, and these can be rescued with normal Merlin isoform 1 (Bashour et al., 2002).

1.1.4.3. ERM Association Domains and activation of Merlin

Merlin has ERMADs as well, but their interactions are weaker and more dynamic than those in ezrin, radixin and moesin (Nguyen et al., 2001). Phosphorylation of a serine residue is required to break the association rather than the conserved threonine, but it has not yet been determined which form of merlin is active. It has been proposed that in fact the merlin oligomeric or 'closed' conformation is active, based on evidence that the ERMAD interaction and dephosphorylation is a requisite step in merlin function (Shaw et al., 2001). Hetero-oligomers of ezrin and merlin have been detected using affinity binding assays of their domains (Nguyen et al., 2001), coimmunoprecipitation, yeast two-hybrid, blot overlay and affinity precipitation (Gronholm et al., 1999; Meng et al., 2000), and it has been observed that the merlin C-ERMAD has a much stronger affinity for the ezrin N-ERMAD than its own (Meng et al., 2000; Nguyen et al., 2001). It is possible that this interaction exists in a regulatory capacity to control the activity of ezrin and/or merlin (Gautreau et al., 2002). This seems to coincide with their opposing functions in growth regulation.

1.1.5. FERM-containing proteins in Drosophila melanogaster

Because of its short reproductive cycle and simpler genetics compared to vertebrates, the fruit fly *Drosophila melanogaster* has been used as a model organism for research since the early 20th century; its complete genome was sequenced in 2000 (Ashburner and Bergman, 2005). It contains several FERM-domain containing proteins, apparently fulfilling many of the functions of their vertebrate homologues. Loss of function studies for these genes have provided valuable insight into the function of their protein products.

1.1.5.1 DMoesin

Drosophila have only one ERM protein homologue, DMoesin, which has 58% sequence homology with human moesin, including 26% identity in the C-terminal divergent region (McCartney and Fehon, 1996). This unique expression makes it possible to side-step the problem of redundant function found in vertebrate mutants (see section 1.1.3.2). In a molecular context, loss of DMoesin show that this protein is essential for cytoskeletal distribution, maintenance of apical-basal polarity, and epithelial integrity; this study also suggests that DMoesin acts antagonistically to the Rho pathway, contradicting the results discussed in section 1.1.3.4 (Speck et al., 2003), but further *in vivo* studies are required in vertebrates. Its subcellular localisation was found to be primarily in apical membrane regions (McCartney and Fehon, 1996).

Physiologically, loss of DMoesin causes severe developmental problems, with the posterior structures missing completely from the fly embryos; in addition, imaginal discs, adherens junctions and photoreceptors are all dependent on DMoesin for correct organisation and assembly (Polesello and Payre, 2004).

1.1.5.2. DMerlin and expanded

DMerlin shows a 55% identity with human Merlin, with particular similarity at the C-terminus (McCartney and Fehon, 1996). It shows a subcellular expression at the membrane and cytoplasmic puncta, indicating that it may have an endocytic function (LaJeunesse et al., 1998). Maitra et al. (2006) found that DMerlin mutants showed defects in endocytic trafficking of signalling receptors from the membrane, and suggested that DMerlin's growth-suppressive function was at least in part due to the regulation it thus exerts on expression of positive growth signals at the membrane.

As with the human protein, DMerlin exerts a growth-suppressive function at the plasma membrane (LaJeunesse et al., 1998). In the developing eye, DMerlin appears to regulate normal apoptosis, with mutants exhibiting overgrowth due to a higher number of cells than the normal fly (Pellock et al., 2007), and wings show broadening and cross-vein disruption (McCartney et al., 2000).

Recent work has shown that DMerlin acts closely with another FERM-containing protein, expanded, to regulate growth, proliferation and differentiation in Drosophila tissues (McCartney et al., 2000). Like DMerlin mutants, expanded mutants show overgrowth phenotypes in various tissues (Boedigheimer and Laughon, 1993); (Blaumueller, and Mlodzik 2000) due to overproliferation (Boedigheimer et al., 1997).

DMerlin and expanded co-localise in Drosophila cells, both in tissues and in culture (McCartney et al., 2000). The two act through the Hippo tumour suppressor signalling pathway, causing downstream activation of the Hippo/Salvador complex and Warts/Mats complex (Hamaratoglu et al., 2006), inhibiting the transcriptional coactivator Yorkie, which induces growth (Huang et al., 2005); this leads to further activation of the *DMerlin* and *expanded* genes, as well as repression of *cyclin E* and *Drosophila inhibitor of apoptosis protein 1* (*diap1*) genes (Hamaratoglu et al., 2006). Cyclin E induces entry into S-phase from G1 (Richardson et al., 1995), so DMerlin and expanded are in this case preventing re-entry into the cell cycle; DIAP1, meanwhile, plays an essential role in cell survival through its inhibition of caspase-induced apoptosis (Wang et al., 1999), so the role of DMerlin and expanded here is to allow this apoptotic pathway to operate during differentiation.

The Hippo pathway is conserved in vertebrates: Mst2 (Hippo) activates the NDR type kinases Lats1 and Lats 2 (Warts) in a growth-suppressive pathway (Chan et

al., 2005), and the Mats homologues (MOB proteins) also associate with NDR type kinases (Tamaskovic et al., 2003).

Figure 1.7 shows a summary of this overall regulatory pathway as proposed by Edgar (2006); the receptor that initiates DMerlin and expanded signalling was not yet elucidated at the time, but has since been proposed to be Fat, a protocadherin already implicated in growth regulation in Drosophila development (Cho et al., 2006; Silva et al., 2006). This also has a vertebrate homologue, FAT4 (Silva et al., 2006), but the function of any pathway for this protein is not clear (Cho et al., 2006).

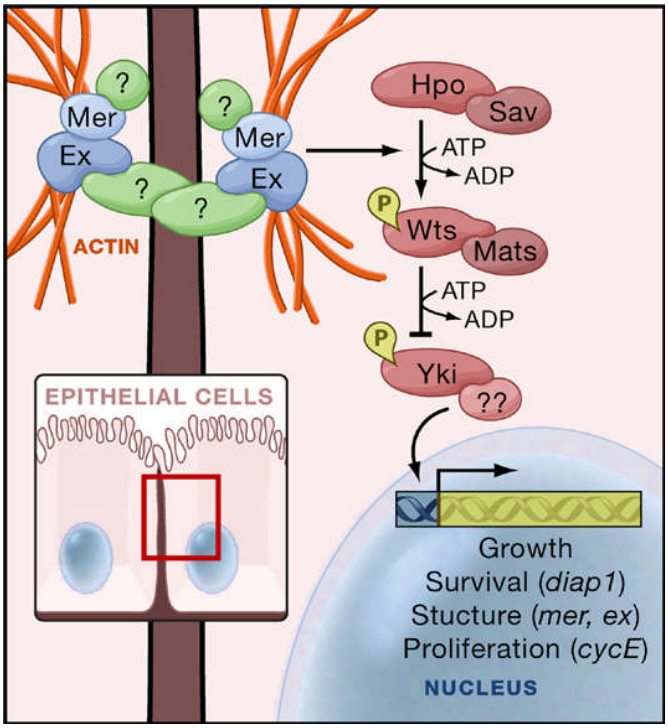

Figure 1.7. The Hippo pathway in *Drosophila* epithelial cells. A membrane receptor, possibly Fat, activates DMerlin and expanded, which in turn regulate the Hippo signalling pathway. Hippo is modulated by Salvador and phosphorylates the Warts/Mats complex, leading to inhibition of Yorkie and continuing growth suppression and apoptosis in a feedback loop. Image taken from Edgar 2006.

1.1.5.3. Coracle

Coracle is a *Drosophila* homologue of protein 4.1, with over 60% sequence identity with the FERM domain of 4.1 and over 35% identity with the final 100 amino

acids of the C-terminus, but lacks the spectrin-actin binding domain (Fehon et al., 1994). Coracle localises to the septate junctions of epithelial cells, where it is required for correct septate junction structure, but unlike protein 4.1, not apical-basal polarity or structural integrity of epithelial cells (Lamb et al., 1998). This septate junction role is probably linked to correct proliferation in embryonic development, as coracle mutants show defects in proliferative aspects such as dorsal closure and cuticle thickness (Ward et al., 2001).

1.1.6. FERM-binding motifs

Several proteins have shown conserved motifs that recognise FERM domains for binding. One such site, MDWxxxxx(L/I)Fxx(L/F), is found in the C-terminus of Na^+/H^+ exchanger regulatory factor (NHERF), an ERM binding partner that anchors ion channels and receptors, as a motif that binds to the F3/C lobe of the FERM domain (Terawaki et al., 2006). Another, and better-characterised, FERM-binding motif, (R/K/Q)xxT(Y/L)xx(A/G), is found in cell adhesion molecules at the juxtamembrane region of their cytoplasmic tails (Dickson et al., 2002; Hamada et al., 2003; Terawaki et al., 2006) and been observed to bind ERMs. A similar motif is also found at the C-terminus of neurofascin (Gunn-Moore et al., 2006).

The interaction of cell adhesion molecules of the L1 family with FERM-containing proteins has been a particular interest of our laboratory for some time, and these will now be discussed.

1.2 The L1 family of cell adhesion molecules

The L1 family of cell adhesion molecules share an overall structure of six IgG-like domains and three to five fibronectin III-like domains extracellularly, a single transmembrane domain, and a short (~110 amino acids) cytoplasmic C-terminus that is highly conserved (Hortsch, 2000). The high level of conservation of the cytoplasmic C-terminus implies similar roles in intracellular signalling, and perhaps even shared binding partners. One known partner of L1 family members is the ankyrin family, a cytoskeletal molecule that binds to a highly conserved 36 amino acid domain found in all L1 proteins (Hortsch, 2000). This cytoskeletal link suggests a role in the regulation of cell morphology and structure for the L1 family.

Members of the family include the prototype, L1 (also known as Neuron-glia cell adhesion molecule or NgCAM), Close Homolog of L1 (CHL1), Neuron-glia-related cell adhesion molecule (NrCAM), and neurofascin in mammals, and neuroglian in *Drosophila* (Figure 1.8). The NrCAM and neurofascin genes are subject to extensive alternative splicing, a process which is tightly linked to development and tissue type (Hassel et al., 1997; Lane et al., 1996). In all, L1 family members make up about 1% of the total membrane protein in brain (Davis et al., 1996).

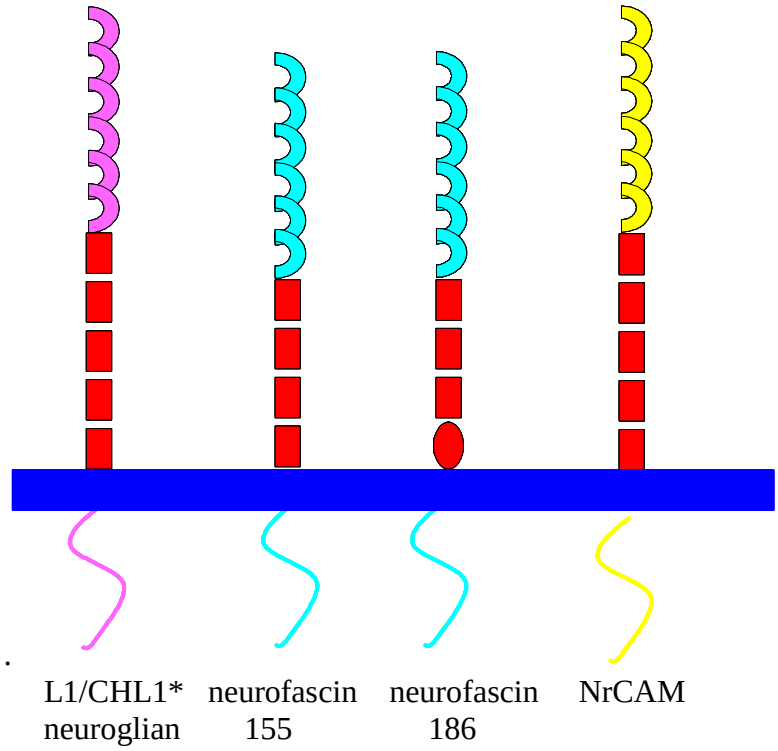

Figure 1.8. Overall structures of the L1 family of cell adhesion molecules. L1 and neuroglian each have 6 IgG-like and 5 fibronectin III-like repeats, while CHL1 has half of the last fibronectin repeat; neurofascin has either 4 fibronectin III domains (neurofascin155) or 3 fibronectin III domains and 1 mucin-like domain (neurofascin 186); NrCAM, like L1, has 6 IgG domains and 5 fibronectin domains.

1.2.1. L1

L1 was first discovered as the cell-surface antigen of L1 monoclonal antibody (Rathjen and Schachner, 1984). Two splice variants, a neuronal-specific and a non-neuronal, exist, with the neuronal form containing the four amino acids arginine, serine, leucine and glutamate (RSLE) in the cytoplasmic C-terminus (Kamiguchi and Lemmon, 1998). L1 plays an important role in the development of the nervous system, promoting neurite outgrowth and neuron survival (Chen et al., 1999), and guiding the differentiation of neural precursor cells to a non-proliferating neuronal, rather than glial, outcome (Dihne et al., 2003). L1-null mice show abnormal cortical dendrites, enlarged ventricles, septal defects, malformed corpus callosum and a lower

number of hippocampal neurons (Demyanenko et al., 1999). Schwann cell-axon interactions are also disrupted, leading to abnormal myelination (Itoh et al., 2005).

Mutations in L1, located on the X chromosome, cause a range of human syndromes known collectively as CRASH (corpus callosum hypoplasia, retardation, adducted thumbs, spastic paraplegia, hydrocephalus), and which show a great deal of diversity in both appearance and severity of symptoms depending on which mutation is present (Yamasaki et al., 1997).

1.2.2. CHL1

CHL1, like L1, promotes neuron survival and neurite outgrowth (Chen et al., 1999); it is believed to interact with integrins for regulation of cell migration, but with perhaps a differential preference for extracellular binding partners than L1 (Buhusi et al., 2003). Its expression during nervous system development is also distinct from L1, and in contrast to L1, the soluble form of CHL1 can promote neurite outgrowth (Hillenbrand et al., 1999).

1.2.3. NrCAM

In the nervous system, NrCAM is found in both glia and neurons, with most studies focusing on its neuronal functions. It is localised at the nodes of Ranvier and axon initial segment, where Na^+ channels cluster (Hillenbrand et al., 1999). Intracellular binding partners of NrCAM have only recently been elucidated, and include the cytoskeletal linker Ankyrin G (Davis and Bennett, 1994), Synapse Associated Protein 102 (SAP102) (Davey et al., 2005), post-synaptic density-95 (PSD95), also known as SAP90, and SAP97 (Dirks et al., 2006). These three related proteins are involved in many processes, but particularly synaptic activities such as vesicle trafficking and receptor modulation (Davey et al., 2005). Interfering with

SAP102-NrCAM binding prevented neurite outgrowth (Davey et al., 2005), and it is required for axonal pathfinding in at least some neuronal systems, through mediation of growth cone-substrate interactions (Zelina et al., 2005).

NrCAM has been implicated in psychiatric disorders, particularly autism (Sakurai et al., 2006) and vulnerability to drug addiction (Ishiguro et al., 2006). Outside the nervous system, cancers such as melanomas (Reed et al., 2005), colon cancer (Conacci-Sorrell et al., 2002) and pancreatic cancer (Dhodapkar et al., 2001) are seen to upregulate NrCAM, and this may be a factor in tumour migratory behaviour (Conacci-Sorrell et al., 2002).

1.2.4. Neurofascin

Like NrCAM, neurofascin is extensively alternatively spliced (Volkmer et al., 1992); Hassel et al., 1997), with isoforms of 186kDa, 155kDa and 140kDa found in the brain (Davis et al., 1993). Alternative splicing strictly controls tissue localisation of neurofascin, with neurofascin186 localising to the Node of Ranvier in axons (Davis et al., 1996), while neurofascin155 localises to unmyelinated axons and the paranodal loops of glial cells in the CNS and PNS (Sherman et al., 2005; Tait et al., 2000). The 140kDa isoform is a minor component, and is present mainly in cerebellum (Davis et al., 1996).

Neurofascin is essential for node of Ranvier formation. Compared to wild-type, neurofascin-null mice have large gaps between the paranodal loops and septate-like junctions are no longer present; myelin appears normal but conduction velocity is decreased (Figure 1.9; Sherman et al. 2005).

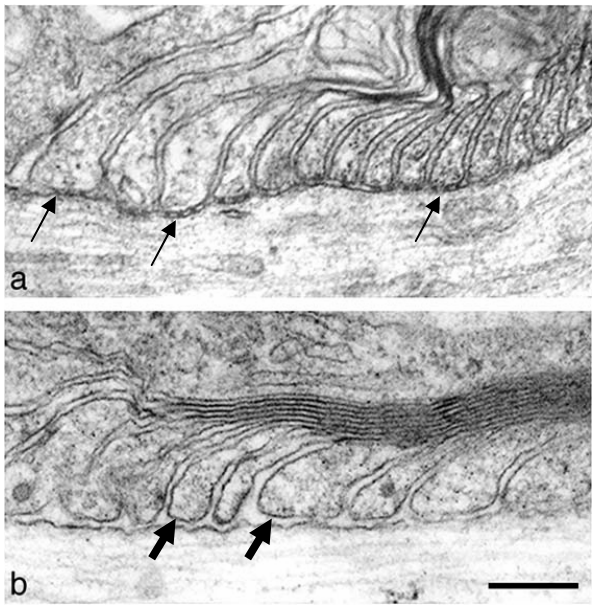

Figure 1.9. Electron micrographs of paranodes in wild type and neurofascin-null mice. In wild-type mice, paranodal loops connect to the axons with septate-like junctions as indicated by arrows (a), but these connections are disrupted and the gaps between loops and the axon (block arrows) are greater in neurofascin-null mice (b). Taken from Sherman et al., 2005.

In the PNS, neurofascin186 is anchored to the node by gliomedin, a component of Schwann cell microvilli, and can then act as a pioneer molecule for recruiting other binding partners, such as NrCAM, ankyrin and sodium channels (Na_V). Neurofascin155, meanwhile, guides formation of the septate-like junctions of the paranodal loops with the axons, via interactions with Caspr and contactin (Charles et al., 2002; Sherman et al., 2005). This is summarised in Figure 1.10.

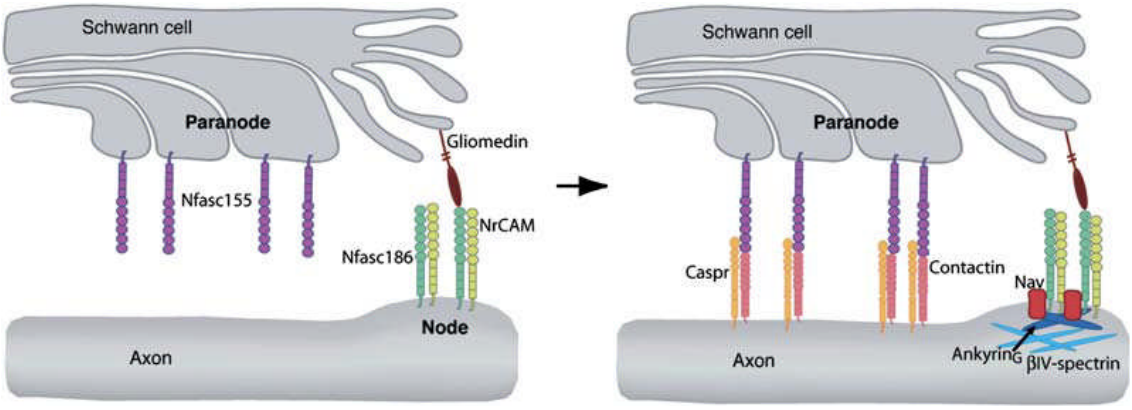

Figure 1.10. Construction of the node of Ranvier. Neurofascin186 and NrCAM in the axon and gliomedin in the Schwann cell microvilli establish the node, and neurofascin and NrCAM recruit additional binding partners to the node. In the paranodal loops, neurofascin 155 arrives independently of Caspr and contactin, and recruits them from the axonal side to form the paranodal complex. Taken form Sherman et al., 2005.

1.2.4.1. Neurofascin and multiple sclerosis

In multiple sclerosis (MS) demyelinating lesions, neurofascin155 expression is spread from its discreet paranodal localisation towards the juxtaparanode, and this leads to movement of juxtaparanode components, such as potassium channels (K_V) towards the node. After demylenation, neurofascin186 and Na_V expression is also disrupted, with both being distributed throughout the axon rather than in distinct nodes. During remyelination of lesions, neurofascin155 paranodal connections are abnormal, with triple structures separating close nodes. These connections seem to be temporary, with separate nodes fusing in remyelinated tissue (Howell et al., 2006). A model of the changes that occur during MS demyelination/remyelination is shown in Figure 1.11.

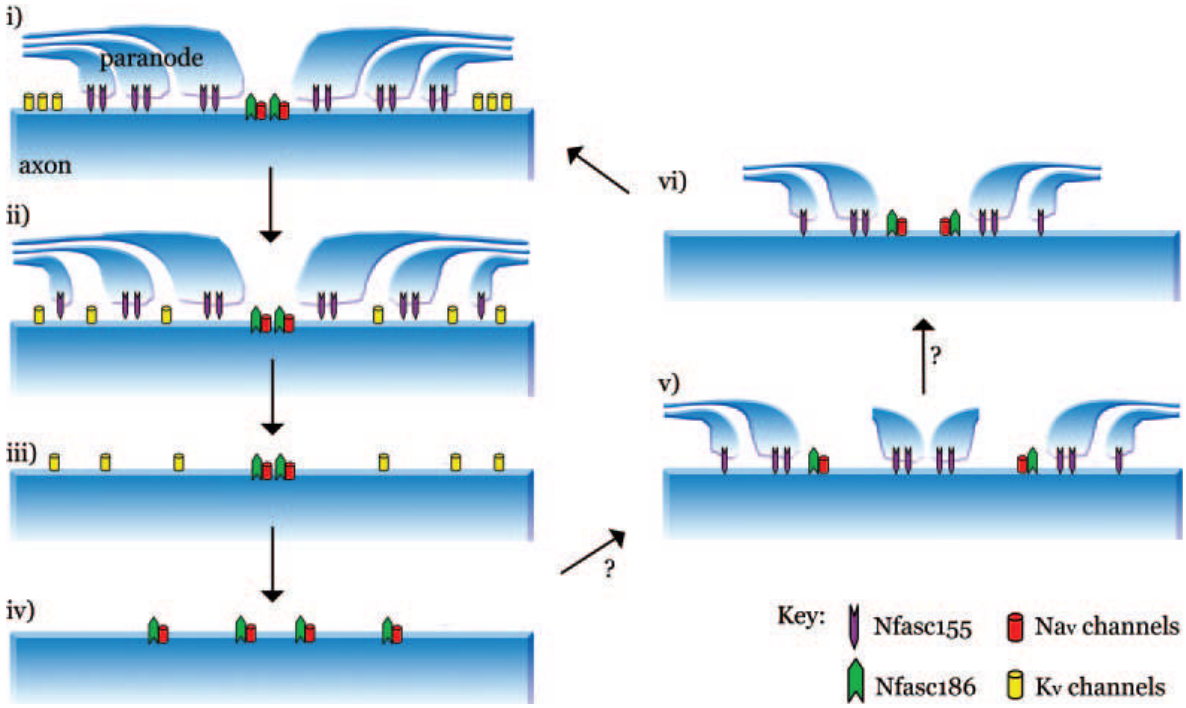

Figure 1.11. i) Neurofascin155 joins the paranodal loops to the axon, with neurofascin186 and Na_V channels in the node and K_V channels in the juxtaparanode. ii) Demyelination leads to neurofascin155 disruption and movement of K_V channels towards the node. iii) Neurofascin155 is lost and the axon is demyelinated. iv) Nodes are disrupted, with neurofascin186 and Na_V channels distributed throughout the axon. v) Abnormal triplicate neurofascin155 paranodal contacts occur during remyelination. vi) Binary nodes fuse, displacing the abnormal triplicate from the remyelination process. Taken from Howell et al., 2006.

1.2.4.2. Neurofascin localisation to lipid rafts is important in paranode formation

Neurofascin155 has been shown to localise to lipid rafts in oligodendrocytes (Schafer et al., 2004), and this is presumably the case in Schwann cells, though it has not been studied in the PNS. Raft localisation is developmentally-regulated, with neurofascin155 found to be soluble prior to paranode formation, and localised to rafts once the paranode is anchored (Schafer et al., 2004). The proper establishment of detergent-resistant membrane microdomains seems to be essential to survival of oligodendrocytes, as their depletion prevents PDGF-mediated signalling (Decker and ffrench-Constant, 2004). Axon-glial contact and myelination are also dependent on lipid raft complexes. Mutant mice lacking the galactosylceramide sulfotransferase

gene, disrupting production of two major glycolipids, show improper ion channel clustering, altered nodal length and diffuse distribution of Caspr along the internode (Ishibashi et al., 2002). Active MS lesions that show disrupted paranodes also have reduced neurofascin155 localisation to lipid rafts (Maier et al., 2007).

1.2.5. Neuroglian

Drosophila have only one L1 family member, neuroglian. Like the other family members, neuroglian interacts with and may be necessary for membrane localisation of ankyrin (Dubreuil et al., 1996). In the *Drosophila* nervous system, neuroglian is important in neuronal pathfinding (Hall and Bieber, 1997) and axonal substrate choice (Garcia-Alonso et al., 2000); in other tissues, it is important for stabilisation of epithelial tissue at points of cell-to-cell contact (Wei et al., 2004), and indeed it has been found to localise to the ladder-like pleated septate junctions of the epithelium (Genova and Fehon, 2003) along with neurexin IV (Baumgartner et al., 1996) and contactin (Faivre-Sarrailh et al., 2004). These three adhesion molecules allow the formation of the Drosophila blood-brain barrier, which keeps the potassium-rich hemolymph separate from neurons. Septate junctions also form between insulating glia around axon in a homologous structure to the vertebrate septate-like junctions of the paranodes (Banerjee et al., 2006).

1.2.6. The interaction of L1 family members and FERM-containing proteins

While the behaviour of the extracellular component of L1 family proteins is relatively well-defined, cytoplasmic binding partners have not been well-elucidated. In fact, despite the high degree of conservation among the L1 family members, ankyrin is the only mammalian universal binding partner found to date (Davey et al.,

2005; Davis et al., 1993). Yeast two-hybrid screens for binding partners of the C-terminus of L1 family members have revealed multiple sites capable of bind ERM proteins in both L1 and neurofascin, but not NrCAM (Cheng et al., 2005; Dickson et al., 2002; Gunn-Moore et al., 2006).

1.2.6.1. L1 interaction with Ezrin is important for normal axonal morphogenesis

Dickson et al. (2002) first screened for cytoplasmic binding partners and found that the FERM domain of Ezrin bound to the neuronal isoform of L1 at a region encompassing the RSLE motif, a region previously shown to regulate sorting of L1 to the axonal growth cone (Kamiguchi and Lemmon, 1998). A second, juxtamembrane region also mediates ERM-binding, and both regions are involved in regulation of neurite outgrowth and branching (Dickson et al. 2002; Cheng et al. 2005). The L1-ERM interaction occurs in early *in vitro* development, with active, phosphorylated ERM expression peaking at 3 days *in vitro* (DIV) and diminished by 21 DIV; between 21 and 28 DIV, mainly inactive ERMs are expressed, but after injury active ERMs are re-expressed for regeneration of neurites (Haas et al., 2004).

1.2.6.2. Neurofascin interacts with Ezrin in the microvilli of Schwann cells

A yeast two-hybrid screen of neurofascin C-terminus against a rat sciatic nerve cDNA library was performed to identify novel intracellular binding partners, and Ezrin was identified as a positive interaction. Experiments with truncated constructs showed it was the FERM domain of Ezrin that bound to neurofascin, while only the extreme C-terminus of neurofascin was required for the interaction (Gunn-Moore et al., 2006). This is a different mechanism for the interaction with Ezrin than that used by L1.

Immunohistochemical staining of neurofascin155 and Ezrin in teased sciatic nerve fibre shows that the two proteins co-localise in the microvilli of Schwann cells that project from the paranode into the node (Figure 1.12); however, neurofascin155 expression is not required for localisation of Ezrin to these microvilli (Gunn-Moore et al., 2006).

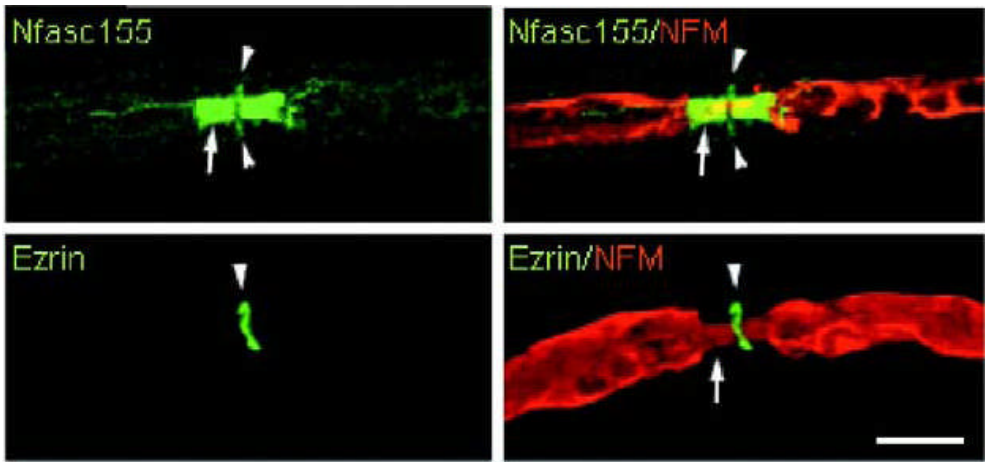

Figure 1.12. Immunofluorescence localization of both neurofascin155 and Ezrin to the microvilli of Schwann cells. The axon is visualized using an antibody against the neurofilament M subunit (NFM). The location of the microvilli in this teased sciatic nerve fiber is shown by arrowheads and the paranodal axoglial junctions are identified by arrows. Scale bar 10 μm. Images taken from Gunn-Moore et al. 2006.

1.2.6.3. Drosophila septate junctions are analogous to vertebrate paranode septate-like junctions

The vertebrate paranodal septate-like junction (Figure 1.13) is similar to the invertebrate septate junction both functionally and structurally. Both perform a selective barrier function at an important point of contact between two different cell types, with the paranodal junction maintaining correct localisation of ion channels in the node of Ranvier and the invertebrate septate junction acting as a trans-epithelial diffusion barrier and maintainer of cell polarity in addition to the previously discussed

function (see section 1.2.5) in the insect blood-brain barrier (Tepass and Tanentzapf, 2001).

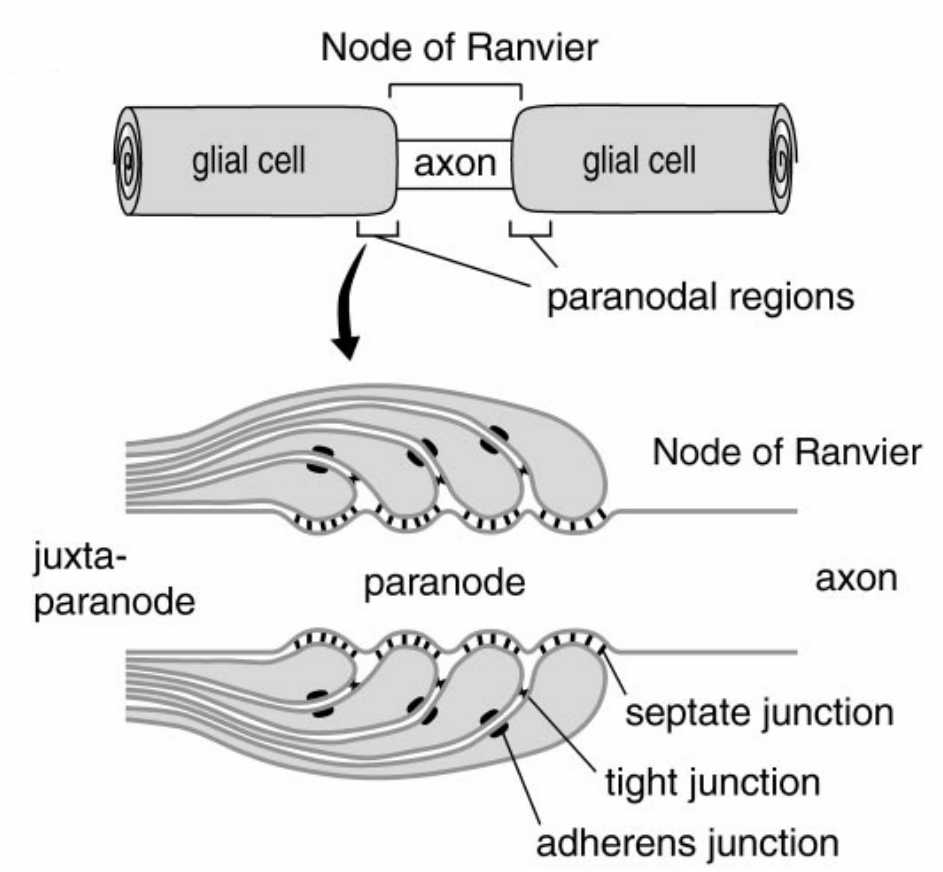

Figure 1.13. At the paranode, glia form septate-like junctions with the axon. Between paranodal loops are tight junctions and adherens junctions. Image from Tepass et al., 2001.

Several molecules have been identified in both junction types: Caspr is a vertebrate homologue of neurexin IV and localises to the paranodal septate-like junctions of myelinated axons (Einheber et al., 1997). It can also bind the neuronal isoform of protein 4.1, the homologue of coracle (Menegoz et al., 1997). Interestingly, neuroglian interacts genetically with coracle in septate junctions, forming a protein complex along with other junction components including neurexin IV (Genova and Fehon, 2003); as Caspr has also been shown to bind neurofascin155

(Charles et al., 2002), an analogous set of structures becomes clear and is summarised in Figure 1.14.

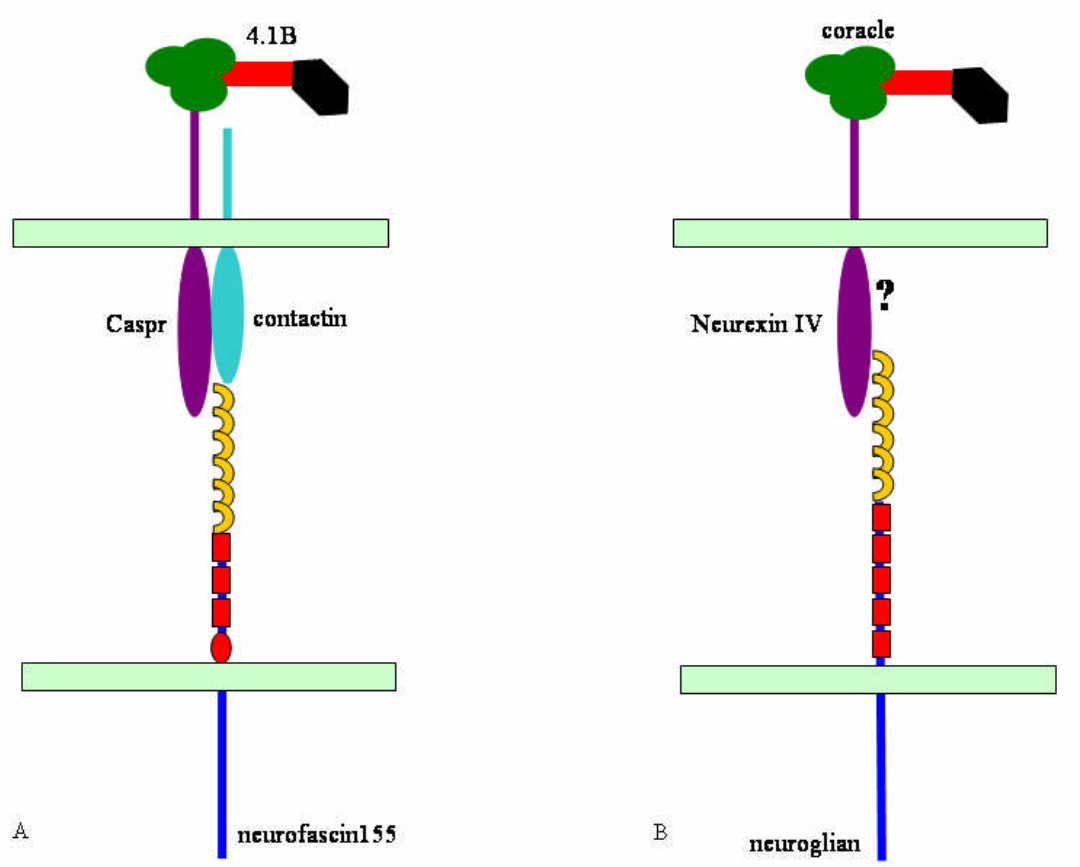

Figure 1.14. The vertebrate paranodal septate-like junction (A) consists of neurofascin155 on the glial side with its extracellular domains interacting with Caspr and contactin on the axonal side. The intracellular domain of Caspr interacts with the neuronal isoform of protein 4.1. The invertebrate septate junction (B) consist of neuroglian, the neurofascin homologue, neurexin IV, the Caspr homologue, and coracle, the 4.1 homologue. It is not known if the *Drosophila* contactin homologue localises to septate junctions.

The knowledge that neurofascin155 is capable of binding and colocalising with Ezrin *in vivo* adds another degree of complexity to this picture. The structure of the septate junction would suggest that neuroglian interacts with coracle only as part of a complex, rather than a direct interaction between the FERM domain of coracle and the C-terminus of neuroglian. Could there then be another FERM-containing

protein that interacts with neuroglian as Ezrin does with neurofascin155? As yet, all other FERM-containing proteins in Drosophila have been observed to localise to adherens, not septate, junctions (Boedigheimer et al., 1997; McCartney and Fehon, 1996), but as will be discussed in Chapter 6, this picture is not as clear cut as it may seem, and leaves some scope for further speculation.

1.2.6.4. A novel protein discovered from a yeast two-hybrid screen of neurofascin

During a yeast two-hybrid screen of the neurofascin C-terminus against a rat sciatic nerve library, a novel FERM-containing cDNA was identified and called 163ScII (accession number AF441249). This sequence was found to have 86% identity at the DNA level and 91% identity at the protein level to a full-length cDNA human clone (MGC:17921 image: 3941276) which has also been identified as Open Reading Frame 31 Chromosome 14 (accession number BC020521). The cDNA image clone, obtained from a human uterine leiomyosarcoma, was acquired from the MRC IMAGE consortium and termed Willin, after the founder of the Royal (Dick) School Veterinary College of the University of Edinburgh, William Dick, and is also known as FRMD6.

1.3. Willin

Upon complete sequencing, the protein was found to have 614 amino acids, with a predicted molecular weight of approximately 71kDa and a FERM domain between residues 14 and 322. It was found to have a FERM domain most closely related to the human ERMs (see Figure 1.15), and is predicted to have a similar overall structure, with a central coiled-coil domain and a C-terminal domain. Like the other family members, it co-localises with actin, but neither the C-terminal actin-

binding motif nor the putative N-terminal actin-binding regions of the ERMs and Merlin are conserved; to date, only the FERM domain is confirmed to be present (see Figure 1.16).

A

```
Radixin   ------------MPKPINVRVTTMDAELEFAIQPNTTGKQLFDQVVKTVGLREVWFFGLQ 48
Moesin    ------------MPKTISVRVTTMDAELEFAIQPNTTGKQLFDQVVKTIGLREVWFFGLQ 45
Ezrin     ------------MPKPINVRVTTMDAELEFAIQPNTTGKQLFDQVVKTIGLREVWYFGLH 47
Willin    MNKLNFHNNRVMQDRRSVCIFLPNDESLNIIINVKILCHQLLVQVCDLLRLKDCHLFGLS 60
                                . . * .*:: *: :   :**: ** . : *::   ***
Radixin   YVDSKGYSTWLKLNKKVT---QQDVKKEN---------PLQFKFRAKFFPEDVSEELIQE 96
Moesin    YQDTKGFSTWLKLNKKVT---AQDVRKES---------PLLFKFRAKFYPEDVSEELIQD 93
Ezrin     YVDNKGFPTWLKLDKKVS---AQEVRKEN---------PLQFKFRAKFYPEDVAEELIQD 95
Willin    VIQNN-EHVYMELSQKLYKYCPKEWKKEASKGIDQFGPPMIIHFRVQYYVENG-RLISDR 118
            :.:   .:::*.:*:     :: :**          *: ::**.::: *:  . : :
Radixin   ITQRLFFLQVKEAILNDEIYCPPETAVLLASYAVQAKYGDYNKEIHKPGYLANDRLLPQR 156
Moesin    ITQRLFFLQVKEGILNDDIYCPPETAVLLASYAVQSKYGDFNKEVHKSGYLAGDKLLPQR 153
Ezrin     ITQKLFFLQVKEGILSDEIYCPPETAVLLGSYAVQAKFGDYNKEVHKSGYLSSERLIPQR 155
Willin    AARYYYYWHLRKQVLHSQCVLREEAYFLLAAFALQADLGNFKRNKHYGKYFEPEAYFPSW 178
           ::  :: :::: :* .:     *: .**.::*:*:. *::::: *   *:  :  :*.
Radixin   VLEQHKLTKEQWEERIQNWHEEHRGMLREDSMMEYLKIAQDLEMYGVNYFEIKNKKG--- 213
Moesin    VLEQHKLNKDQWEERIQVWHEEHRGMLREDAVLEYLKIAQDLEMYGVNYFSIKNKKG--- 210
Ezrin     VMDQHKLTRDQWEDRIQVWHAEHRGMLKDNAMLEYLKIAQDLEMYGINYFEIKNKKG--- 212
Willin    VVSKR--GKDYILKHIPNMHKDQFALTASEAHLKYIKEAVRLDDVAVHYYRLYKDKREIE 236
          *:.:: : ::   .:*   * :: .   .:: ::*:* *  *:  .::*: : :.*
Radixin   TELWLGVDALGLNIYE-HDDKLTPKIGFPWSEIRNISFNDKKFVIKPIDKKAP-DFVFYA 271
Moesin    SELWLGVDALGLNIYE-QNDRLTPKIGFPWSEIRNISFNDKKFVIKPIDKKAP-DFVFYA 268
Ezrin     TDLWLGVDALGLNIYE-KDDKLTPKIGFPWSEIRNISFNDKKFVIKPIDKKAP-DFVFYA 270
Willin    ASLTLGLTMRGIQIFQNLDEEKQLLYDFPWTNVGKLVFVGKKFEILPDGLPSARKLIYYT 296
          :.* **:   *::*::  ::.     .***::: :: * .*** * * .  :. .:::*:
Radixin   PRLRINKRILALCMGNHELYMRRRKP 297
Moesin    PRLRINKRILALCMGNHELYMRRRKP 294
Ezrin     PRLRINKRILQLCMGNHELYMRRRKP 296
Willin    GCPMRSRHLLQLLSNSHRLYMNLQPVLRHIRKLEENEEKKQYRESYISDNLDLDMDQLEK 356
               .:::* *  ..*.** . :

Willin    RSRASGSSAGSMKHKRLSRHSTASHSSSHTSGIEADTKPRDTGPEDSYSSSAIHRKLKTC 416
Willin    SSMTSHGSSHTSGVESGGKDRLEEDLQDDEIEMLVDDPRDLEQMNEESLEVSPDMCIYIT 476
Willin    EDMLMSRKLNGHSGLIVKEIGSSTSSSSETVVKLRGQSTDSLPQTICRKPKTSTDRHSLS 536
Willin    LDDIRLYQKDFLRIAGLCQDTAQSYTFGCGHELDEEGLYCNSCLAQQCINIQDAFPVKRT 596
Willin    SKYFSLDLTHDEVPEFVV                                             614
```

B

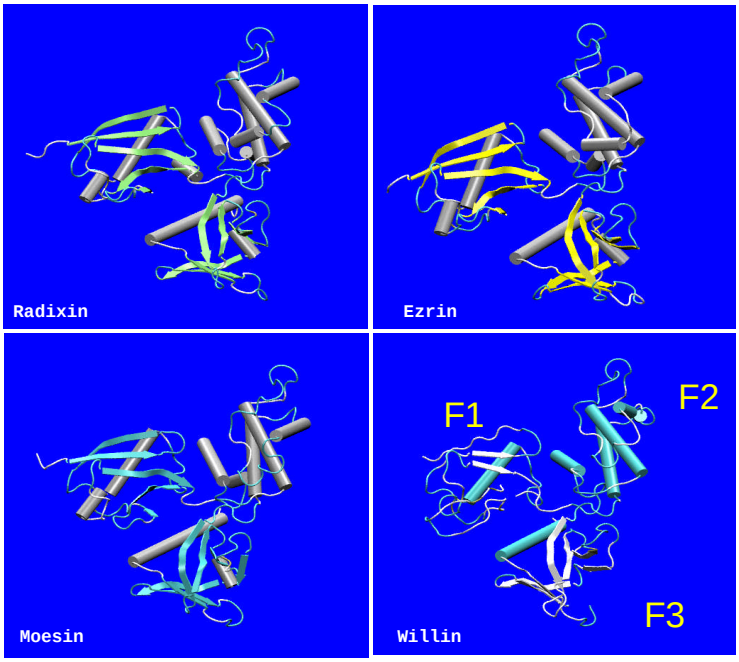

F1 (ubiquitin like subdomain)

F2 (acyl-CoA binding like sub-domain)

F3 (phosphotyrosine binding (PTB)/pleckstrin homology (PH) like subdomain)

Figure 1.15. A) Sequence alignments of Willin and the FERM domains of Ezrin, Radixin and Moesin. * = identical residue, **:** = conserved substitution, **.** = semi-conserved substitution. B) Predicted 3-dimensional structure of Willin FERM domain compared with Ezrin, Radixin and Moesin FERM domains from crystal structures. Structural prediction performed by V. Zaitsev.

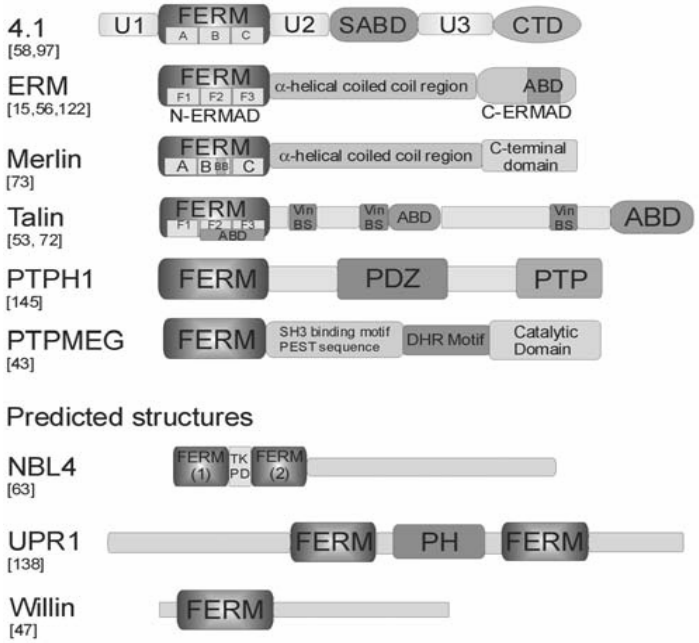

ABD: Actin binding domain
BB: blue box
CTD: carboxy terminal domain
DHR: *Drosophila* hormone receptor
PDZ: postsynaptic density-95 /discs large/zonula occludens-1 domain
PH: pleckstrin homology domain
PTP: protein tyrosine phosphatase domain
SABD: spectrin-actin-binding domain
TKPD: tyrosine kinase phosphorylation domain
U1-3: unique regions
VinBS: vinculin binding site

Figure 1.16. Structural domains present in the Band 4.1 superfamily. The FERM domain is the only confirmed domain in Willin. Image taken from Diakowski et al., 2006.

Like the ERMs and Merlin, Willin has been observed in the cytoplasm and nucleus (Madan et al., 2006). We have also shown that Willin has a phosphoinositol binding profile comparable to that of Moesin (Figure 1.17), and Willin-GFP is often localised to the membrane; this is particularly true in adjoining cells.

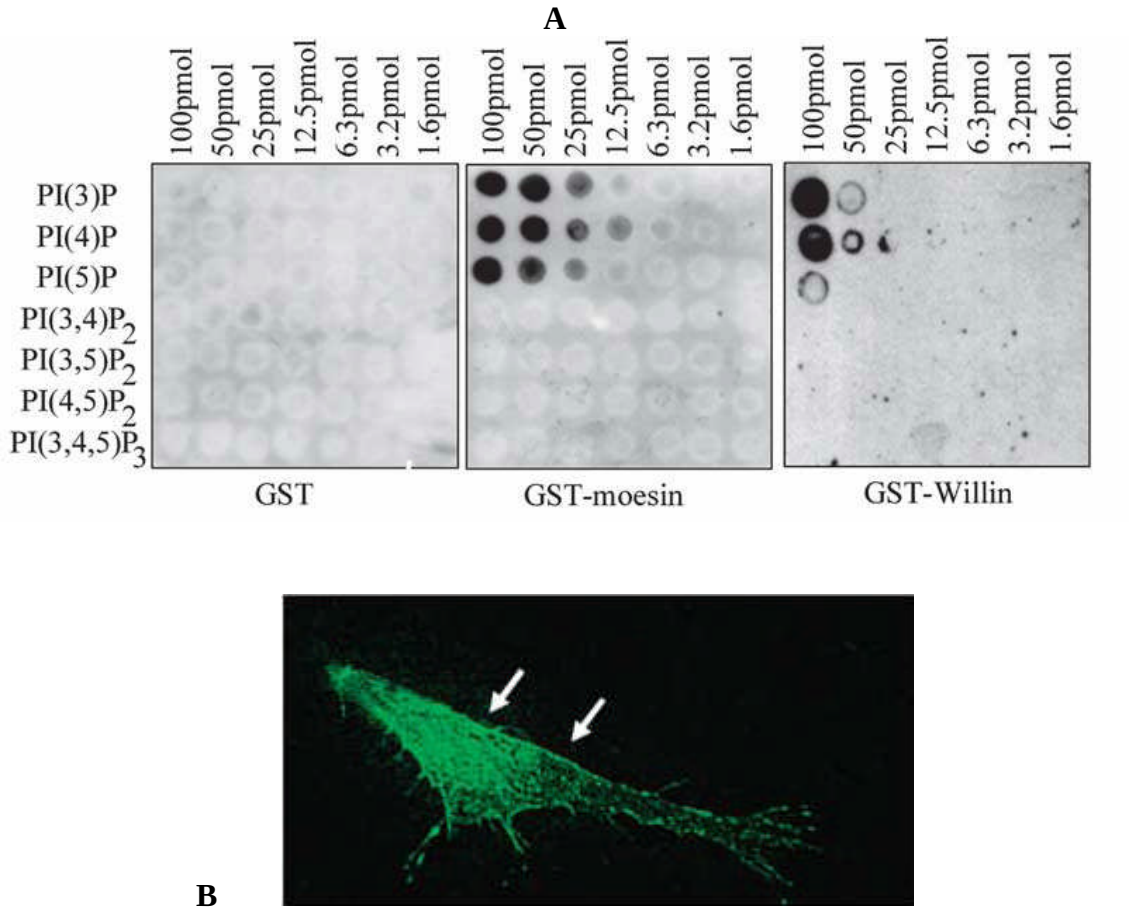

Figure 1.17. A) A phospholipid blot overlay experiment using purified GST, GST-Moesin and GST-Willin. Image provided by Dr. Kanamarlapudi Venkateswarlu. B) A HEK-293 cell expressing Willin-GFP. Membrane localisation indicated by arrows. Image obtained by Dr. Frances Brannigan.

In PC12 cells, a cytoplasmic pool of Willin-GFP is seen to translocate to the membrane when the cells are treated with growth factors, even in adjoining cells where Willin-GFP is already present in the membrane (Gunn-Moore et al., 2005). This effect occurred under the influence of both epidermal growth factor (EGF;

Figure 1.18) and nerve growth factor (NGF; data not shown), but the translocation is not blocked when the cells are treated with wortmannin (Figure 1.19). This indicates that phosphatidylinositol 3-kinase (PI3K) activity is not required to translocate Willin (Venkateswarlu et al., 1999). It is probable that, like Ezrin, EGF is causing tyrosine phosphorylation of Willin; EGF is a known activator of Ras (Marshall, 1995), Rho and Rac (Maddala et al., 2003), which in turn interact with ERM proteins (see section 1.1.3.4), so Rho family activation is a possible pathway for Willin translocation. These and other possibilities have yet to be studied.

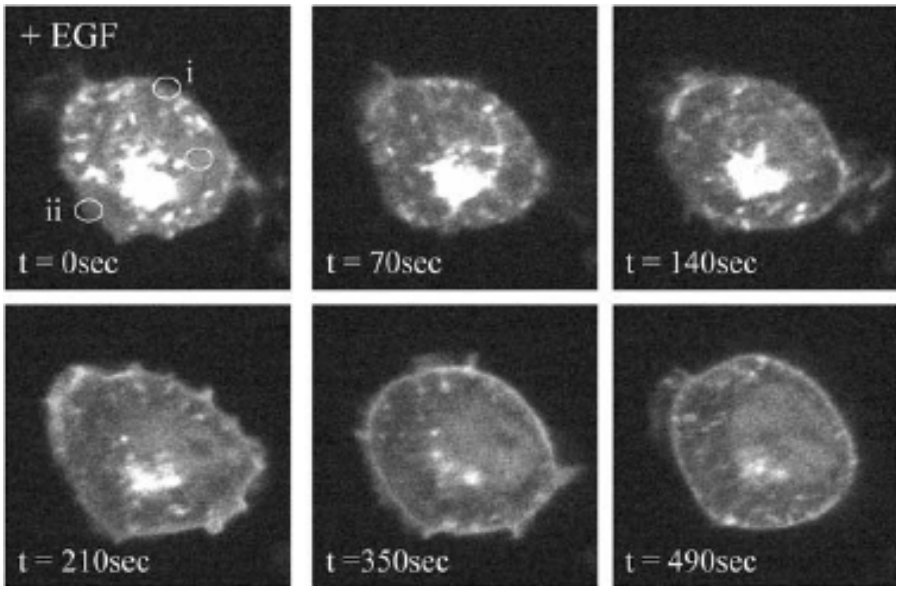

Figure 1.18. A PC-12 cell expressing Willin-GFP, mostly in the cytoplasm. Upon addition of 100 ng/mL of EGF, the majority of cytoplasmic pool of Willin-GFP translocates to the plasma membrane in under 10 minutes. t = time after addition of EGF. Images taken from Gunn-Moore et al., 2005.

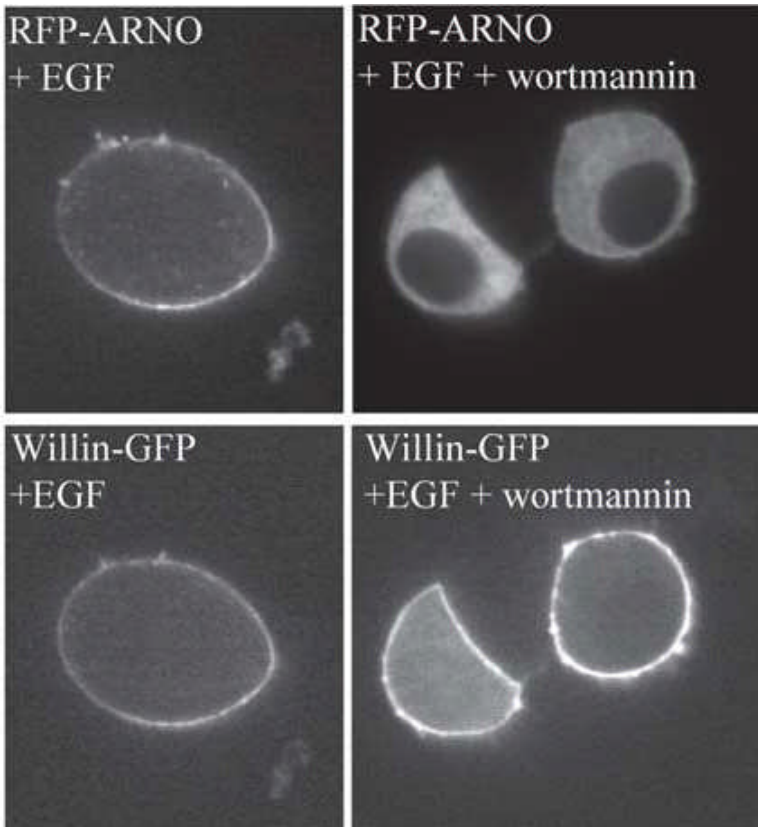

Figure 1.19. PC12 cells co-expressing RFP-ARNO and Willin-GFP were treated with 100 ng/mL EGF alone (left) or pretreated with 100nM wortmannin 30 minutes before addition of 100 ng/mL EGF (right). ARNO, a PH-domain-containing protein, is dependent on PI3K activation for its transolaction, which is thus blocked by wortmannin, a PI3K inhibitor. Willin-GFP translocation is not blocked by wortmannin.

The human Willin gene is found on chromosome 14, open reading frame 31. Interestingly, the 14q region at which it is found has been implicated in a variety of human cancers, such as uterine leiomyoma and leiomyosarcoma (Levy et al., 2000), meningiomas (Tse et al., 1997), gastronintestinal stromal tumours (Fukasawa et al., 2000), neuroblastomas (Theobald et al., 1999) and gliomas (Dichamp et al., 2004). 14q mutations and loss of heterozygosity (LOH) have also been linked with mutations and LOH on chromosome 22q12- the site of the *NF2* gene (Fukasawa et al., 2000; Leone et al., 1999). This raises the intriguing possibility that Willin is a tumour suppressor, a concept that is further bolstered by the recent suggestions that Willin

could be the mammalian homologue of the *Drosophila* tumour suppressor Expanded (Hamaratoglu et al., 2006).

The aims of this project were: to characterise further the novel protein Willin, with particular emphasis on elucidation of potential binding partners, subcellular localisation and function; to test several antibodies to Willin which were raised in chicken, rabbit and mouse; and to perform an initial comparison between the 614 amino acid isoform of Willin and a 622 amino acid splice variant that was found late in this project.

CHAPTER 2: MATERIALS AND METHODS

Chapter 2: Materials and Methods

Unless otherwise stated, chemical reagents were obtained from Sigma. See appendix 4 for a list of suppliers.

2.1 Molecular biology and cloning

2.1.1 Polymerase Chain Reaction (PCR)

PCR was performed using PfuTURBO DNA Polymerase (Stratagene or Rovalab,Teltow, Germany) or Expand High Fidelity Taq Polymerase (Roche) according to manufacturer's instructions in the buffer supplied and adding 200μM dNTPs (Promega), 0.5μM forward and reverse primers (Invitrogen) and 200-300ng template. Thermal cycling was then done in a Biometra Tpersonal Combi thermal cycler (Biometra, Goettingen, Germany) as follows:

1. 94ºC for 5 minutes
2. 94ºC for 1 minute.
3. 54ºC for 1 minute.
4. 72ºC for 2minutes 30 seconds. (steps 2-4 repeated 34 times for a total of 35 cycles)
5. 72ºC for 10 minutes.

PCR products were run on a 1% or 2% agarose gel alongside a 1kb DNA ladder for size analysis.

2.1.2 Restriction enzyme digest

Restriction enzymes were acquired from Promega or New England Biolabs. Restriction digests were performed according to manufacturer's instructions with supplied buffers and either single enzymes or in double digests. Generally, 10 units of enzyme were used to digest 1μg of plasmid DNA or PCR product. Digests were

incubated at 37°C for 1-5 hours. They were then either heat inactivated at 65°C for 15 minutes for further treatment with alkaline phosphatase (see section 2.1.3) or run directly on an agarose gel for analysis or purification.

2.1.3 Alkaline phosphatase treatment of digested plasmids

To prevent religation of sticky ends in digested plasmids, phosphate groups were removed from their 5' overhangs by the addition of 1 unit of calf intestinal alkaline phosphatase (CIAP) (Promega) incubated for 30 minutes at 37°C, followed by addition of another unit of CIAP and a further 30 minute incubation at 37°C. Blunt ends and 3' overhangs were treated by addition of 1 unit CIAP for 15 minutes at 37°C and then 15 minutes at 56°C, repeated with a second unit of CIAP.

2.1.4 Klenow reaction

For cloning strategies where a blunt end was required for ligation, sticky ends were filled in using Klenow fragment and supplied buffer (Promega) according to manufacturer's instructions.

2.1.5 Ligation reaction

Ligations were performed using T4 DNA ligase (Promega) according to manufacturer's instructions.

2.1.6 Agarose gel electrophoresis

DNA fragments were separated by molecular weight using agarose gel electrophoresis. Agarose was melted in Tris-borate ethylenediamine tetra acetic acid (TBE) buffer (0.45M Tris-borate, 10mM EDTA, pH 8.3) with ethidium bromide added to a final concentration of 0.5μg/mL, and poured into an AGTI submarine gel casting apparatus unit (VWR) to set. A 1% (w/v) agarose solution was used for DNA

fragments ≥ 1kb, and 2% (w/v) for fragments <1kb. The samples had 20% 6x agarose gel loading buffer (50% glycerol, 49.75% TBE, 0.25% bromophenol blue) added. For analytical gels, 1kb or 100bp DNA ladders were loaded into a lane in 1% and 2% gels respectively for sizing and quantification of DNA bands. Gels were run at 60-80V for 30-60 minutes. Analytical gels were visualised with a UV lamp and photographed by a digital camera (Mitsubishi 85mm lens, Thistle Scientific), while preparation gels were visualised with a low intensity UV lamp (230V-50Hz, Ultratec, Ltd.) and desired bands excised from the gel with a sterile scalpel blade.

2.1.7 Gel purification of digested DNA

Digested DNA was separated on a 1% agarose purification gel and purified with the Wizard SV Gel and PCR Cleanup Kit (Promega) according to manufacturer's instructions.

2.1.8 Preparation of plasmid DNA

Small scale plasmid purification was done with the Qiagen Spin Miniprep Kit according to manufacturer's instructions. Large scale purifications were done with the Qiagen Endofree Maxi Kit or the Promega PureYield Midi Prep kit according to manufacturer's instructions.

2.1.9 Preparation of $CaCl_2$-competent E. coli

A 5mL overnight culture of DH5α or BL21/DE3 *E. coli* was grown shaking overnight at 37°C in LB without antibiotics. The next day, 50mL of LB without antibiotics were inoculated with 500μL of preculture and grown shaking at 37°C until A_{600} was 0.3-0.4. Cells were then harvested by centrifugation at 3500*g* for 10 minutes at 4°C. The cell pellet was resuspended in 20mL of chilled sterile 100mM $CaCl_2$ and incubated on ice for 30 minutes-2 hours. The suspension was again centrifuged at

3500*g* for 5 minutes at 4°C and the pellet resuspended in 1mL 100mM $CaCl_2$ for an additional 30 minute incubation on ice. Competent cells were then used for transformation or frozen at -80°C for later use.

2.1.10 Preparation of 'super'-competent E. coli

DH5α *E. coli* were streaked from a glycerol stock onto an LB-Agar plate and grown overnight at 37°C. The following day, 10-12 colonies were picked to inoculate 250mL of SOB medium (2% (w/v) Bacto-tryptone, 0.5% (w/v) Bacto yeast extract, 10mM NaCl, 2.5mM KCl, 10mM $MgCl_2$, 10mM $MgSO_4$), which was the grown at 18°C with shaking until $O.D._{600}$ reached 0.6. The cells were then incubated on ice for 10 minutes before being centrifuged at 2500*g* for 10 minutes at 4°C. The pellet was gently resuspended in 80mL ice-cold TB (10mM PIPES, 15mM $CaCl_2$, 250mM KCl, pH 6.7, 55mM $MnCl_2$, 0.45μm filter sterilised), and aliquots snap frozen and stored in liquid nitrogen. These cells were used for more difficult transformations.

2.1.11 Transformation of competent E. coli

The desired amount of plasmid or ligation was added to a 100-200μL aliquot of competent cells in a 15mL tube, and the mixture was incubated on ice for 30 minutes. Cells were heat-shocked at 42°C for 45 seconds, incubated on ice for a further 2 minutes, then left to shake at 37°C in SOC medium (2% w/v tryptone, 0.5% bacto-yeast extract, 10mM NaCl, 2.5mM KCl, 10mM $MgCl_2$, 10mM $MgSO_4$, 20mM glucose) for 1 hour. Cells were plated onto LB-Agar plates containing the appropriate antibiotic for selection of transformed colonies (100μg/mL ampicillin, 34μg/mL chloramphenicol, 50μg/mL kanamycin) and left to grow upside down overnight at 37°C.

2.2 Cell culture

2.2.1 Cell culture

All plasticware and glass coverslips were from Nunc/VWR. All cells were cultured in T-75 flasks (80cm^3) at 37^{o}C in the presence of 5% CO_2. COS-7 (laboratory stocks) cells were routinely cultured in Dulbecco's modified Eagle medium (DMEM) supplemented with 10% (v/v) foetal calf serum (FCS) (Globepharm), 2mM L-glutamine, 100 units/mL penicillin (pen) and 0.1mg/mL streptomycin (strep). PC12 cells were routinely cultured in DMEM, 10% FCS, 10% horse serum (HS), 1mM L-glutamine, 100 units/mL pen and 0.1mg/mL strep. SK-UT-1 (Cell Lines Service, Eppelheim, Germany) cells were routinely cultured in minimum essential medium (MEM), 10% FCS, 2mM L-glutamate, 100 units/mL pen, 0.1mg/mL strep, 1% (v/v) non-essential amino acids (NEAA), and 1mM sodium pyruvate. Human embryonic kidney (HEK-293) cells (laboratory stocks) were routinely cultured in MEM, 10% FCS, 2mM L-glutamate, 100 units/mL pen, 0.1mg/mL strep and 1% NEAA. Stable cell lines were maintained in their normal medium supplemented with 1mg/mL G-418 sulfate (geneticin) (Melford Laboratories).

2.2.2 Passage of cell lines

Cells were passaged prior to reaching confluence by washing the flask with trypsin-EDTA (0.25% (w/v) trypsin, 0.5mM EDTA in PBS) warmed to 37^{o}C, then incubating the flask in with trypsin-EDTA for the amount of time required to loosen them according to cell type. HEK293 cells were incubated for 30 seconds-2 minutes in the hood and the trypsin-EDTA removed prior to striking the flask to dislodge them. COS-7 cells were incubated for 5 minutes in the hood and struck without

removing the trypsin-EDTA. SK-UT-1 cells were incubated for 2 minutes in the hood, then the trypsin-EDTA was removed and the flask incubated at 37^{o}C for a further 8-10 minutes before being struck. Detached cells were harvested with 15mL medium by pipetting and seeded into flasks or Petri dishes at appropriate seeding densities as required.

2.2.3 Cryogenic storage of mammalian cell lines

Frozen stocks of cells were prepared by treating confluent cells as for passage, but upon harvesting the suspension was pelleted by centrifugation at 2000*g* for 5 minutes at room temperature. The pellet was resuspended in 40% FCS, 50% normal growth medium, and 10% DMSO and 1.5mL aliquots pipetted into cryotubes. Cryotubes were slowly brought to -80^{o}C by placing in a 'Mr. Frosty' cryo 1^{o}C freezing container (Nalgene) in a -80^{o}C freezer for 5-12 hours, then transferred to liquid nitrogen for long-term storage.

2.2.4 Rescue of frozen cell lines

Cell lines were rescued by rapid thawing of the cryotube at 37^{o}C and seeding into a T-75 flask with 15mL usual medium. Medium was then changed 8-24 hours later to remove DMSO.

2.2.5 Transfection of mammalian cells with Lipofectamine Transfection Reagent

Cells were grown to 40-80% confluence, depending on cell type, in a dish, with or without coverslips, of desired size and transfected according to manufacturer's instructions. Optimem medium was prewarmed to 37^{o}C and aliquoted into two sterile tubes. To one tube was added the desired amount of plasmid DNA, and to the other the appropriate amount of Lipofectamine (Invitrogen). The contents were then added together and left to incubate for at least 30 minutes. Meanwhile, the dish was gently

rinsed twice with Optimem to remove all serum, and a final volume of Optimem left on the dish. The contents of the tube were then added on top and the cells were left in usual growth conditions for 5-6 hours before the medium was replaced with normal growth medium. Table 2.1 shows the amounts of all reagents for the various sizes of dishes used in all experiments. Due to the high toxicity and low efficiency of Lipofectamine transfection, its use was discontinued and replaced with GeneJammer.

Dish size (mm)	μg of Lipofectamine	μL of Optimem (each tube)	μg of DNA	mL Optimem (dish)	mL medium after 5-6 hrs
35	4	100	1	0.6	2
60	8	300	2	2.4	6
90/T75	16	800	4	6.4	10

Table 2.1. Reagent volumes for Lipofectamine transfection of different sized dishes.

2.2.6 Transfection of mammalian cells with GeneJammer Transfection Reagent

Cells were grown to 40-80% confluence, depending on cell type, in a dish, with or without coverslips, of desired size and transfected according to manufacturer's instructions. First, the appropriate quantity of Optimem medium was placed in a tube and the appropriate amount of GeneJammer (Stratagene) was added and mixed well. This mixture was left to incubate 5-10 minutes before the desired quantity of plasmid DNA was added and further incubated for 10 minutes. Meanwhile, medium was removed from the dish and replaced with the appropriate amount of fresh normal serum-containing medium and the transfection mixture was added to the dish. After 3-5 hours in usual growth conditions, normal medium was added to the correct final volume. Table 2.2 shows the amounts of all reagents used for the various sizes of dishes used in all experiments.

Dish size (mm)	µL of GeneJammer	µL of Optimem	µg of DNA	mL medium	mL medium after 3 hrs
35	6	100	2	0.9	1
60	15	250	5	2.25	2.5
90/T75	30	750	10	5.75	6.5
150	60	1000	20	10	11

Table 2.2. Reagent volumes for GeneJammer transfection of different sized dishes.

An updated protocol released by Stratagene in 2007 removed the media replacement step and changed the DNA/GeneJammer incubation time to 15-45 minutes. The amounts of DNA and GeneJammer per dish were also reduced as show in table 2.3.

Dish size (mm)	µL of GeneJammer	µL of Optimem	µg of DNA
35	3	100	1
60	6	200	2
90/T75	18	600	6

Table 2.3. Updated reagent volumes, GeneJammer transfection of different sized dishes.

2.2.7 Making stable cell lines

Stable cell lines were made by transfecting four T75 flasks using either the Lipofectamine or GeneJammer protocol as described above. Cells were grown for 48 hours in normal medium, which was then supplemented with 1mg/mL G418-sulfate. The cells were maintained in this medium thereafter.

2.2.8 Fixing cells and immunocytochemistry for fluorescence microscopy

All cell types except PC12 cells were grown on uncoated coverslips in 35mm dishes and transfected as usual. PC12 cells were grown on collagen-coated coverslips. Post-transfection, dishes were washed 3 times in PBS pH 7.4, then fixed in ice-cold paraformaldehyde (PFA; 4% (w/v) in PBS, pH 7.4) for 20 minutes at room temperature or neutral buffered formalin (NBF; 10% (v/v) formalin, 0.4% (w/v)

$NaH_2PO_4 \cdot H_2O$, 0.65% (w/v) Na_2HPO_4) for 10 minutes at room temperature. They were then washed three further times and either mounted directly onto glass slides for fluorescent proteins or used for immunocytochemistry or other labelling. For phalloidin staining of actin cytoskeleton, cells were permeabilised with 0.2% Triton X-100 for 10 minutes and washed three times, then phalloidin tagged with Alexa 568 (Molecular Probes/Invitrogen) was added 1/100 in PBS onto the coverslip and incubated at room temperature in the dark for 15 minutes. For immunocytochemistry, coverslips were incubated for 1 hour at room temperature in the dark in blocking reagent and 0.2% Triton X-100 with primary antibody (anti-FLAG-FITC 1:100 in TBS pH 7.4; anti-FLAG M2 1:100 in 3% BSA; anti-FLAG polyclonal 1:100 in 3% BSA; pAP914[3] 1:100 in 3% BSA; anti-neurofascin 1:2000 in 5% fish skin gelatin PBS). After another 3 washes, coverslips were either mounted directly to glass slides (for primary antibodies with fluorescent tags) or continued for another incubation for 1 hour at room temperature in the dark in blocking reagent with secondary antibody conjugated with fluorescent tag (Alexa 568 goat anti-rabbit 1:1000-1:20,000 in 3% BSA or 5% goat serum; Alexa 568 goat anti-mouse 1:1000-1:10,000 in 3% BSA or 5% goat serum). After the final 3 washes, coverslips were mounted onto glass slides using Mowiol with DAPI.

2.3 Protein assays and Western blot

2.3.1 Large-scale GST fusion protein production

A 5mL culture of BL21/DE3 *E. coli* strain, transformed with pGST-Willin, was grown overnight shaking at 37^{o}C in Luria Broth (LB) supplemented with 100μg/mL ampicillin and 34 μg/mL chloramphenicol. The following morning, 500mL of LB without antibiotics was inoculated with the 5mL overnight culture and

grown shaking at 30°C until absorbance at 600nm (A_{600}) was between 0.5-1. At this point a 1mL sample was taken as a control. Protein production in the remaining culture was induced by addition of 0.2mM isopropyl-β-D-thiogalactopyranoside (IPTG), continuing for three hours shaking at 30°C. A 500μL sample was taken at this point to test for induction. The remaining culture was harvested by centrifugation at 5000*g* for ten minutes at 4°C. The pellet was resuspended in 5mL PBS with 1x Roche protease inhibitor, snap frozen in N_2(l), and stored at -70°C until use. Uninduced and induced samples were centrifuged at 16000*g* for 1 minute and resuspended in 50μL and 100μL of 2x PSB respectively and boiled for SDS-PAGE.

2.3.2 Preparation of glutathione sepharose 4B beads

1.33mL of bead slurry was centrifuged at 2000*g* for 5 minutes and washed three times in 10 mL PBS. The final bead pellet was resuspended in 1mL PBS to make a 50% slurry.

2.3.3 GST protein purification

Frozen pellets were thawed on ice and lysed by sonication in 4 x 30 seconds bursts with 30 seconds rest on ice between bursts. Triton X-100 was added to a final concentration of 1% and the lysate tumbled at room temperature for 30 minutes. The lysate was centrifuged at 12000*g* for 15 minutes at 4°C and the supernatant added to the glutathione sepharose bead slurry. This mixture was tumbled at room temperature for 30 minutes or 4°C for 2 hours. Beads were then washed 4 times with PBS. To elute pure GST proteins, 0.5mL reduced glutathione (GSH) buffer (0.5mL 1M Tris pH8.0, 1mL 0.1M GSH, 8.5mL MQ, 0.1% Triton X-100) was added to the beads and tumbled at room temperature for 10 minutes. Eluate was collected by centrifugation at 1500*g* for 5 minutes. Three further elutions were performed and the eluates pooled.

Samples were concentrated in a 30,000MW Vivaspin column (Sigma) according to the manufacturer's instructions. Protein concentrations were determined by Bradford assay.

2.3.4 Bradford assay

A mixture consisting of 1μL protein sample, 499μL MQ and 500μL Bradford Reagent was made and its absorbance at 595nm measured. Concentration of the sample was determined by comparison with a standard curve created with known concentrations of BSA.

2.3.5 Small-scale GST induction (for positive control samples)

A 5mL overnight was grown as described for large scale GST production. The following morning, 50mL LB supplemented with 100μg/mL ampicillin and 34 μg/mL chloramphenicol was inoculated with 100mL of pre-culture and grown shaking at 37^{o}C until A_{600} reached 0.3-0.4. Several 1mL samples were taken as an uninduced control, and the remaining culture induced by addition of 0.2mM IPTG. Three hours post-induction, 500μL aliquots were taken and all samples centrifuged at 16000*g* for 1 minute. Uninduced samples were resuspended in 50μL of 2x protein sample buffer (PSB; 2% SDS, 20% glycerol, 20mM Tris HCl pH 8.0, 2mM EDTA pH 8.0, 0.1mg/mL bromophenol blue, 2% β-mercaptoethanol) and induced samples in 100μL of 2x PSB, and all were boiled for SDS-PAGE.

2.3.6 Preparation of samples for SDS-PAGE

Mammalian cells were grown in 35, 60 or 90mm dishes and transfected as required for 24-48 hours. For whole cell extracts, dishes were washed 4x with PBS and harvested with 50, 100 or 200μL (respectively) PBS supplemented with PI. For RIPA extraction, dishes were washed 4x with PBS, removed with a cell scraper and

harvested with 50, 100 or 200μL (respectively) of radio-immunoprecipitation assay (RIPA) buffer (50mM Tris HCl pH 7.4, 1% NP-40, 0.25% Na-deoxycholate, 150mM NaCl, 1mM EDTA, 1μg/mL aprotinin, 1μg/mL leupeptin, 1μg/mL pepstatin, Roche protease inhibitor cocktail, 1mM PMSF), then centrifuged for 15 minutes and the supernatant separated from the pellet. An equal amount of 2x PSB was added and samples were boiled as usual for SDS-PAGE.

2.3.7 SDS-PAGE

Unless otherwise stated, samples were diluted in 2X protein sample buffer and boiled for 5-10 minutes. For rat sciatic nerve, hot 2% SDS was added to the nerve, which was then boiled for 15 minutes, then centrifuged at 16000*g* for 5 minutes; the supernatant was removed to a new tube, diluted in 2x protein sample buffer and boiled for an additional 5 minutes. Pre-cast Invitrogen NuPage 3-8% Tris-Acetate were prepared according to manufacturer's instructions with provided Tris-Acetate running buffer. The desired amount of sample was loaded into lanes with SeeBlue Plus2 molecular weight marker. Gels were run at 150V for 1 hour. After a short period of use, it was decided that the separation of proteins between 70-100kDa was not as clear as desired, and thus Tris-Acetate was abandoned and replaced with 4-12% Bis-Tris gels and provided MOPS or MES running buffer. Bis-Tris gels were run at 200V for 1 hour with MOPS or 35 minutes with MES.

2.3.8 Coomassie staining of SDS-PAGE gels

Gels were stained for 10-20 minutes at room temperature in Coomassie stain solution (0.1% (w/v) Coomassie brilliant blue R-250, 45% (v/v) methanol, 10% (v/v) glacial acetic acid). The stain was then removed with multiple changes of destain

solution (10% (v/v) glacial acetic acid, 40% (v/v) methanol) for several hours at room temperature.

2.3.9 Transfer of proteins to nitrocellulose

The Invitrogen NuPage blot module was used to transfer proteins to a nitrocellulose membrane according to manufacturer's instructions with provided transfer buffer supplemented with either 10% methanol for single gel transfer or 20% methanol for double gel transfer. Transfer was completed at 30V for 1-2 hours and verified by staining with Ponceau S solution (0.1% Ponceau S (w/v), 5% acetic acid). Ponceau was washed off with distilled water and Tris-buffered saline (0.05M Tris, 0.138M NaCl, 0.0027M KCl, pH 8.0) with added 0.1% Tween-20 (TBS-T).

2.3.10 Western blotting

Antibody-specific protocols are detailed in appendix 3. In general, membranes were blocked overnight in 5% (w/v) fat-free powdered milk in TBS-T either overnight at 4^{o}C or 2 hours at room temperature. The blot was then washed once in TBS-T and incubated with primary antibody for 1 hour at room temperature in 3% (w/v) fat-free powdered milk in TBS-T. Primary antibody was removed by three 10 minute washes in TBS-T at room temperature. The blot was then incubated with HRP-conjugated secondary antibody (Santa Cruz or Abcam) in 3% milk TBS-T for 1 hour at room temperature and washed three further times as before. All incubations and washes were done with rocking. Bands were visualised with SuperSignal West Pico enhanced chemiluminescence reagent (Pierce) according to the manufacturer's instructions.

2.3.11 Triton X-100 Solubility Assay

Cells were grown on 90mm dishes and transfected as usual. After 24-48 hours they were washed two times with PBS and harvested with 200μL 1% ice-cold Triton X-100 (Triton X-100). They were then incubated on ice for 15 minutes to lyse, and centrifuged at 16,000*g* for 15 minutes at 4^{o}C. The supernatant (S/N) was transferred to another tube and the pellet (P) was resuspended in an additional 200μL 1% ice-cold Triton X-100. Both fractions were mixed with 200μL 2x PSB and boiled for SDS-PAGE.

2.3.12 S100/P100 subcellular fractionation

Cells were washed twice with PBS and harvested by centrifugation at 1500*g* for 5 minutes at 4^{o}C. They were then resuspended in 5mL hypotonic buffer (20mM Tris-HCl, 10mM KCl, 1mM EDTA, 1mM DTT, 1% aprotinin, pH 7.4) with 1mM phenylmethylsulfonyl flouride (PMSF) and incubated on ice for 10 minutes for cells to swell. Cells were gently lysed by 40 strokes in a Dounce homogeniser and equilibrated to 125mM NaCl. The lysate was centrifuged at 1500*g* for 10 minutes at 4^{o}C to remove whole cells and nuclei (P1 fraction), and the supernatant was collected into Beckman Ultraclear centrifuge tubes to be centrifuged in a SW55Ti rotor at 100,000*g* for 30 minutes or 1 hour at 4^{o}C. The supernatant (S100) was incubated with 4 volumes of ice-cold acetone for 45 minutes to precipitate soluble proteins. The pellet was resuspended in 200μL 1% ice-cold Triton X-100 and incubated on ice for 15 minutes, then centrifuged at 16,000*g* for 15 minutes at 4^{o}C. The Triton-soluble supernatant (P100s) was removed and mixed with 200μL 2x PSB, while the Triton-insoluble pellet (P100i) was resuspended in 200μL 1% Triton X-100 and 200μL 2x

PSB. The P1 fraction was also resuspended in 200μL 1% Triton X-100 and 200μL 2x PSB, and all samples were boiled for ten minutes.

2.3.13 Optiprep Density Gradient Fractionation

Optiprep Fractionation for separation of lipid rafts was carried out as described in Stickney et. al., 2004. COS-7 and HEK-293 cells were grown on 35mm dishes and transfected with pWillin-GFP, pMerlin1-GFP, pGFP-Ezrin or pcDNA3 neurofascin155. After 24-48 hours, cells were washed two times with TBS and harvested with 267μL of chilled optibuffer (50mM Tris pH 7.5, 150mM NaCl, 1mM DTT, 1mM PMSF, 1 tablet PI, 1% Triton X-100, 10% sucrose), then left on ice for thirty minutes to lyse. Additional lysis was achieved by freeze-thawing at -20^{o}C. To make the 40% fraction, 533mL of 60% Optiprep (Sigma) was added to the lysate and mixed well in a 5mL Ultraclear centrifuge tube (Beckman). Fractions 35%-20% were made by diluting 60% stock with appropriate amounts of optibuffer, and 800μL of each were overlaid in the centrifuge tube. Samples were centrifuged at 100,000*g* for at least 16 hours at 4^{o}C, forming a continuous gradient that was separated by removing 800μL fractions into 1.5mL Eppendorf tubes. Samples were then prepared as usual for SDS-PAGE and Western blotting. Lipid rafts floated to 20% and 25% fractions.

2.3.14 Actin binding biochem kit protocol

Actin binding experiment was performed as described by the manufacturer (Cytoskeleton). GST-tagged protein was purified and concentrated as described in section 2.3.3 to a concentration of at least 20mM for maximum likelihood of binding. All other reagents were provided in the kit unless otherwise specified. A 250μg aliquot of actin was thawed and resuspended in General Actin Buffer and left on ice

for 30 minutes, at which point 25μL of Actin Polymerisation Buffer was added and the mixture left to incubate at room temperature for 1 hour to make the 23μM F-actin stock. Meanwhile, GST-tagged test protein was centrifuged at 150,000*g* for 1 hour at 24^{o}C and the supernatant kept. 1mL of F-actin buffer was made with 900μL General Actin Buffer and 100μL of Actin Polymerisation Buffer and put on ice. Centrifuge tubes were labelled 1a, 1,2,3 and 4 and the tubes were filled as shown in Table 2.4.

1	40μL F-actin buffer	10μL test protein
2	40μL F-actin stock	"
3	"	8μL F-actin buffer + 1μL α-actinin + 1μL Tris-HCl pH 7.0
4	"	8μL F-actin buffer + 1μL BSA or GST

Table 2.4. Experimental setup for actin binding kit protocol. Tubes 1, 3 and 4 were controls.

These were then incubated at room temperature for 30 minutes. This was followed by a centrifugation at 150,000*g* for 1.5 hours at 24^{o}C. The supernatants were separated and supplemented with user-supplied 10μL 5X PSB; pellets were resuspended in user-supplied 30μL 2X PSB and all samples were prepared for SDS-PAGE as usual. The gel was stained with Coomassie stain and the bands interpreted according to manufacturer's instructions.

2.3.15 Tandem Affinity Purification - Stratagene

HEK-293 cells were grown on a 150mm dish as instructed by the manufacturer to obtain sufficient protein for Western blot analysis. Cells were then transfected with 10μg Willin-CTAP A and left to express for 48 hours. Tandem affinity purification was performed according to the manufacturer's instructions. Test aliquots were taken at various sample points and all samples were boiled in 2X protein sample buffer and used for SDS-PAGE and Western blotting as usual.

2.3.16 Tandem Affinity Purification – pCMV5/TAP

HEK-293 cells were grown on ten 150mm dishes and transfected as usual with 10μg pWillin-FLAG or pFLAG-Ezrin and 10μg of either pCMV5/TAP (NTAP) or pCMV5/TAP-neurofascin155 (NTAPNF). pCMV5/TAP inserts a tandem affinity purification tag to the N-terminus of neurofascin155, and was a kind gift from Professor Ron Hay (University of Dundee). 36 hours post-transfection, dishes were washed twice with PBS and harvested in 10mL PBS by centrifugation at 1500*g* for 5 minutes at 4^{o}C. Cells were resuspended in lysis buffer (50mM Tris-HCl pH 7.4, 150mM NaCl, 1mM EDTA pH 7.4, 1% NP-40, 15% glycerol, 1X protease inhibitor, 1mM PMSF) and tumbled at 4^{o}C for 30 minutes. These were then centrifuged at 14000*g* for 5 minutes at 4^{o}C and the supernatants pooled, with a 250μL aliquot taken as the input sample. 200μL of Rabbit IgG bead slurry was added to the lysate and the mixture tumbled at 4^{o}C for 2 hours, then centrifuged at 2000rpm in a benchtop centrifuge for 1 minute at 4^{o}C. An aliquot was taken of the supernatant before it was discarded and the beads washed 3 times with 10mL TBS pH 7.4 0.05% Tween, then twice more with 500μL TEV cleavage buffer (10mM Tris-HCl pH 8.0, 150mM NaCl, 0.1% NP-40, 0.5mM EDTA pH 8.0, 1mM DTT) and the mixture was moved to a 1.5mL tube. After another spin, beads were resuspended in 200μL TEV cleavage buffer with 5μL TEV protease (Invitrogen) and tumbled overnight at 4^{o}C.
The following day, the tube was centrifuged at 2000rpm for 1 minute at 4^{o}C and the supernatant kept, and a second elution with 200μL TEV cleavage buffer done. Supernatants were kept both times and an aliquot taken, and 0.6μL of 1M $CaCl_2$ per 200μL of supernatant was added. Meanwhile, 40μL of calmodulin resin slurry was aliquoted and washed twice with 1mL calmodulin binding buffer (CBB: 10mM β-mercaptoethanol, 10mM Tris-HCl pH 8.0, 150mM NaCl, 1mM Mg-acetate, 1mM

imidazole, 2mM $CaCl_2$, 0.1% NP-40) and resuspended in 20μL CBB. 3 volumes of CBB were added to the TEV-cleaved supernatant, the mixture was added to the calmodulin resin, and tumbled at 4°C for 2 hours. This was then centrifuged at 2000rpm for 2 minutes at 4°C and the supernatant discarded. Beads were washed 5 times with 1mL CBB. Purified proteins were eluted 4 times with 50mL calmodulin elution buffer (CEB: 10mM β-mercaptoethanol, 10mM Tris-HCl pH 8.0, 150mM NaCl, 1mM Mg-acetate, 1mM imidazole, 2mM EGTA, 0.1% NP-40), then 1 time with Extra buffer (50mM Tris-HCl pH 8.0, 2mM EGTA, 1M NaCl), centrifuging at 14000*g* for 10 seconds each time. To ensure all proteins were accounted for, the calmodulin beads were then boiled for 5 minutes in PSB and centrifuged at maximum speed for 15 seconds, with the supernatant containing any protein that may have remained bound to the beads. All samples were prepared for SDS-PAGE and Western blot as usual. A shortened protocol was also used which stopped after TEV protease cleavage, and the rabbit IgG beads were boiled instead of the calmodulin beads; this protocol was used to minimise protein loss caused by the second purification step.

2.3.17 GST Pulldown

HEK-293 cells were cultured on two 90mm dishes and transfected with pcDNA3 neurofascin155 for 48 hours, then washed twice with PBS and harvested with 500mL RIPA extraction buffer. The cells were then sonicated 4 x 30 seconds. Glutathione sepharose 4B beads were separated into two 37.5μL aliquots and one 75μL aliquot and washed 3 times with RIPA extraction buffer. The cell lysate was added to the 75mL aliquot as a pre-clearing step, and 10μg of purified GST were added to one 37.5μL aliquot while 10μg of purified GST-Willin were added to the

other, and 250μL of RIPA were added to both. All three aliquots were rotated overnight at 4°C. The following day, the cell lysate fraction was centrifuged at 16000*g* for 20 seconds, leaving a cleared cell lysate, from which an input sample was taken before being split into 2 x 250μL aliquots. The GST- and GST-Willin-conjugated beads were centrifuged at 2000rpm for 1 minute and one 250μL aliquot of the cleared lysate was added to each tube of beads. These were then rotated for 2 hours at 4°C and centrifuged at 2000rpm for 1 minute. The beads were washed 5 times with 50μL RIPA and 5 times with 50μL PBS, then boiled in 2X PSB and centrifuged at maximum speed for 1 minute. The supernatant was kept as the final sample. Input and final samples were prepared for SDS-PAGE and Western blotting as usual.

2.3.18 Immunoprecipiation with monoclonal FLAG antibody and protein A

FLAG immunoprecipitation was carried out as described in Crawford et al.(2005). HEK-293 cells were grown on 90mm dishes and co-transfected with pcDNA3 neurofascin155 and either pWillin-FLAG or empty FLAG vector. After 2 PBS washes, cells were harvested in 1mL IP buffer (50mM NaF, 50mM Tris-HCl, 150mM NaCl, 1mM NaPPi, 1mM EDTA, 1mM EGTA, pH 6.8; 1mM DTT and protease inhibitors added just before use) and sonicated 3 X 20 seconds. FLAG M2 monoclonal antibody (Sigma) was conjugated with Protein A from *Staphylococcus aureus* immobilised on polyacrylic beads and tumbled with 500μL IP buffer and 100-200μL whole cell lysate at room temperature for 2 hours. The beads were then washed 3 times in IP buffer brought up to 1M NaCl and centrifuged at 16,000*g* for 45 seconds after each wash, and again 3 times in normal IP buffer; with all washes, the pellet was not disturbed. The entire bead-protein complex was then resuspended in a

loading volume of IP buffer and protein sample buffer and heated at 70°C for 10 minutes, then loaded as usual for Western blotting.

2.4 Yeast two-hybrid

2.4.1 Media for yeast growth

Untransfected Y190 were grown in YPAD 1% (w/v) yeast extract (Difco), 2% (w/v) peptone (Difco), 2% (w/v) glucose, 0.01% (w/v) adenine hemisulfate) medium or YPAD agar plates. Transfected Y190 were grown in omission liquid medium (0.67% (w/v) Yeast nitrogen base without amino acids (Difco), 2% (w/v) glucose, 0.067% synthetic dropout mix) or omission medium agar plates. Synthetic dropout mix included all of the following amino acids excluding the amino acid(s) being selected for: 2.0g adenine hemisulfate, 2.0g arginine-HCl, 2.0g histidine-HCl, 2.0g isoleucine, 4.0g leucine, 2.0g lysine-HCl, 2.0g methionine, 3.0g phenylalanine, 2.0g serine, 2.0g threonine, 3.0g tryptophan, 2.0g tyrosine, 1.2g uracil and 9.0g valine. Glycerol stocks of Y190 were prepared from overnight cultures of Y190 grown in YPAD. 600µL of culture was mixed with 400µL of 50% sterile glycerol and stored at -70°C.

2.4.2 LiAc transformation

The lithium acetate/single-stranded carrier DNA/polyethylene glycol (LiAc/ssDNA/PEG) transformation protocol developed by the Gietz laboratory (Agatep et al, 1998) was used to transform Y190. A YPAD plate was streaked with the Y190 glycerol stock and grown for 2-3 days at 30°C. From this plate, 3-4 colonies were used to inoculate 5mL of YPAD liquid medium, grown overnight at 30°C with shaking. The following morning, 2.5 x 10^8 cells were inoculated into 50mL YPAD

medium and grown to a titre of 2 x 10^7 cells per mL. They were then harvested by centrifugation at 3000*g* for 5 minutes at room temperature. They were washed in 25mL sterile distilled water and centrifuged again. Cells were now resuspended in 1mL 0.1M LiAc and moved to a 1.5mL microcentrifuge tube, where it was centrifuged again at maximum speed for 15 seconds. The pellet was again resuspended in 400µL 0.1M LiAc and divided into the required number of 50µL aliquots in fresh 1.5mL tubes. Aliquots were centrifuged again at maximum speed for 15 seconds and resuspended by vortexing for ~1 minute in transformation mix added in the following order: 240µL PEG (50% polyethylene glycol 3350, filter sterilised), 36µL 1M LiAc, 50µL (10µg) ssDNA, sterile distilled water, pAS2-1 bait (1µg) and pACT2 contruct (1µg). This mixture was incubated at 30^{o}C for 30 minutes, then heat shocked in a water bath at 42^{o}C for 30 minutes and pelleted at 7000*g* and gently resuspended in 1mL sterile distilled water. 200µL of cell suspension was plated onto an omission plate lacking tryptophan and leucine (Trp^-Leu^-) and grown at 30^{o}C for 3-4 days.

The overnight culture was also used to prepare a Y190 glycerol stock. This was made with 600µL of culture and 400µL of sterile 50% glycerol and stored at -70^{o}C.

2.4.3 Filter lift assay

Positive interaction between proteins was tested for by β-galactosidase activity as described by Parchaliuk (1999). Sterile 7.5cm diameter Whatman grade 1 paper was soaked in a solution of 10mL Z buffer (60mM $Na_2HPO_4 \cdot 7H_2O$, 40mM $NaH_2PO_4 \cdot H_2O$, 10mM KCl, 1mM $MgSO_4 \cdot 7H_2O$, pH 7.0), 0.5mL of 20mg/mL 5-bromo-4-chloro-3-indolyl-D-galactopyranoside (X-gal) in N,N-dimethylformamide

(DMF) and 27μL β-mercaptoethanol, and placed into an 8cm diameter Petri dish. Clean, dry filter paper was placed over the surface of the colonies growing on Trp^- Leu^- plates to transfer the colonies onto the filter paper, which was then placed in liquid nitrogen. After the paper was completely frozen, it was removed and allowed to thaw at room temperature. Freeze-thaw was repeated and the defrosted paper placed on top of the wetted filter paper in the Petri dish. The dishes were then incubated at 37^{o}C for up to 6 hours, checked at 30 minutes, 1 hour, then each subsequent hour up to 6 hours for colour change, and overnight at room temperature in the dark. To be consistent with previous studies in the laboratory (Davey et al, 2005), filter lift assays of β-galactosidase activity were scored semi-quantitatively by the time taken for the development of blue colonies: ++++, <30 min; +++, 30–60 min; ++, 1–2 h, +, 2–6 h, – > 6 h.

CHAPTER 3: CHARACTERISATION OF NOVEL ANTIBODIES TO WILLIN

Chapter 3: Characterisation of novel antibodies to Willin

3.1 Introduction

Biochemical studies of proteins require specific, high quality antibodies to the protein of interest for detection of native protein expression and to avoid the use of tags that may confound data. Prior to this project, a polyclonal rabbit antibody had been produced to the peptide sequence KEASKGIDQFGPPMIIH, which is found in the N-terminal FERM domain of Willin (residues 86-102, see appendix I), and was characterised as discussed by Brannigan (Ph.D. thesis, 2006). This antibody, called '914^{3}', was affinity purified and, due to cross-reactivity with Bovine Serum Albumin (BSA), also 'panned' against BSA-coupled sepharose beads (Brannigan, 2006). The purified antibody, termed 'pAP914^{3}', detected expressed Willin reasonably well, results were mixed when attempting to detect native Willin. The primary problem was the appearance of multiple bands, even when BSA contamination had been eliminated; it could not be determined if these bands were different isoforms of Willin, breakdown products or non-specific binding. Furthermore, peptide competition assays, whereby the antibody was pre-incubated with the peptide to which it was raised in order to determine band specificity, gave mixed results as well.

Therefore it was deemed necessary to develop and purify a better antibody to use in future studies. In this chapter I describe three attempts that were made to identify such an antibody. Additionally, in the course of my studies a second isoform of the Willin protein was predicted (See section 4.7), and the relationship of the peptide sequences for each antibody to this isoform is discussed.

3.2 Characterisation of a custom-made polyclonal chicken antibody

Two polyclonal antibodies were raised in two separate chickens by the company Davids Biotechnologie (Regensburg, Germany) The two chicken antibodies, termed 'Hen1' and 'Hen2', were raised against the extreme C-terminal peptide of Willin (residues 598-614): KYFSLDLTHDEVPEFVV. This peptide is present in both isoforms of Willin, in both human and mouse (see appendix 1). Antibodies from the two different hens were provided in both pre- and post-affinity purified forms by the company (Hen1 and APHen1 or Hen2 and APHen2).

Initial studies focused on developing the best blotting conditions for these antibodies; this involved varying concentrations of the antibodies as well as different blocking conditions. In most of these studies the source of Willin to be tested was from whole cell extracts of *E. coli* bacteria BL21/DE3 pGST-Willin (see section 2.3.5) either before ('uninduced') or after ('induced') IPTG treatment to induce expression of a GST-Willin chimeric protein; this protein is ~100kDa in size. SDS-PAGE and transfer were performed as described in sections 2.3.7 and 2.3.9.

The initial conditions used for Western blotting were based on previous results for 914[3] (Brannigan, 2006) and are as follows: overnight blocking in 5% milk in PBS at 4^{o}C with rocking, followed by washes and antibody incubation in a 0.2% porcine gelatin 0.1% Tween-20 PBS solution. Primary and secondary antibodies were incubated at room temperature for one hour, with three ten-minute washes in between using the same buffer as for antibody incubation. Varying concentrations of antibody from both hens, standard and affinity purified versions, were attempted. The following figures are examples of the Western blots that were performed, with arrows indicating the bands presumed to be expressed Willin protein.

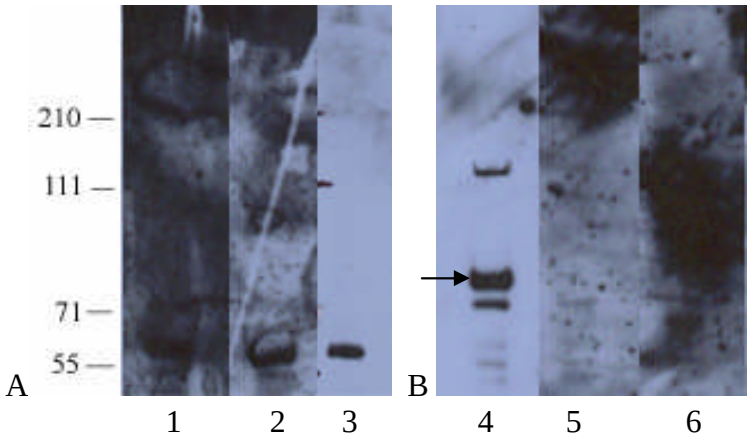

Figure 3.1. **A**) Whole cell extract from IPTG induced BL21/DE3 pGST-Willin cells was separated on a 3-8% Tris-Acetate SDS-PAGE gel. The subsequent nitrocellulose membrane was probed with Hen1 at concentrations of 1:500 (Lane 1), 1:1000 (Lane 2) and 1:2000 (Lane 3). The secondary anti-chicken-HRP antibody (Sigma, UK) was used at a concentration of 1:2000. To the left are shown the Molecular weights (kDa). **B**) Whole cell extract from IPTG induced BL21/DE3 pGST-Willin cells was separated on a 3-8% Tris-Acetate SDS-PAGE gel. The subsequent nitrocellulose membrane was probed with pAP914[3] 1:1000 and secondary anti-rabbit-HRP 1:5000 (Uptate) (Lane 4); AP Hen1 1:1000 and secondary anti-chicken-HRP 1:5000 (Sigma) (Lane 6); APHen1 1:2000 and secondary anti-chicken-HRP 1:5000 (Sigma) (Lane 6).

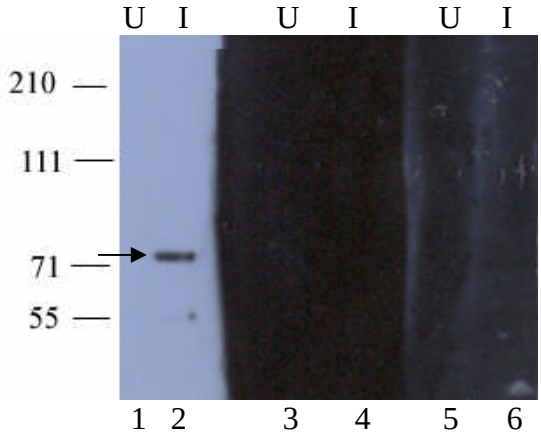

Figure 3.2. Whole cell extract from uninduced (U) IPTG induced (I) BL21/DE3 pGST-Willin cells were separated on a 3-8% Tris-Acetate SDS-PAGE gel. The subsequent nitrocellulose membrane was probed with pAP914[3] 1:1000 and secondary anti-rabbit-HRP 1:5000 (Uptate) (Lanes 1 and 2); Hen2 1:1000 and secondary anti-chicken-HRP 1:5000 (Sigma) (Lanes 3 and 4); APHen2 1:1000 and secondary anti-chicken-HRP 1:5000 (Sigma) (Lanes 5 and 6). To the left are shown the Molecular weights (kDa).

These preliminary experiments showed that the blocking method previously used for 914[3] was not successful in blocking background staining and non-specific binding with the chicken antibodies. Changing the overnight blocking to 3% BSA

improved the blot quality for very short exposures as seen in figure 3.3, but exposures longer than 30 seconds began to show background. APHen2 was also observed to have a binding profile similar to pAP914[3].

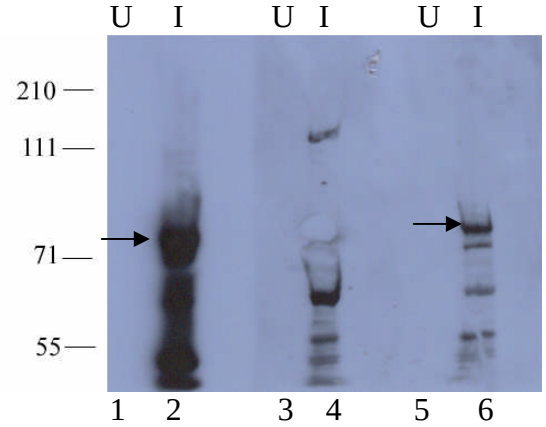

Figure 3.3. Whole cell extracts from uninduced (U) and IPTG induced (I) BL21/DE3 pGST-Willin cells were separated on a 3-8% Tris-Acetate SDS-PAGE gel. The subsequent nitrocellulose membrane was probed with either pAP914[3] 1:1000 and secondary anti-rabbit-HRP 1:5000 (Upstate) (Lanes 1 and 2); Hen2 1:1000 and secondary anti-chicken-HRP 1:5000 (Sigma) (Lanes 3 and 4); Hen2AP 1:1000 and secondary anti-chicken-HRP 1:5000 (Sigma) (Lanes 5 and 6). To the left are shown the Molecular weights (kDa). Arrows indicate presumed GST-Willin bands.

As a means of trying to improve this further, an internet search was performed to determine whether a particular blocking reagent was considered optimal for use with chicken IgY antibodies. Aves Labs, a company that produces chicken antibodies, advocates their cold-water fish skin gelatin (FSG) blocking buffer, 'BlokHen', as ideal for chicken antibodies and is featured in the protocol at url: http://www.aveslab.com/commerce/misc/protocols.jsp;jsessionid=C3F791817B28CEF00F72F849D10C727D?czuid=1179848967757. As the concentration of FSG in BlokHen is not given, initial concentrations were chosen as 0.6% (w/v) FSG in PBS overnight (4^{o}C) and 0.2% FSG in PBS 0.1% Tween-20 for antibody incubations based on the concentration of porcine gelatin already being used for this protocol. At this time the gels used were changed from 3-8% Tris-Acetate to 4-12% Bis-Tris gels in

order to get better separation at ~70kDa and ~100kDa. Figure 3.4 shows the result of the FSG protocol.

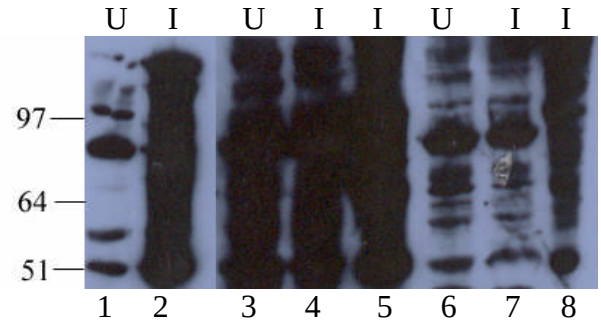

Figure 3.4. Whole cell extract from uninduced (U) and IPTG induced (I) BL21/DE3 pGST-Willin cells were separated on a 4-12% Bis-Tris SDS-PAGE gel. The subsequent nitrocellulose membrane was probed with pAP914[3] 1:1000 and secondary anti-rabbit-HRP 1:5000 (Uptate) (Lanes 1 and 2); Hen1 1:1000 and secondary anti-chicken-HRP 1:5000 (Sigma) (Lanes 3-5); Hen2 1:1000 and secondary anti-chicken-HRP 1:5000 (Sigma) (Lanes 6-8). To the left are shown the Molecular weights (kDa).

Background was reduced but a high number of non-specific bands appeared. It was presumed that the concentration of FSG in the overnight block was too low; therefore different conditions of initial blocking with FSG were tried, with two different concentrations at both room temperature for 2.5 hours and overnight at 4^{o}C, as shown in Figure 3.5. Antibody incubations continued to be in 0.2% FSG. Increased FSG concentration in the initial block was not sufficient to overcome the appearance of non-specific bands in either the room temperature (Figure 3.5) or overnight (data not shown) blocks.

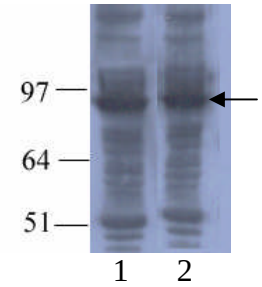

Figure 3.5. Whole cell extract from IPTG induced BL21/DE3 pGST-Willin cells was separated on a 4-12% Bis-Tris SDS-PAGE gel. The subsequent nitrocellulose membrane was probed with Hen1 1:1000 and secondary anti-chicken-HRP 1:5000 (Sigma). Lane 1 was blocked with 1% FSG at room temperature for 2.5 hours and Lane 2 was blocked with 2% FSG for 2.5 hours. To the left are shown the Molecular weights (kDa). Arrow indicates presumed GST-Willin band.

As FSG still did not provide the desired result, 5% milk was again used for blocking overnight, with 0.2% FSG still used during antibody incubation. In addition, the concentration of primary antibody was reduced from 1:1000 to 1:2000 in the hope of reducing non-specific binding. This method proved more successful, with fewer bands appearing as shown in Figure 3.6. Unfortunately, the non-affinity purified chicken antibodies did not appear to detect the induced GST-Willin as the pAP914[3] control did.

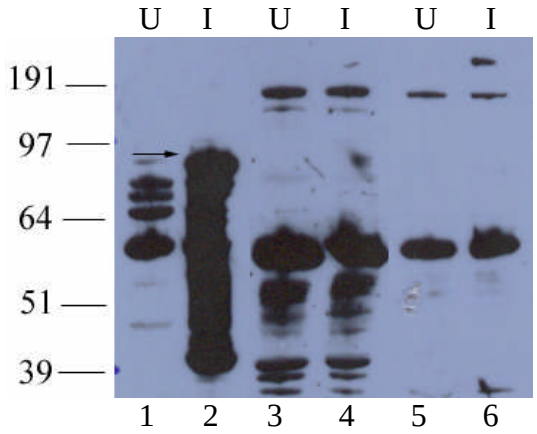

Figure 3.6. Whole cell extract from uninduced (U) and IPTG induced (I) BL21/DE3 pGST-Willin cells were separated on a 4-12% Bis-Tris SDS-PAGE gel. The subsequent nitrocellulose membrane was probed with pAP914[3] 1:1000 and secondary anti-rabbit-HRP 1:5000 (Upstate) (Lanes 1 and 2); Hen1 1:2000 and secondary anti-chicken-HRP 1:5000 (Sigma) (Lanes 3 and 4); Hen2 1:2000 and secondary anti-chicken-HRP 1:5000 (Sigma) (Lanes 5 and 6). To the left are shown the Molecular weights (kDa). Arrow indicates presumed GST-Willin band.

APHen1 and APHen2 were then tested under the same blocking conditions, and APHen2 did detect a band of the same size to that detected by pAP914[3] (Figure 3.7).

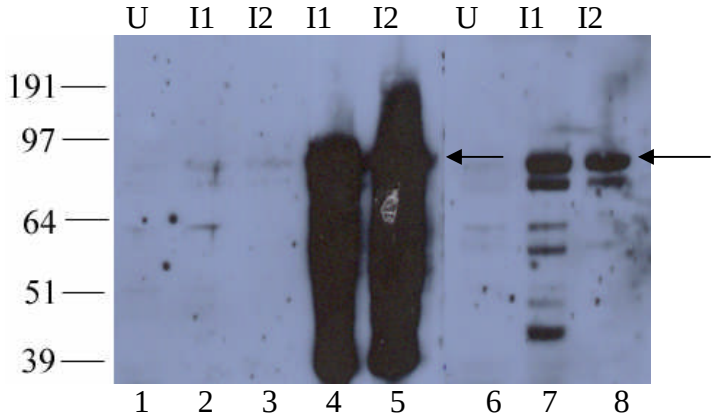

Figure 3.7. Whole cell extract from uninduced (U) and IPTG induced (I) BL21/DE3 pGST-Willin cells were separated on a 4-12% Bis-Tris SDS-PAGE gel. The subsequent nitrocellulose membrane was probed with APHen1 1:1000 and secondary anti-chicken-HRP 1:5000 (Sigma) (Lanes 1-3); pAP914[3] 1:1000 and secondary anti-rabbit-HRP 1:5000 (Upstate) (Lanes 4 and 5); APHen2 1:1000 and secondary anti-chicken-HRP 1:5000 (Sigma) (Lanes 6-8). To the left are shown the Molecular weights (kDa). Arrows indicate presumed GST-Willin bands.

With a positive result thus obtained, a whole cell extract of COS-7 cells was separated on a gel. It is not known for certain whether COS-7 cells express Willin, but it was desirable to see what band profile the antibody would show. A band of approximately 70kDa was expected. It was also necessary to verify that APHen2 would not cross-react with BSA as 914[3] had done, so a high concentration (>5μg) of BSA was also loaded on this gel to test for cross-reactivity; whole cell extract from IPTG induced BL21/DE3 pGST-Willin cells was used as a positive control. APHen2 dilution was kept at 1:1000, but secondary antibody concentration was reduced to 1:10,000 in an attempt to reduce non-specific bands. APHen2 still detected GST-Willin and did not detect BSA, but unfortunately it detected many bands in the COS-7 samples (Figure 3.8).

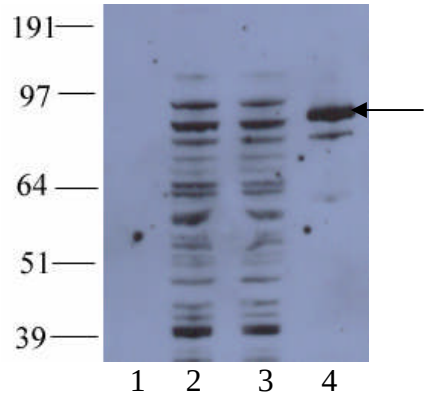

Figure 3.8. BSA (Lane 1), COS-7 whole cell extract (Lanes 2 and 3) and whole cell extract from IPTG induced BL21/DE3 pGST-Willin cells (Lane 4) were separated on a 4-12% Bis-Tris SDS-PAGE gel. The subsequent nitrocellulose membrane was probed with APHen2 1:1000 and secondary anti-chicken-HRP 1:10,000. To the left are shown the Molecular weights (kDa). Arrow indicates presumed GST-Willin band.

Despite the low concentration of anti-chicken-HRP, it was possible that secondary antibody was causing the non-specific bands in Figure 3.8, so another secondary antibody (Davids Biotechnologie) was compared with the original one (Sigma), and different concentrations were tried as well. Against COS-7 cells neither gave satisfactory results at previously established concentrations; furthermore, both antibodies, but especially Sigma, gave some background when tested with no primary antibody (Figure 3.9).

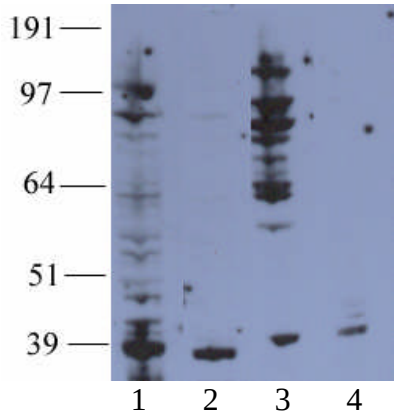

Figure 3.9. COS-7 whole cell extract was separated on a 4-12% Bis-Tris gel and the subsequent nitrocellulose membrane was probed with APHen2 1:1000 and secondary anti-chicken-HRP (Davids) 1:2000 (Lane 1); APHen2 1:1000 and secondary anti-chicken-HRP (Davids) 1:5000 (Lane 2); secondary anti-chicken-HRP (Sigma) 1:5000 only (Lane 3); and secondary anti-chicken-HRP (Davids) 1:2000 only (Lane 4). To the left are shown the Molecular weights (kDa).

Concentrations of secondary antibody were reduced and tested against whole cell extract from IPTG induced BL21/DE3 pGST-Willin cells. Here both versions were satisfactory and similar, with Davids being slightly weaker (Figure 3.10). It was decided to keep using the Sigma secondary anti-chicken-HRP.

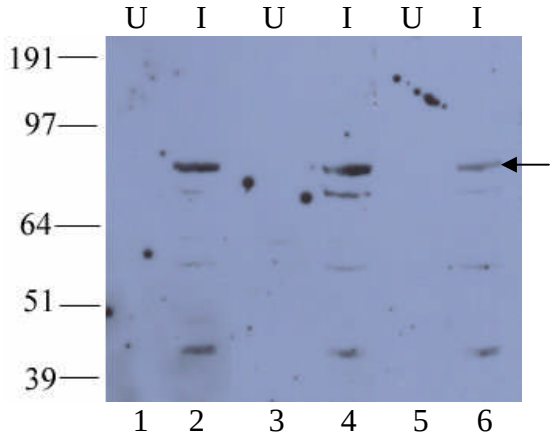

Figure 3.10. Whole cell extract from uninduced (U) and IPTG induced (I) BL21/DE3 pGST-Willin cells were separated on a 4-12% Bis-Tris SDS-PAGE gel. The subsequent nitrocellulose membrane was probed with APHen2 1:1000 and secondary anti-chicken-HRP (Sigma) 1:10,000 (Lanes 1 and 2); APHen2 1:1000 and secondary anti-chicken-HRP (Sigma) 1:20,000 (Lanes 3 and 4); and APHen2 1:1000 and secondary anti-chicken-HRP (Davids) 1:10,000 (Lanes 5 and 6). To the left are shown the Molecular weights (kDa). Arrow indicates presumed GST-Willin band.

After several further attempts and inconsistent Western blotting results, the blocking method was changed once again on the advice of Dr. Fleur Davey. As described in section 2.3.10, membranes were blocked overnight in 5% milk TBS 0.5% Tween, and antibody incubations were in 3% milk TBS 0.1% Tween (TBS-T), with washes between antibodies using TBS-T. The APHen2 antibody was tested with this method as well, as shown in Figure 3.11. This blocking method produced the most consistently clean results and was subsequently used as standard for all Western blotting with APHen2. Whole cell extract from IPTG induced BL21/DE3 pGST-Willin cells was used as a positive control, and homogenised sciatic nerve from one adult rat was loaded to test for native expression. As the nerves were extracted in hot

2% SDS and loaded directly onto the gel as a whole cell extract, no quantitation of protein amounts was done, but Ponceau staining showed that protein was present in abundance in the sample.

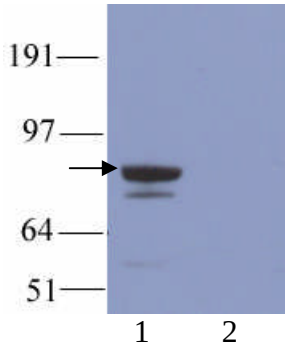

Figure 3.11. Whole cell extract from IPTG induced BL21/DE3 pGST-Willin cells (Lane 1) and homogenised sciatic nerve from one rat (Lane 2) were separated on a 4-12% Bis-Tris gel. The subsequent nitrocellulose membrane was probed with APHen2 1:750 and secondary anti-chicken-HRP 1:10,000. To the left are shown the Molecular weights (kDa). Arrow indicates presumed GST-Willin band.

Unfortunately, there were problems with sample preparation and loading due to the high myelin content of the nerve, so the lack of bands in this lane was not thought to be indicative of the ability of APHen2 to bind native Willin, nor of the presence of Willin in rat sciatic nerve.

An attempt was then made to detect native Willin in HEK-293 cells; again it was not known whether these cells expressed Willin, but as these are human cells it was thought to be more likely to have a matching sequence to the APHen2 epitope. As with the COS-7 samples, many bands (indicated by arrows) appeared as seen in Figure 3.12.

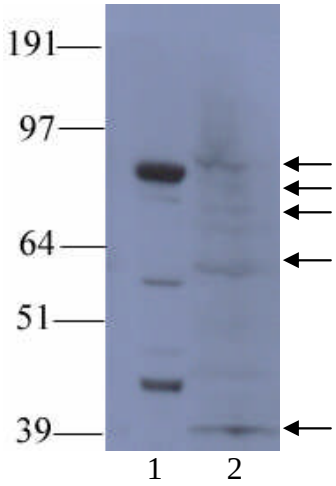

Figure 3.12. Whole cell extract from IPTG induced BL21/DE3 pGST-Willin cells (Lane 1) and HEK-293 whole cell extract (Lane 2) were separated on a 4-12% Bis-Tris gel. The subsequent nitrocellulose membrane was probed with APHen2 1:750 and secondary anti-chicken-HRP 1:10,000. To the left are shown the Molecular weights (kDa).

Because of the large number of bands, it was difficult to determine if APHen2 was detecting native Willin. To determine which, if any, bands were specific to the epitope against which APHen2 had been raised, a peptide blocking experiment was performed. 100μg/mL of the pure peptide were incubated with APHen2 about 2 hours at room temperature. Antibodies were incubated in TBS-T only to avoid milk interference with the peptide. Figure 3.13 shows that, while the peptide blocking was apparently successful for whole cell extract from IPTG induced BL21/DE3 pGST-Willin cells, no blocking appeared to occur for the HEK-293 whole cell extract.

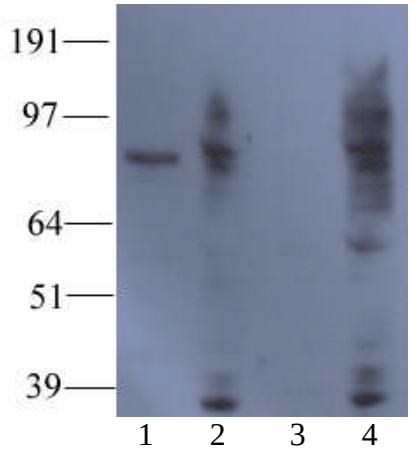

Figure 3.13. Whole cell extract from IPTG induced BL21/DE3 pGST-Willin cells (Lanes 1 and 3) and HEK-293 whole cell extract (Lanes 2 and 4) were separated on a 4-12% Bis-Tris gel. The subsequent nitrocellulose membranes were probed with either APHen2 1:1000 secondary anti-chicken-HRP (Sigma) 1:10,000 (Lanes 1 and 2); or APHen2 1:1000 + 100μg/mL peptide and secondary anti-chicken-HRP 1:10,000 (Lanes 3 and 4). To the left are shown the Molecular weights (kDa).

During the course of these investigations, a 622 amino acid isoform of Willin was found which could not be detected by 914[3] due to the insertion of an octapeptide in the same sequence to which 914[3] was made. However, the epitope to which APHen2 was made is present in the longer isoform, and thus may be detectable by this antibody. A human clone of this isoform was not available, so a highly-conserved mouse version was obtained from the IMAGE consortium and tagged with GFP (see section 4.7). Unfortunately, the antibody was unable to detect the GFP-tagged version of this protein (Figure 3.14A). It is not yet known why this occurs, though there may be a problem with the GFP tag, which is directly adjacent to the APHen2 epitope.

Figure 3.14. Whole cell extract from IPTG induced BL21/DE3 pGST-Willin cells (Lane 1) and whole cell extract from HEK-293 cells either untransfected (Lanes 2 and 4) or transfected with mouse Willin-GFP (Lanes 3 and 5) were separated on a 4-12% Bis-Tris gel. The subsequent nitrocellulose membrane was probed with APHen2 1:1000 and secondary anti-chicken HRP1:5000 (Lanes 1-3) or anti-GFP 1:1000 and secondary anti-mouse HRP 1:5000 (Lanes 4 and 5).

3.3 Characterisation of the custom-made polyclonal rabbit antibody αWR1 & 2

The chicken antibody was found to be too inconsistent and unable to detect native protein with any certainty; therefore another custom antibody was produced. Two polyclonal antibodies were raised in two separate rabbits by the company Genovac (Freiburg, Germany), using the same peptide sequence as the more-successful 914[3]: KEASKGIDQFGPPMIIH. Antibodies from the two different rabbits were provided in both pre- and post-affinity purified forms by the company, but because they were more likely to yield clean results, only the affinity purified versions were tested. These were called αWR1 and αWR2. Initial concentrations were as recommended by the manufacturer.

Because 914[3], the previous antibody with this sequence, cross-reacted with BSA and thus required panning before use, it was first desirable to test the new antibody for the same reactivity. Whole cell extract from uninduced (U) and IPTG induced (I) BL21/DE3 pGST-Willin cells and 5μg of BSA were separated on a gel; pAP914[3] was used as a positive control for GST-Willin expression. Blocking and antibody incubations were used as for APHen2; the membrane was first blocked overnight in 5% milk TBS 0.5% TWEEN-20, and antibody incubations were done in

3% milk TBS 0.1% TWEEN-20 (TBS-T), with three TBS-T washes after each antibody incubation. Figure 3.16 indicates that neither antibody was detecting BSA, but both did detect the proteins which had been induced in the bacteria. This confirmed that the αWR antibodies did not cross-react with BSA, and therefore did not need to be panned. The pAP914[3] lanes give the expected result; however, αWR1 and 2 seem to detect a band in the uninduced samples (figure 3.15). However, the signal is very strong in the induced sample, so it is likely that the aWR antibodies are detecting GST-Willin expressed prior to induction; this occurs in pGEX expression systems because lac promoter expression is known to be leaky (Krebber et al., 1996).

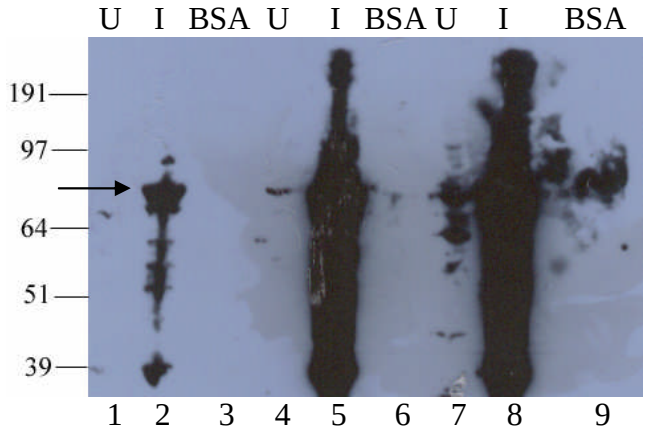

Figure 3.15. Whole cell extract from uninduced (U) and IPTG induced (I) BL21/DE3 pGST-Willin cells and BSA were separated on a 4-12% Bis-Tris gel. The subsequent nitrocellulose membrane was probed with pAP914[3] 1:1000 and secondary anti-rabbit-HRP 1:5000 (Lanes 1-3); αWR1 1:1000 and secondary anti-rabbit-HRP 1:5000 (Lanes 4-6); and αWR2 1:2000 secondary anti-rabbit-HRP 1:5000 (Lanes 7-9). To the left are shown the Molecular weights (kDa). Arrow indicates presumed GST-Willin band.

This showed that the αWR antibodies were capable of giving a signal; therefore mammalian cell lines were used for further characterisation. COS-7 cells were either untransfected or transfected with Willin-GFP and extracted using a RIPA extraction buffer (see section 2.3.6). Both whole cell extracts and separated supernatant and pellet fractions were separated on a gel and the membrane probed as described in Figure 3.17. A brief exposure (10 seconds) indicated a distinct band of

about 70kDa in the transfected whole cell extract samples probed by αWR1 and 2 (Figure 3.16A); because of its exclusive presence in the transfected lane, it was thought that this could be a breakdown product of Willin-GFP, as without the GFP tag Willin would be about 70kDa. However, a slightly longer exposure time (30 seconds) showed high non-specific binding, making it difficult to analyse whether Willin-GFP expression, confirmed by anti-GFP in lane 2, was detected by αWR1 and 2 in the transfected samples (Figure 3.16B).

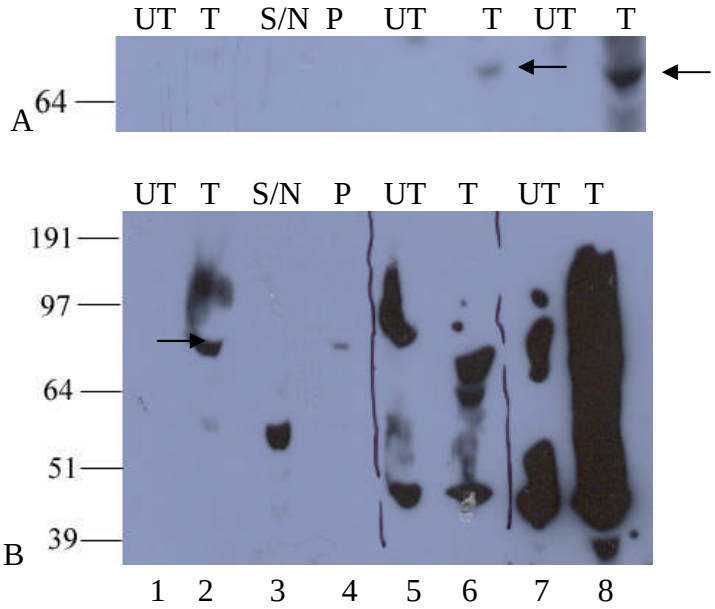

Figure 3.16. Whole cell extracts of RIPA-extracted COS-7 cells, both untransfected (UT) and transfected with Willin-GFP (T), were taken prior to separation of supernatant (S/N) and pellet (P). Samples were separated on a 4-12% Bis-Tris gel as shown. The subsequent nitrocellulose membrane was probed with anti-GFP 1:1000 and secondary anti-mouse-HRP 1:5000 (Lanes 1-4); αWR1 1:200 and secondary anti-rabbit-HRP 1:2000 (Lanes 5 and 6); or αWR2 1:200 and secondary anti-rabbit-HRP 1:2000. A) Exposure time of 10 seconds yields a potential band of correct size, as indicated by the yellow arrow. B) Exposure time of 30 seconds; the yellow arrow indicates the Willin-GFP band. To the left are shown the Molecular weights (kDa).

This result was still not satisfactory, so another attempt was made, this time using HEK-293 cells instead of COS-7 cells. Both untransfected and Willin-GFP-transfected HEK-293 whole cell extracts were separated on a gel. As shown in figure 3.17, a band matching that detected by anti-GFP was weakly detected by both αWR1

and 2. αWR2 also detected a band of ~70kDa as in figure 3.16, while αWR1 detected a higher band of unknown origin. In addition, a portion of the blot was probed with secondary anti-rabbit-HRP only to ensure that bands were due to primary antibodies only.

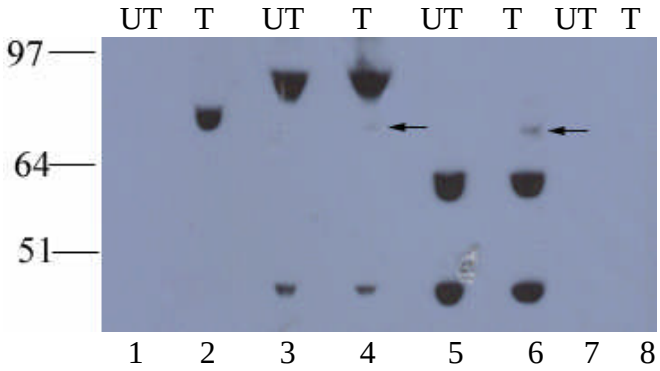

Figure 3.17. Untransfected (UT) and Willin-GFP-transfected (T) HEK-293 whole cell extracts were separated on a 4-12% Bis-Tris gel. The subsequent nitrocellulose membrane was probed with anti-GFP 1:1000 and secondary anti-mouse-HRP 1:5000 (Lanes 1 and 2); αWR1 1:500 and secondary anti-rabbit-HRP 1:2000 (Lanes 3 and 4); αWR2 1:500 and secondary anti-rabbit-HRP 1:2000 (Lanes 5 and 6); and secondary anti-rabbit-HRP 1:2000 only, no primary (Lanes 7 and 8). Arrows indicate suspected Willin-GFP bands detected in transfected samples. To the left are shown the Molecular weights (kDa).

As occurred with the chicken antibodies, unexpected bands on the membrane made it difficult to interpret the ability of αWR to detect Willin. It was decided to perform peptide blocking experiments with the antibody to see if any bands could be specifically blocked. Whole cell extracts from uninduced and IPTG induced BL21/DE3 pGST-Willin were separated on a gel and the membrane probed with either αWR1 or 2 as normal or αWR1 or 2 pre-incubated with 100μg/mL peptide. αWR2 showed detection of GST-Willin as in figure 3.15, but pre-incubation with the peptide showed only high background and no blocking (data not shown). However, for αWR1, uninduced samples show leaky expression of GST-Willin, and this is completely blocked by the peptide. Induction was very high in this sample, but the band is still mostly blocked by the peptide (Figure 3.18).

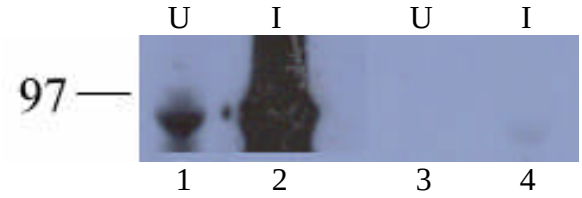

Figure 3.18. Whole cell extract from uninduced (U) and IPTG induced (I) BL21/DE3 pGST-Willin cells was separated on a 4-12% Bis-Tris gel. The subsequent nitrocellulose membrane was probed with αWR1 1:500 and secondary anti-rabbit-HRP 1:5000 (Lanes 1 and 2) or αWR1 1:500 + 100mg/mL peptide and secondary anti-rabbit-HRP 1:5000 (Lanes 3 and 4). To the left are shown the Molecular weights (kDa).

HEK-293 cells transfected with Willin-GFP were also tested, this time with a lower concentration of antibody to ensure that peptide was in excess. As seen in Figure 3.19, the suspected Willin-GFP band, based on detection by anti-GFP, runs below an unidentified high molecular weight band, and this lower band is blocked by the peptide (Figure 3.19).

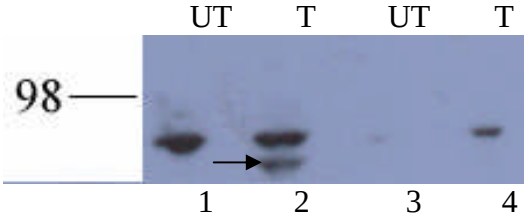

Figure 3.19. Whole cell extracts from HEK-293 cells either untransfected (UT) or transfected with Willin-GFP (T) were separated on a 4-12% Bis-Tris gel. The subsequent nitrocellulose membrane was probed with αWR1 1:1000 and secondary anti-rabbit-HRP 1:10,000 (Lanes 1 and 2) or αWR1 1:1000 + 100mg/mL peptide and secondary anti-rabbit-HRP 1:10,000 (Lanes 3 and 4). Blocked band is indicated by an arrow. To the left are shown the Molecular weights (kDa).

3.4 Characterisation of the commercial antibody αFRMD6

In 2006, the Atlas Antibodies company (Stockholm, Sweden) released an antibody to the FRMD6 protein, which is identical to Willin, based on a sequence from the Human Protein Atlas project:

EEDLQDDEIEMLVDDPRDLEQMNEESLEVSPDMCIYITEDMLMSRKLNGHSG
LIVKEIGSSTSSSSETVVKLRGQSTDSLPQTICRKPKTSTDRHSLSLDDIRLYQK
DFLRIAGLCQDTAQSYTFGCGHELDEE

This sequence is found in the C-terminal at residues 440-574 in Willin human isoform 2 and 447-551 in human isoform 1. It was therefore expected that this antibody would detect both isoforms of Willin. Information provided by the company showed Western blots with bands of ~70kDa in human tissue samples, as seen in figure 3.20.

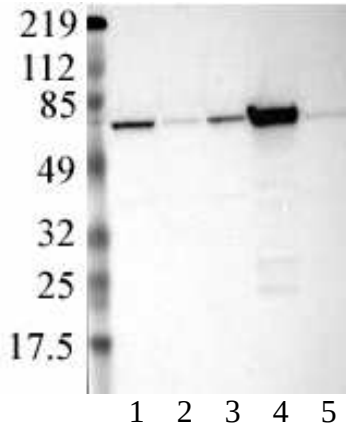

Figure 3.20. Taken from http://www.atlasantibodies.com. Total protein lysate from human cell line RT-4 (Lane 1), total protein lysate from human cell line EFO-21 (Lane 2), total protein lysate from human cell line A-431 (Lane 3), total protein lysate from human liver (Lane 4), and total protein lysate from human tonsil (Lane 5) were separated on an SDS-PAGE gel and the subsequent nitrocellulose membrane was probed with αFRMD6 1:500 and anti-rabbit-HRP 1:3000. To the left are shown the Molecular weights (kDa).

In order to determine whether αFRMD6 would detect expressed Willin, whole cell extract from uninduced (U) and IPTG induced (I) BL21/DE3 pGST-Willin cells were separated by SDS-PAGE and the subsequent nitrocellulose membrane probed using the same blocking and antibody incubation conditions as for APHen2 and αWR. As shown in figure 3.21A, no difference was seen between the uninduced and induced samples. A repeat of this experiment with less protein loaded to reduce smearing gave the same result (figure 3.21B). These results indicated that perhaps the GST-Willin was not expressing properly, so a control was done with pAP914[3] to see if it could detect the induced protein compared to αFRMD6. Figure 3.21C shows

that, while pAP914[3] is able to detect induced GST-Willin as normal, αFRMD6 still does not.

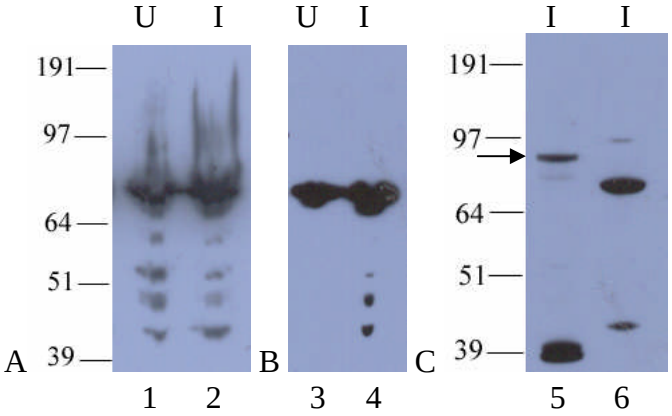

Figure 3.21. A) Whole cell extracts from uninduced (U) and IPTG induced (I) BL21/DE3 pGST-Willin cells were separated on a 4-12% Bis-Tris gel. The subsequent nitrocellulose membrane was probed with αFRMD6 1:500 and secondary anti-rabbit-HRP 1:3000. There is no difference between the samples, and a band appears just above 64kDa. B) The same conditions with reduced protein loading to reduce smearing. C) Whole cell extracts from IPTG induced BL21/DE3 pGST-Willin cells were separated on a 4-12% Bis-Tris gel. The subsequent nitrocellulose membrane was probed with pAP914[3] 1:1000 and secondary anti-rabbit-HRP 1:5000 (Lane 5) or αFRMD6 1:500 and secondary anti-rabbit-HRP 1:3000 (Lane 6). To the left are shown the Molecular weights (kDa).

It was determined that αFRMD6 does not detect GST-Willin. An attempt was then made to see if αFRMD6 could detect Willin-GFP expressed in mammalian cells. First, HEK-293 cells were either untransfected or transfected with plasmids expressing Willin-GFP, Merlin1-GFP, GFP-Moesin or GFP-Ezrin. Whole cell extracts were prepared as usual (section 2.3.6) and separated on a gel, and the subsequent nitrocellulose membrane was probed with αFRMD6 as described in figure 3.22. Willin-GFP and Merlin1-GFP were expected to be approximately 98kDa, while GFP-Moesin and GFP-Ezrin were expected to be approximately 108kDa. It was expected that αFRMD6 would react exclusively with Willin and not the other ERM

proteins. Figure 3.22 shows an approximately 39kDa band and an approximately 60kDa band in all lanes, and an approximately 85kDa band in all transfected lanes.

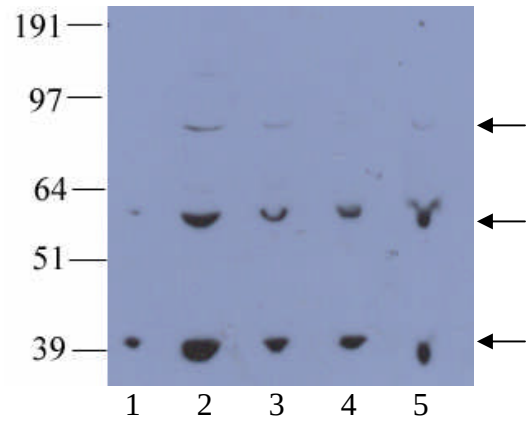

Figure 3.22. HEK cells were either untransfected (1) or transfected with Willin-GFP (2), M1GFP (3), GFP-Moesin (4) or GFP-Ezrin (5); whole cell extracts were separated on a 4-12% Bis-Tris gel and the subsequent nitrocellulose membrane was probed with αFRMD6 1:500 and secondary anti-rabbit-HRP 1:3000. To the left are shown the Molecular weights (kDa).

This experiment showed possible detection of a band of similar size to previous Willin-GFP samples, but it also appeared in lanes with other ERM proteins. To determine if this band was Willin-GFP, whole cell extracts from COS-7 cells either untransfected or transfected with Willin-GFP were separated on a gel and the subsequent nitrocellulose membrane probed with αFRMD6 and αGFP as a control. Figure 3.23A shows that, while αGFP detected an expressed band, αFRMD6 did not; increasing the exposure time to 15 minutes (figure 3.23B) still did not bring up Willin-GFP bands in αFRMD6.

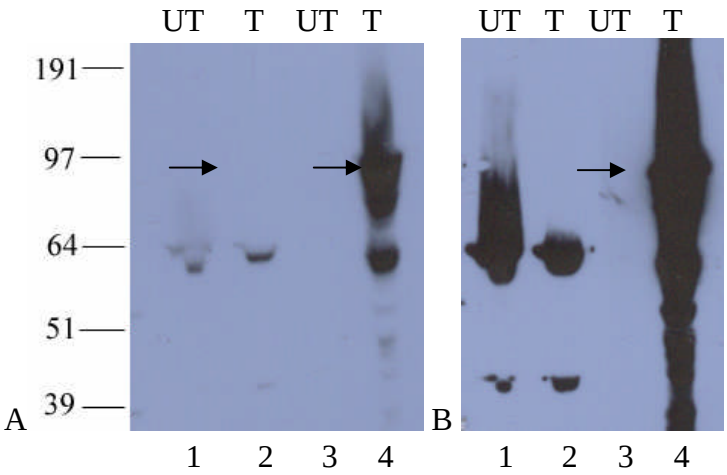

Figure 3.23. Untransfected (UT) and Willin-GFP-transfected (T) COS-7 whole cell extracts were separated on a 4-12% Bis-Tris gel, and the subsequent nitrocellulose membrane was probed with αFRMD6 1:500 and secondary anti-rabbit-HRP 1:5000 (Lanes 1 and 2) or αGFP 1:1000 and secondary anti-mouse-HRP 1:5000 (Lanes 3 and 4). **A**) 30 second exposure time. **B**) 15 minute exposure time. To the left are shown the Molecular weights (kDa).

Atlas Antibodies stated that αFRMD6 was suitable for immunocytochemistry. Therefore, further characterisation of αFRMD6 was done under my supervision by project student Chris Cozens, who performed immunocytochemistry on COS-7 cells transfected with Willin-GFP. While the Willin-GFP expressed as expected, αFRMD6 staining did not overlay with Willin-GFP, and in fact showed a punctate cytoplasmic distribution reminiscent of mitochondria (data not shown). To confirm the suspicion that αFRMD6 was staining a mitochondrial protein rather than Willin, COS-7 cells were transfected with mito-ABAD-GFP, a construct previously shown to localise almost exclusively to mitochondria (M. Taylor, unpublished data). Transfected dishes were fixed and stained as described in section 2.2.8, using αFRMD6 at a concentration of 1:100 and Alexa568-conjugated anti-rabbit secondary antibody at a concentration of 1:000. Figure 3.27 shows perfect colocalisation between the αFRMD6 staining and mitochondria.

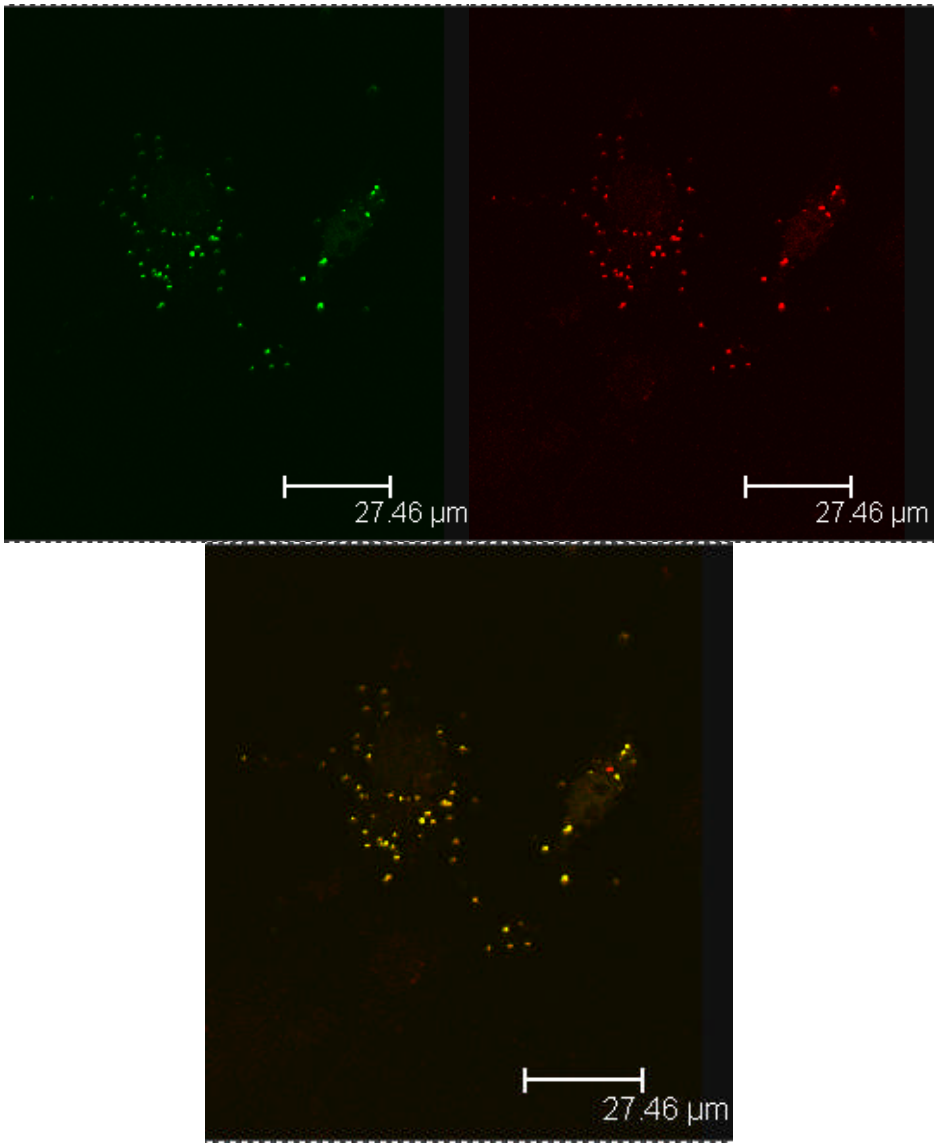

Figure 3.27. COS-7 cells were transfected with mito-ABAD-GFP and grown at 37^{o}C for 48 hours before being fixed and stained with αFRMD6 1:100/Alexa568-conjugated αrabbit 1:1000.

3.5 Discussion

3.5.1 914^3 and αWR Antibodies and the 622 Amino Acid Isoform of Willin

The rabbit polyclonal antibodies 914^3 and αWR were made against the peptide sequence KEASKGIDQFGPPMIIH. The panned, affinity purified version of 914^3 detects expressed Willin reasonably well in Westerns, but has been mostly unsuccessful in detecting native Willin; affinity purified versions of αWR had the same problems. All of the expressed proteins used in our experiments were the 614 amino acid length version, called isoform 2, but there is another isoform, isoform 1, that is 622 amino acids in length. This version has 8 additional amino acids within the very sequence to which 914^3 was raised (KEASKVRQYEVTWGIDQFGPPMIIHC). If the native form of Willin expressed in the cell types studied is isoform 1, it is clear that 914^3 and αWR are unlikely to detect it. As yet it is unknown what difference there is in expression and function between the two different isoforms of Willin, but it would be advisable to avoid this sequence in the design of future antibodies against Willin. However, once more is known about Willin isoform distribution, it is possible that either of these antibodies can be used as an isoform-specific detection method if the need arises.

3.5.2 APHen2

APHen2 was found to be no better than $pAP914^3$ in detecting expressed Willin and inconclusive as to whether it could detect native Willin in cultured cells and rat sciatic nerve. COS-7 cells are from African green monkey (*Chlorocebus sabaeus*), so it is possible that the APHen2 epitope is not present in the monkey version, if indeed there is a green monkey homologue. In addition, BLAST searches of the rat Willin sequence led to the discovery that a rat sequence with a complete C-terminus had not

been cloned at the time, and it was as yet impossible to know if the antibody peptide is even present in the rat protein. This line of inquiry was therefore abandoned. A recent BLAST search has shown a predicted 615 amino acid rat version (accession number XP_001080473) with a C-terminal sequence of VLFSGPHSRRGPRVPCL, which matches only 2 amino acids of the APHen2 sequence (KYFSLDLTHDEVPEFVV). Although this is only a predicted sequence, this may explain why APHen2 was unable to detect Willin in rat sciatic nerve. The mouse protein does have this sequence, but the C-terminal GFP tag may prevent binding of the antibody to expressed protein. To study the antibody further, the mouse Willin sequence should be expressed in another mammalian expression vector without a C-terminal tag. Unfortunately this was outwith the scope of this project.

3.5.3 αWR

The αWR rabbit antibody was made to the same sequence as 914[3], but did not cross-react with BSA. Unfortunately, it was also inconsistent with its detection of Willin. Non-specific binding was high and peptide blocking seemed to work only for expressed protein. Further characterisation was done by project student Amy Cameron, and her results also showed a high level of inconsistency with this antibody. For these reasons, it was abandoned.

3.5.4 αFRMD6

The commercial antibody αFRMD6 was shown not to bind expressed Willin in cultured mammalian cells and bacteria. The ~70kDa band that appeared in Western blots with cultured cells also appeared in bacterial samples. FERM proteins are not found in bacteria, so it is very unlikely that this band is Willin. In addition, the immunocytochemistry results show that αFRMD6 staining is exclusive to the

mitochondria, but does not overlap with expressed Willin-GFP. As further confirmation, Professor Simon Harrington, a pathologist at the University of St. Andrews, observed the original immunocytochemistry images made available on the Atlas Antibodies website, and suggested that the granular staining is typical of mitochondria (CS Herrington, personal communication). Therefore, αFRMD6 should not be used as an antibody to Willin.

3.6. Conclusion

Overall, the antibodies so far raised to Willin have not been successful despite several attempts. After the conclusion of this work, a monoclonal antibody was raised to GIDQFGPPMIIH, found in both splice variants; initial testing has indicated that this has also been unsuccessful. The use of peptides to produce antibodies can be difficult, as it cannot be known for certain whether a peptide sequence will prove to be a good antigen without cross-reactivity. In future it may be useful to raise an antibody to purified protein rather than a peptide, but with a protein as labile and difficult to purify (see section 5.9.4) as Willin, this will also prove challenging.

CHAPTER 4: INTRACELLULAR LOCALISATION AND BEHAVIOUR

Chapter 4: Intracellular localisation and behaviour of Willin

4.1 Introduction

As discussed in Chapter 3, antibodies against Willin have not been as specific as desired for the study of native protein. Therefore, tagged constructs have been expressed in cells to observe the protein's behaviour in cell lines. Prior to the start of this project, a pWillin-GFP construct was produced by Frances Brannigan (Gunn-Moore et al., 2005), and has been very useful in characterisation. However, GFP has been shown to be toxic to living cells (Liu et al., 1999), and as it is a large tag of about 27kDa, there was a fear that it could affect localisation of the protein by masking binding sites or simply preventing proper targetting. To determine if the Willin-GFP data was valid, it was determined that a FLAG-tagged construct should be made for comparison; this tag is only 8 amino acids long, so in theory it should not affect the distribution or behaviour of Willin. Also, specific antibodies are available to the FLAG octapeptide, making it a good tag for both immunofluorescence and Western blot studies. In addition, a DsRed-tagged clone of Willin, allowing for double transfectant fluorescence microscopy without the use of antibodies, was produced under my supervision and in collaboration with undergraduate project student Jessica Davis as discussed in section 4.2.3.

Overexpression of proteins in transient transfections is also a concern. It has been observed that overexpression can lead to mistargeting, which is an obvious problem when trying to determine subcellular localisation of a novel protein. To overcome this problem, stable cell lines are usually produced. This involves transfecting a cell line, then selecting the transfected cells with antibiotic until only the cells expressing the construct remain; only the cells that have integrated the gene

will survive, and these cells should produce the gene at close to native expression levels. A stable Willin-expressing cell line had not been made before, so an attempt was made to produce four such lines: COS-7 cells expressing Willin-GFP, COS-7 cells expressing Willin-FLAG, HEK-293 cells expressing Willin-GFP and HEK-293 cells expressing Willin-FLAG.

The purification of Willin has always been fraught with difficulties. The protein has been found to be very labile, preventing any long-term storage of purified protein and whole cell extracts, and the lack of a good antibody has precluded the study of native protein. As will be discussed in section 4.4, cells expressing Willin for longer than 72 hours tend to die, restricting longer-term study of transfected cells and the production of stably-transfected cell lines. This suggests that a function of Willin could be in the regulation of cell growth and proliferation, potentially triggering cell death when it is overexpressed or cells have reached a certain density. There is precedent for this in the FERM proteins, with merlin as a proven tumour suppressor and growth regulator in species as diverse as *Drosophila* and humans (Evans et al., 1992; LaJeunesse et al., 1998). This possibility is further supported by mRNA data showing that the Willin signal is very low in cells (Stewart Gillespie, personal communication), and that in some head and neck cancers, Willin is downregulated (Michael B. Prystowsky, personal communication).

The biggest challenge, however, has been solubility. We have found this protein to be highly insoluble. Traditionally this has been assumed to mean an association with the actin cytoskeleton in mammalian cells, and indeed, because of the often close association and colocalisation with actin, we at first assumed this was the case. However, disruption of the actin cytoskeleton made no difference either to Willin localisation or solubility (Gunn-Moore et al., 2005). This finding led to the

question of what was causing the insolubility of Willin if not the cytoskeleton. Intriguingly, merlin is also highly insoluble, but this is because it localises to lipid rafts (see section 1.1.4.2), special membrane domains that are resistant to solubilisation by ice-cold 1% Triton X-100 due to their unique packing of cholesterols and glycosphingolipids (Stickney et al., 2004). As Willin is often found to localise to the membrane, it was thought that this might be the reason for the insolubility. The association of Willin constructs with lipid rafts was therefore studied, in conjunction with Dr. Wally Ip's group at the University of Cincinnati, Ohio, USA.

During the course of this project, a splice variant of Willin containing 622 amino acids was found. As discussed in section 3.5.1, this variant, referred to here Willin2, has 8 additional amino acids within the part of the sequence used to produce two of our antibodies. Therefore, in order to compare this isoform to the one used previously, a GFP-tagged construct was cloned under my supervision by undergraduate project student Chris Cozens. A human version of Willin2 was not available as an Image clone, so a full-length mouse cDNA was purchased instead (Image Clone 6389695, NCBI accession number: BC053929). Initial characterisation of this clone is presented in section 4.7.

4.2 The distribution and effect of expressed Willin constructs on mammalian cells

4.2.1. Construction of the pWillin-FLAG plasmid

A previously constructed plasmid (pWillin-GFP) expressing Willin fused to the N-terminus of EGFP was shown to express this chimeric protein (Willin-GFP) such that it had an intracellular distribution that was different from the ERMs and Merlin, and that varied according to the cell type within which it was expressed and

even within a cell type it was dependent on growth factor activation, cell-cell contact, and as-yet other undetermined factors (Gunn-Moore et al., 2005). To see if Willin with a smaller tag would behave in the same way, pWillin-FLAG was constructed. The most convenient cloning sites in the pCMV-Tag 4A vector were SacI and BamH I; however, there is a single SacI site within Willin at base pair 1507. Therefore, a two-step cloning strategy was devised. First, pWillin-GFP was digested with the restriction enzyme SacI, releasing the first 1507bp fragment of Willin. Then, using pWillin-GFP as a template, the forward primer 5' CCACCTCGAGCTCTTCAG 3' containing a SacI site, and reverse primer 5' CGGGATCCCACAACAAACTCTGGAAC 3' containing a BamH I site, a PCR product containing the remaining 338bp of Willin was produced and subsequently digested with the restriction enzymes SacI and BamH I. The pCMV Tag-4A vector was also digested with SacI and BamH I, and the shorter fragment of Willin was ligated with it. The ligation mixture was transformed into *E. coli* and prepared as usual, and restriction digest analysis showed the ligated plasmid was present. This plasmid was then digested with SacI, treated with alkaline phosphatase (section 2.1.3) and the longer Willin fragment ligated with it. As two orientations for this insert were possible, several digests were performed to test both the presence and direction of the insert, and the complete plasmid was further confirmed by sequencing. Figure 4.1 summarises the cloning strategy of pWillin-FLAG.

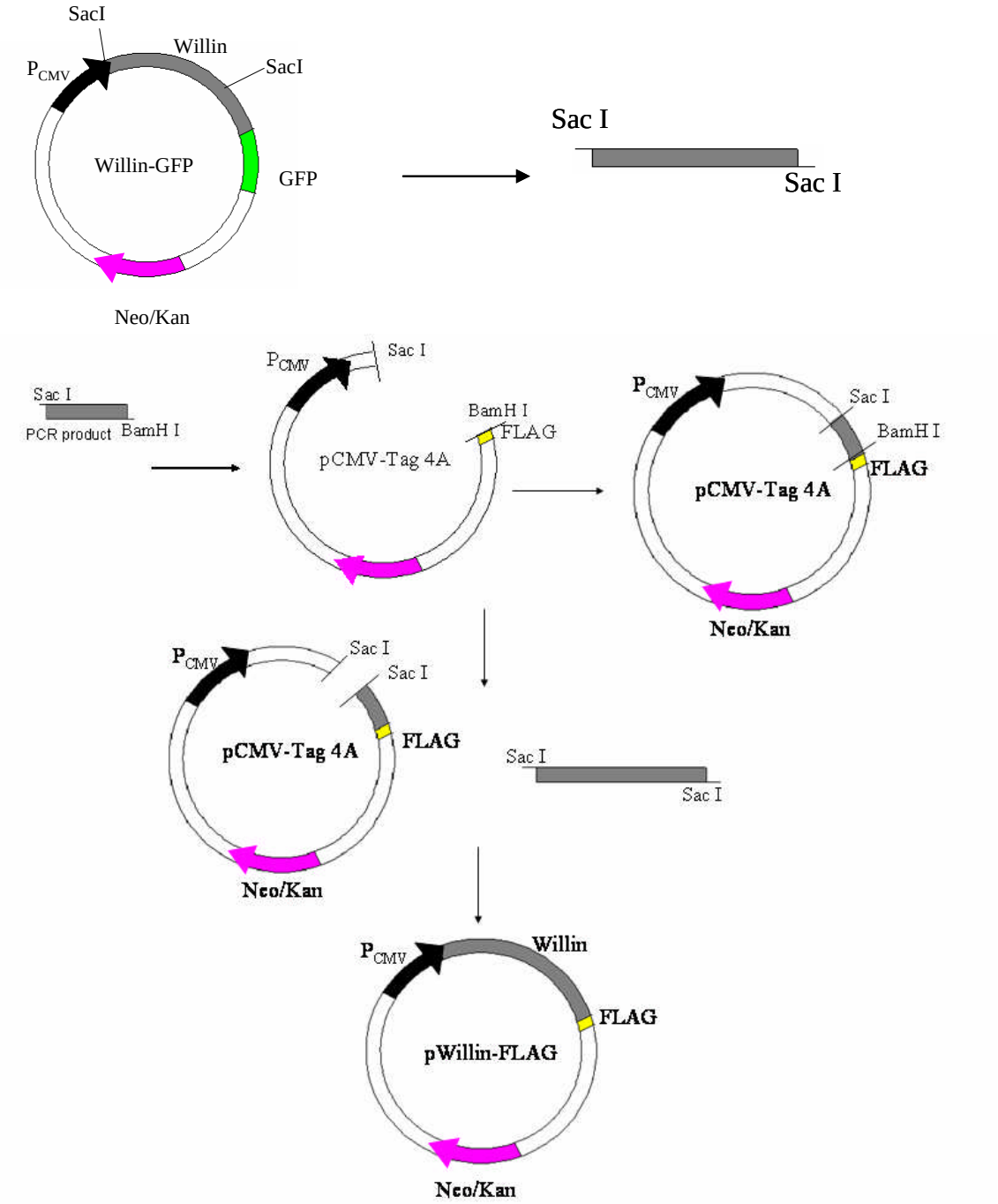

Figure 4.1. Two-step cloning strategy for pWillin-FLAG. pWillin-GFP was digested with SacI to produce a 1507bp fragment; pWillin-GFP was also used as the template for PCR of the last 338bp of Willin. The two fragments were then sequentially ligated into pCMV-Tag4A to produce pWillin-FLAG.

4.2.2. Expression of Willin-FLAG

Willin-FLAG was transfected into HEK-293 cells to test for expression by Western blot analysis. A positive control lysate containing a truncated FLAG-Ezrin protein was provided by Dr. Fleur Davey. The Willin-FLAG protein was expected to

be about 72kDa, but as is usually seen with Willin, the detected protein had a lower apparent molecular weight (Figure 4.2).

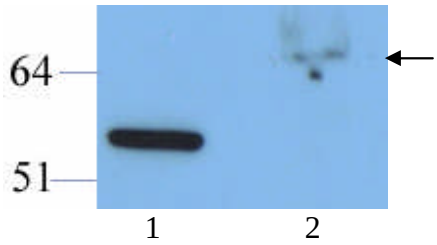

Figure 4.2. Truncated FLAG-Ezrin positive control (Lane 1) and whole cell extract from Willin-FLAG transfected HEK-293 cells (Lane 2) were separated on a 4-12% Bis-Tris gel and the subsequent nitrocellulose membrane probed with anti-FLAG M2 1:500 and secondary anti-mouse-HRP (Santa Cruz) 1:10,000.

Immunocytochemistry was also performed in HEK-293 cells transfected with pWillin-FLAG (see section 2.2.8) to study the distribution of the Willin-FLAG protein. It was observed that Willin-FLAG has a comparable distribution pattern to Willin-GFP (see Figure 1.17B): localisation is punctate throughout the membrane and cytoplasm in the vast majority of cells (Figure 4.3). In addition, Willin-FLAG-expressing cells showed the same tendency towards high levels of cell death 48 hours post-transfection as those expressing Willin-GFP. This indicated that the GFP tag did not have a significant effect on Willin localisation and was not solely responsible for increased levels of cell death, and could thus continue to be used for other studies.

Co-expression of Willin-GFP and Willin-FLAG was attempted, but due to technical problems with the FLAG antibodies that were not FITC-tagged, images could not be obtained to show co-localisation.

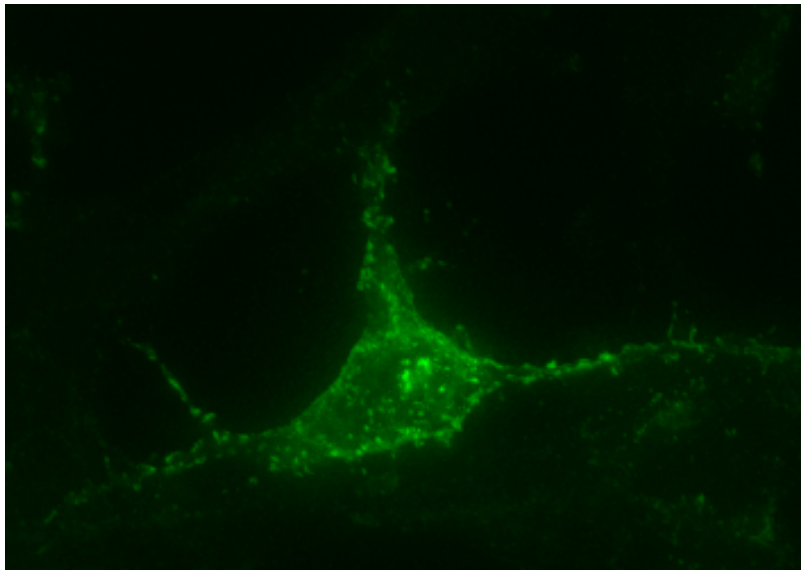

Figure 4.3. HEK-293 cell expressing Willin-FLAG. Image is a maximum projection of 46 Z-sections acquired on Olympus IX70 Deltavision RT microscope with Coolsnap 2HQ camera (Roper Sci). Images were deconvolved and converted to TIF format with SoftWorx (Applied Precision) and projection assembled using ImageJ software. Z-sections were 0.2μm thick.

4.2.3. Construction of the pWillin-DsRed plasmid

Under my supervision, undergraduate project student Jessica Davis constructed a pWillin-DsRed plasmid that could be used for co-localisation studies with GFP-tagged proteins of interest. PCR was not required; instead, the GFP sequence was digested from the pWillin-GFP plasmid using BamHI and NotI and replaced with DsRed2 that had been digested from pDsRed2-Mito with BamHI and NotI (Figure 4.4).

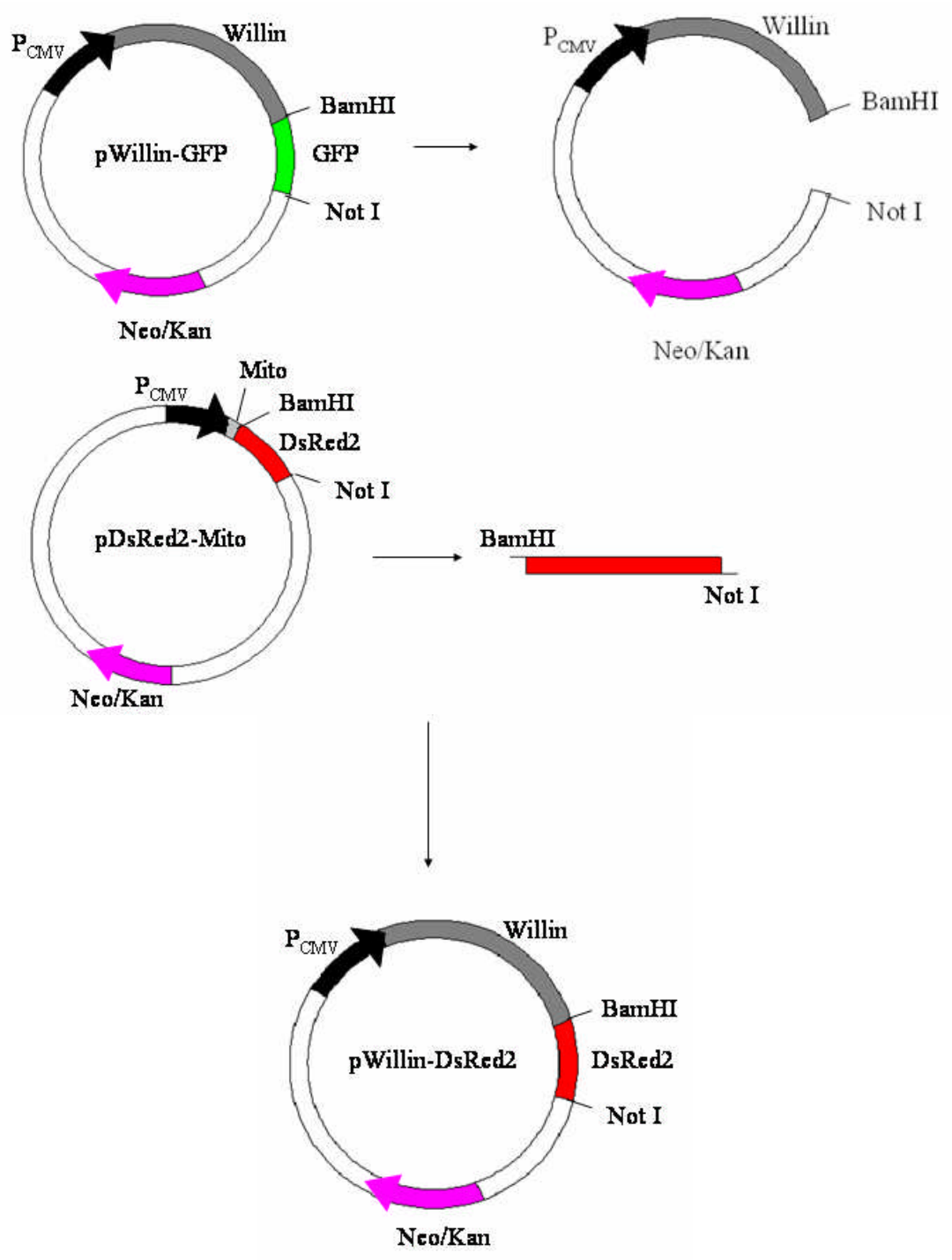

Figure 4.4. Cloning strategy for pWillin-DsRed2. DsRed2 was digested from the pDsRed2-Mito plasmid with BamHI and NotI, while GFP was digested from the pWillin-GFP plasmid. The DsRed2 fragment was then ligated into the Willin vector.

Once the sequence of the plasmid produced was verified by sequencing to ensure it was in frame, COS-7 cells were transfected with the plasmid. As can be seen in Figure 4.5, the Willin-DsRed2 protein was found to form aggregates in the

cytoplasm, and did not display the characteristic Willin distribution usually found with Willin-GFP. DsRed1 previously showed this tendency, and though DsRed2 is supposed to show drastically reduced aggregation (Clontech manual, http://www.clontech.com/upload/images/ctq/full/CTQJUL01.pdf), it is likely that the cause of aggregation is DsRed itself. This construct could therefore not be used.

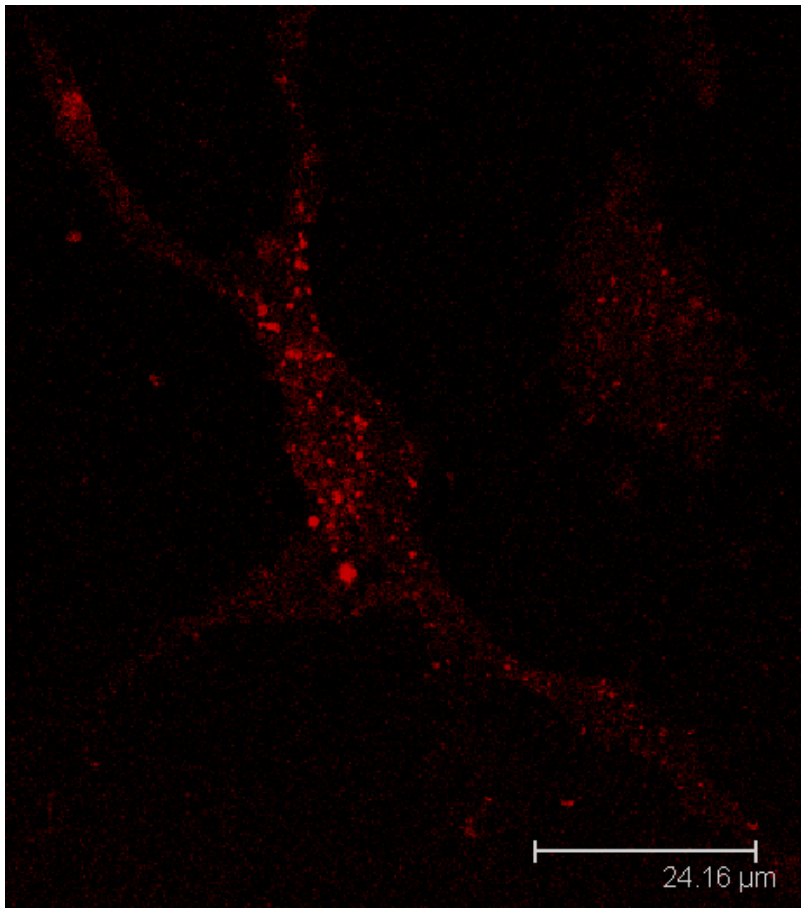

Figure 4.5. A single Z-section snapshot of a COS-7 cell expressing Willin-DsRed2. Single section snapshots were created using LCS Lite V2.61 Build 1538 and cropped with Adobe Photoshop 7.0 (no other post-processing)

4.3. Production of stable cell lines expressing Willin-GFP and Willin-FLAG

To overcome potential overexpression issues, the production of stable cell lines was attempted in two cell lines of interest. As HEK-293 cells were in constant use for many experiments and showed an interesting distribution of Willin, one flask was transfected with Willin-GFP and another with Willin-FLAG as described in

section 2.2.7. In addition, PC12 cells, which showed Willin translocation when stimulated by growth factors (Gunn-Moore et al., 2005), were also selected and transfected with the same constructs.

About 48 hours post-transfection, normal medium was supplemented with 1mg/mL G418-sulfate to select for cells that had incorporated the tagged Willin gene. Almost immediately, problems arose. The cells first continued proliferating until passaged, and once selection did begin, it took over a month for enough cells to grow back to a T-25 flask. At this point, cells were seeded onto coverslips to check for expression, and mixed populations were observed for both cell types and both genes of interest (data not shown). The PC12 cells had a very low (>5%) transfection efficiency to begin with, and upon further selection, the protein expression grew fainter and fewer cells seemed to be expressing the protein in any quantity. The HEK-293 cells, though showing a higher initial transfection rate, also displayed this tendency towards dramatically reduced expression. After only a few passages, it seemed that the cells had expelled the Willin gene but retained the resistance gene, as the G-418 no longer killed any of the cells. The individual remaining cells were too faint for imaging, and were severely stressed. Time constraints prevented a second attempt at producing any of these cell lines.

4.4. Quantitation of cell death in cells expressing Willin-GFP

It had been observed in the laboratory that cells transfected with any of the Willin constructs seemed to have a high level of cell death if left to express the protein for longer than 2-3 days. As discussed in section 4.3.1, stable transfections did not seem to take very well, as the cells that did grow after a significant amount of time expressed Willin only faintly. This was initially unexpected, as the ERM

proteins usually promote cell survival (see section 1.1.3.4), but as Merlin is a growth suppressor (see section 1.1.4), it was hypothesised that Willin may also have a suppressive function. Blind cell counts at two different time points post-transfection were performed under my supervision and in collaboration with undergraduate project students Amy Cameron and Jessica Davis

COS-7 cells were grown on glass coverslips and transfected with either pWillin-GFP, pMerlin1-GFP, or pGFP-Moesin, then left to express the proteins for either 48 or 72 hours before fixation with either PFA in Amy Cameron's experiments, or NBF in Jessica Davis' experiments, as described in section 2.2.8. Coverslips were mounted on glass slides with Mowviol containing DAPI to allow for visualisation of nuclei. These slides were then observed under a 63x oil objective lens on a Zeiss Axioscop microscope. The number of transfected cells in 5 random fields of view were counted, as well as the number of apoptotic nuclei among those transfected cells. The number of apoptotic cells was divided by the total number of transfected cells to give a percentage of transfected cells undergoing apoptosis. All transfected cells could be expected to have some cell death from the transfection process; cells transfected with GFP-Moesin were expected to have the least due to the growth and survival promoting ability of Moesin (see section 1.1.3.4), while Merlin1-GFP was expected to have more, particularly as cell density increased over time and Merlin1 became more active (see section 1.1.4.1). Willin-GFP was also expected to show higher cell death compared to GFP-Moesin, particularly after 72 hours as previously observed. All the data sets were compiled and the outcome shown below in Figure 4.6. As expected, Merlin1-GFP-expressing cells shows a higher level of cell death than GFP-Moesin-expressing cells, and more after 72 hours than after 48 hours. Willin-GFP-expressing cells, however, showed little death at 48 hours, but the

number of apoptotic cells increased markedly after 72 hours. While intriguing, this data is still preliminary, and further cell counts must be done for statistical analysis to be valid.

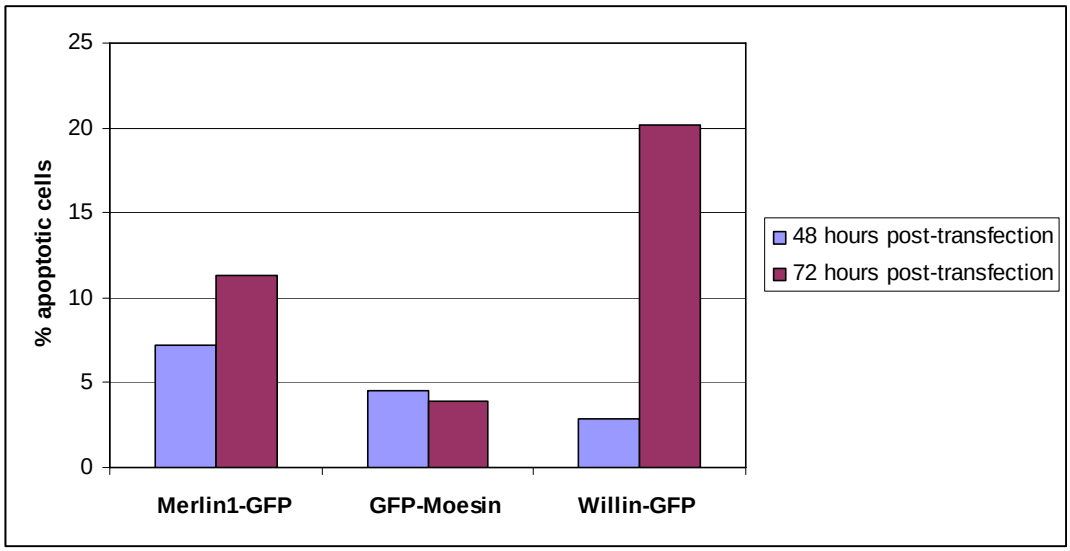

Figure 4.6. Percentage of apoptotic COS-7 cells transfected with either Merlin1-GFP, GFP-Moesin or Willin-GFP. Cells were counted either 48 hours (blue) or 72 hours post-transfection. Cell counts were too small for statistical analysis to be performed.

4.5. Investigation of solubility and lipid raft localisation of Willin

4.5.1. Solubility of Willin in Schwann cells

Brannigan (2006) first observed that Willin tended to localise to the insoluble fraction of detergent extractions. This was mostly the case with expressed Willin, but it was believed that this insolubility may be a characteristic of Willin, possibly because of its association with the cytoskeleton. Ideally this would be tested on native protein, but it was not known which cell lines express Willin. However, Schwann cells seemed a likely candidate because of Willin's discovery as the yeast two-hybrid binding partner of a Schwann cell protein and has been shown to be expressed in sciatic nerves (Gunn-Moore et al., 2005). RIPA extraction was carried out as described in 2.3.6. A confluent T-25 flask of rat Schwann cells was a kind gift from Dr. Sue Barnett, University of Glasgow. These cells were harvested in RIPA buffer

and an aliquot of whole cell extract was taken prior to separation of supernatant and pellet by centrifugation. The samples were separated on a 4-12% Bis-Tris gel and the subsequent nitrocellulose membrane was probed with pAP914[3] antibody, which had previously been shown to detect some native protein. As shown in Figure 4.7, a single band of approximately 64kDa protein is strongly detected in the whole cell extract and insoluble pellet, but only faintly in the soluble supernatant. This confirmed the presence of a Willin antigen in Schwann cells and the probably native insolubility of this protein.

Figure 4.7. Schwann cells were grown in a T-25 flask and harvested in RIPA buffer. Whole cell extract (Lane 1), supernatant (Lane 2) and insoluble pellet (Lane 3) fractions were separated onto a 4-12% Bis-Tris gel and the subsequent nitrocellulose membrane probed with pAP914[3] 1:1000 and anti-rabbit secondary (Santa Cruz) 1:2000.

4.5.2. Detergent resistant membrane subfractionation

It was initially believed that association with the cytoskeleton was the cause of Willin's insolubility. However, disruption of the cytoskeleton did not affect the membrane localisation of Willin (Gunn-Moore et al., 2005), which raised questions about how strong this association might be. A literature search for other causes of insolubility pointed to detergent-resistant membranes (DRMs) as the most likely candidates for investigation (Brown and London, 2000; Simons and Ehehalt, 2002). These patches of membrane are high in sphingolipids and cholesterol, leading to tight packing and resistance to solubilisation by non-ionic detergents (Brown and London, 2000). It was also found that there is precedent for a FERM protein to localise to DRMs; Stickney et al. (2004) found that Merlin1-GFP localised to lipid rafts, and that this localisation appeared to be the main cause for its insolubility. It was therefore

decided to repeat their experiments using Willin-GFP to determine if lipid raft localisation could explain the insolubility of Willin. While detergent-based methods for determining raft association can be prone to artefacts (Kahya et al., 2005), subfractionation results of this kind can provide at least a basis for further investigation into potential raft localisation.

Using a detergent-based high speed centrifugation protocol as described in 2.3.12, cells were gently homogenised and subfractionated into nuclear/cellular debris, cytoplasmic, detergent-soluble membrane and detergent-resistant membrane (DRM) fractions. For Merlin, localisation to DRMs was supported by fluorescence microscopy evidence of punctate membrane expression of the GFP-tagged protein. Willin has also shown this distribution, so DRM extractions under various conditions were attempted on four cell types for which solubility and localisation data already existed for Willin-GFP: COS-7, HEK-293, PC12 and SK-UT-1.

4.5.2.1. COS-7 cells express Willin-GFP in DRM

COS-7 cells were grown on 150mm tissue culture dishes and transfected with 20μg of pWillin-GFP. Cells were harvested forty-eight hours post-transfection and S100/P100 fractionation performed as described in section 2.3.13 and fractions P1, S100, P100s and P100i were boiled in 2X PSB and loaded onto a 4-12% Bis-Tris NuPage gels. Proteins were then transferred to nitrocellulose membranes and detected with a mouse monoclonal antibody to GFP and an HRP-conjugated anti-mouse secondary antibody raised in goat (Figure 4.8). As expected based on previous microscopy data, Willin-GFP in COS-7 cells expresses almost exclusively in the DRM fraction, with some faint detergent-soluble membrane and cytoplasmic expression. P1 is referred to as a nuclear fraction, but while it cannot be proven that it

contains only nuclei, a strong Willin-GFP expression in this fraction correlates to the nuclear localisation of Willin-GFP that is often observed.

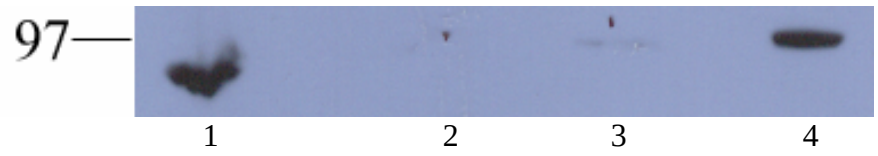

Figure 4.8. COS-7 cells were transfected with pWillin-GFP and subfractionated into P1 (whole cell and nuclei, Lane 1), S100 (soluble cytoplasmic, Lane 2), P100s (Triton X-100 soluble membrane, Lane 3) and P100i (Triton X-100 insoluble membrane, Lane 4) fractions, then separated with equal loading on a 4-12% Bis-Tris gel. The subsequent nitrocellulose membrane was probed anti-GFP 1:2000 and secondary anti-mouse-HRP 1:5000.

4.5.2.2. Willin-GFP DRM localisation in HEK-293 cells is not dependent on actin

HEK-293 cells were grown and transfected with pWillin-GFP as for COS-7 cells. Twenty-four hours post-transfection, the cells were serum-starved for one hour and treated with either 0.2% DMSO or 2μM cytochalasin D in DMSO to disrupt the cytoskeleton and incubated at 37^{o}C 5% CO_2 for thirty minutes. After usual development with GFP antibody, membranes were stripped with 0.1 M glycine-HCl pH 3 for 30 minutes at room temperature in order to be reprobed with the RAD4 pan-ERM antibody to compare Willin-GFP localisation to native ERM localisation. Another dish of HEK-293 cells transfected with pEGFP but not treated with either cytochalasin D or DMSO was also fractionated to determine if DRM localisation could be attributed to the GFP tag. Figure 4.9A shows that there is no apparent difference between cells treated with cytochalasin D and DMSO control, suggesting that Willin-GFP localisation is not dependent on an intact actin cytoskeleton. There is a greater expression of Willin-GFP in the cytoplasmic fraction in HEK-293 cells, which again correlates to observations from microscopy. Figure 4.9B shows that the ERMs are mostly soluble with some localisation as expected to the TX-100 soluble

membrane fraction. Figure 4.9C shows HEK-293 cells transfected with GFP only. Most of the GFP is found in the soluble fraction and none in the DRM fraction, confirming that DRM localisation of Willin-GFP is not an artefact of GFP production.

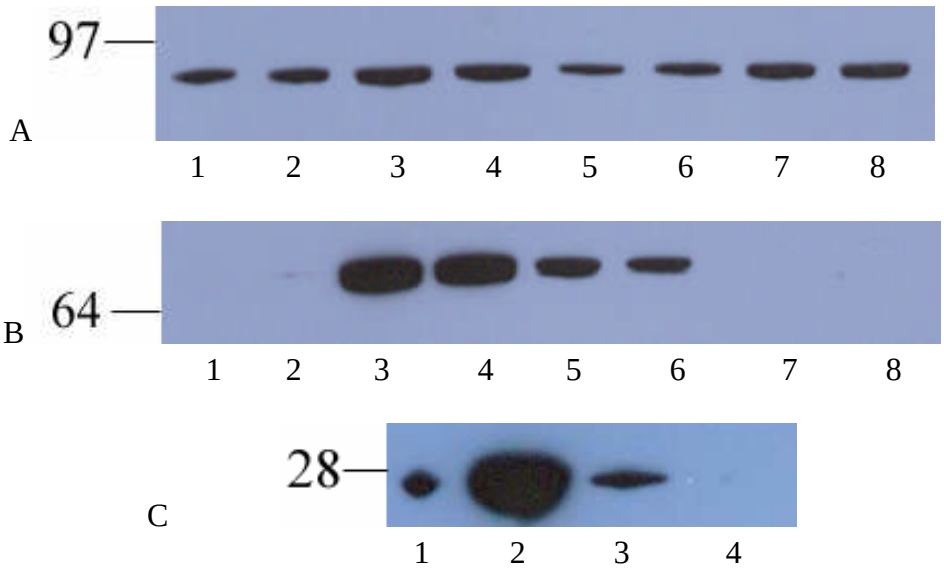

Figure 4.9. HEK-293 cells transfected with pWillin-GFP were treated with either 0.2% DMSO or 2μM cytochalasin D, then fractionated and the samples loaded onto a 4-12% Bis-Tris gel. The subsequent nitrocellulose membrane was probed with anti-GFP 1:1000 and secondary anti-mouse-HRP 1:5000 (A) and then stripped and reprobed for native ERM expression with RAD4 pan-ERM antibody 1:5000 and secondary anti-rabbit-HRP 1:10,000 (B). Some cells were also transfected with pEGFP and fractionated, and the samples loaded onto a 4-12% Bis-Tris gel. The subsequent nitrocellulose membrane was probed with anti-GFP 1:1000 and secondary anti-mouse-HRP 1:5000. A) Odd-numbered lanes were DMSO-treated and even-numbered lanes cytochalasin D-treated. Willin-GFP is present in nuclear/debris (Lanes 1 and 2), cytoplasmic (Lanes 3 and 4), detergent-soluble membrane (Lanes 5 and 6) and DRM (Lanes 7 and 8) fractions. B) ERMs are mostly found in the cytoplasmic (Lanes 3 and 4) and detergent-soluble (Lanes 5 and 6) fractions. C) GFP is expressed strongly in the cytoplasmic fraction (Lane 2), and in nuclear/debris (Lane 1) and detergent-soluble membrane (Lane 3) fractions. There is no GFP present in the DRM fraction (Lane 4).

4.5.2.3. Willin-GFP DRM localisation in PC12 cells does not require stimulation by growth factors

Live imaging experiments with Willin-GFP expressed in PC12 cells showed that stimulation by either nerve growth factor (NGF) or epidermal growth factor (EGF) caused a translocation of Willin-GFP from a cytoplasmic pool to the

membrane, even in contacting cells which already expressed Willin-GFP in the membrane to some extent (Gunn-Moore et al., 2005). However, not all transfected cells responded in this way (Frances Brannigan, personal communication). To test whether this stimulation was required for a membrane, and thus DRM, localisation, PC12 cells were transfected with pWillin-GFP, then 48 hours post-transfection, serum-starved for 3 hours before either no treatment or treatment with 50ng/mL EGF for about 10 minutes. This time was chosen as it had previously been sufficient for Willin-GFP translocation under live imaging conditions (Gunn-Moore et al., 2005). As seen in Figure 4.10, Willin-GFP localises to DRM fractions regardless of growth factor stimulation. Interestingly, no significant difference was seen between treated and untreated cells in terms of membrane localisation, but more Willin does seem to appear in the nuclear fraction.

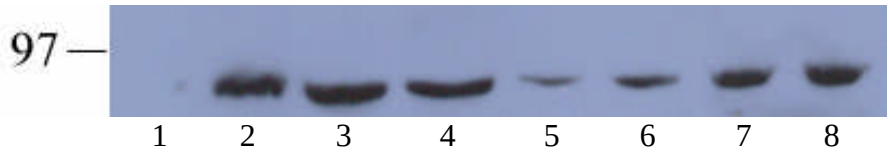

Figure 4.10. PC12 cells were transfected with pWillin-GFP and either treated with 50ng/mL EGF (even-numbered lanes) or left untreated (odd-numbered lanes). No significant difference is seen between the samples in the cytoplasmic (Lanes 3 and 4), detergent-soluble membrane (Lanes 5 and 6) or DRM (Lanes 7 and 8) fractions, but EGF stimulation may cause a shift of Willin-GFP into the nucleus (Lanes 1 and 2).

4.5.2.4. Willin-GFP floats to a lipid raft fraction of an Optiprep gradient

To further characterise the localisation of Willin to lipid rafts, an Optiprep gradient centrifugation was performed as described in 2.3.13. HEK-293 cells were lysed and centrifuged for at least 16 hours at 100,000*xg* at 4^{o}C in a continuous Optiprep gradient ranging from 0% to 40% Optiprep. 800µL fractions representing 0%, 20%, 25%, 30%, 35% and 40% were then taken and run on SDS-PAGE for Western blotting. Merlin1-GFP has been found to float to 20% and 25% fractions

under various conditions (Stickney, 2004), and this was also observed for Willin, as seen in Figure 4.11.

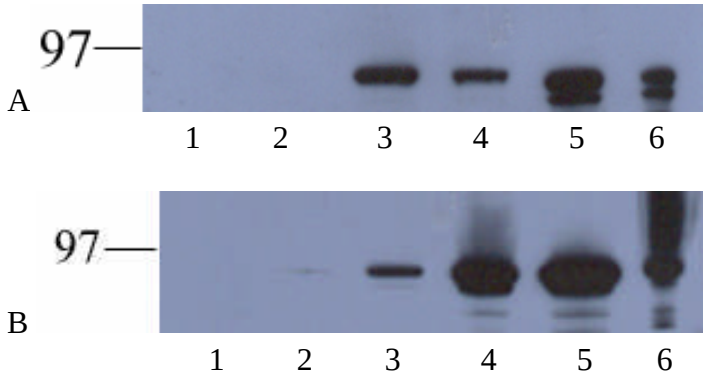

Figure 4.11. A) HEK-293 cells transfected with Merlin1-GFP centrifuged in an Optiprep gradient. A band appears in 25% fraction (Lane 3), indicating the presence of Merlin1-GFP in lipid rafts. B) HEK-293 cells transfected with Willin-GFP centrifuged in an Optiprep gradient. Bands appear in 20% and 25% fractions (Lanes 2 and 3), indicating the presence of Willin-GFP in lipid rafts.

4.6. Characterisation of a novel splice variant of Willin

A BLAST search for Willin in late 2006 brought up a new splice variant of Willin, called Willin2, containing 8 additional amino acids within the FERM domain (accession number Q96NE9). A human cDNA clone was not available, so a highly conserved mouse homologue cDNA (Mouse Willin2) was obtained from the IMAGE consortium (Image clone 6389695, accession number BC053929). To compare its distribution with that of the original Willin, a GFP-tagged plasmid was constructed by project student Chris Cozens under my supervision. PCR with the usual Willin program was performed using the cDNA Image clone as a template, a forward primer containing an EcoRI site (5' GGAATTCGCCATGAACAAACTGACCTTCC 3') and reverse primer containing a BamHI site (5' CGGGATCCGACGACGAACTCTGGGAC 3'). This PCR product was then ligated into the pEGFP-N3 plasmid and confirmed by restriction digest analysis and

sequencing. Figure 4.12 summarises the cloning strategy used to produce Mouse Willin2-GFP.

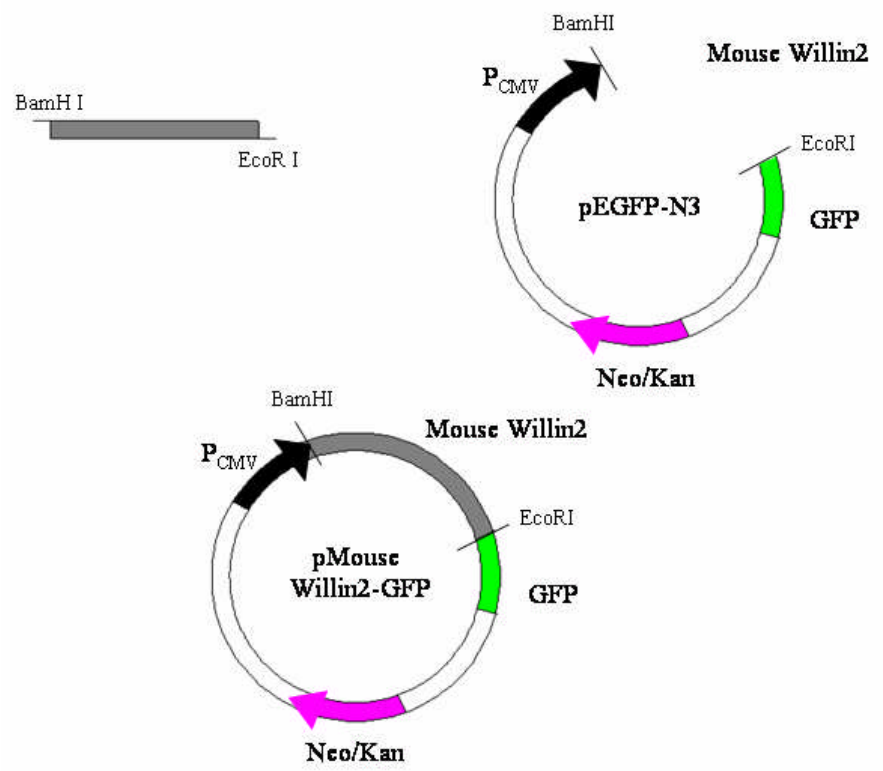

Figure 4.12. Cloning strategy for pMouse Willin2-GFP. The Mouse Willin2 gene was amplified by PCR from the cDNA Image clone and ligated into pEGFP-N3.

This construct was transfected into COS-7 cells to test its expression. First, cells were harvested for SDS-PAGE and Western blotting using the anti-GFP antibody to verify fusion protein expression. Figure 4.13 shows that Mouse Willin2-GFP is detected by anti-GFP and like Willin runs lower than the predicted approximately 99kDa fusion protein.

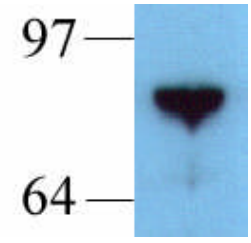

Figure 4.13. COS-7 cells expressing Mouse Willin2-GFP were harvested in PBS and separated on a 4-12% Bis-Tris gel. The subsequent nitrocellulose membrane was probed with anti-GFP 1:1000 and secondary anti-mouse-HRP 1:5000.

Cells grown on coverslips were also transfected and fixed for confocal microscopy. Figure 4.14 shows the expression of Mouse Willin2-GFP, which is strikingly different from Willin. Cytoplasmic distribution is more evenly spread, and there is heavy nuclear staining, while little to no membrane staining is observed.

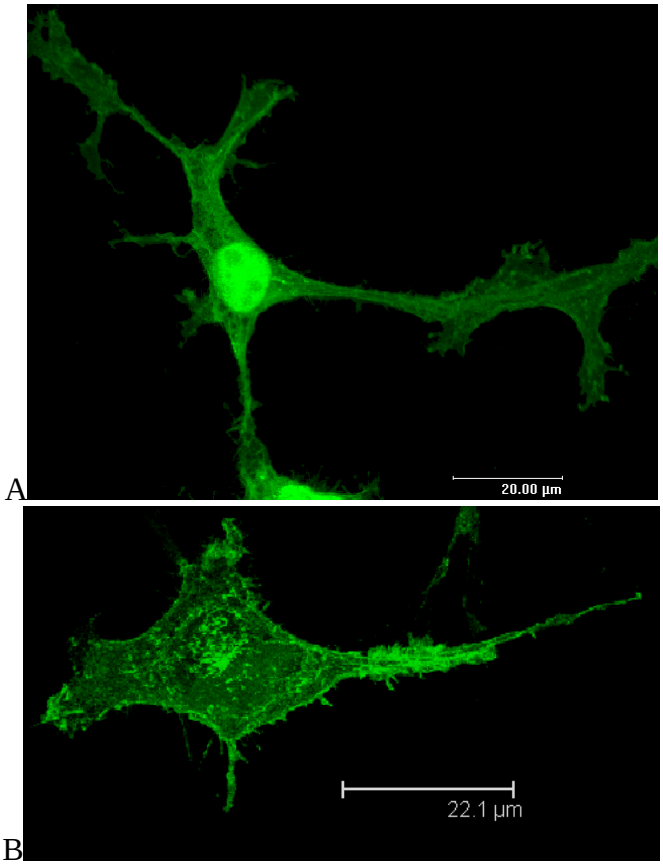

Figure 4.14. A) COS-7 cell expressing Mouse Willin2-GFP. Maximum projection of 14 optical sections acquired with a Leica TCS4D confocal microscope, assembled using LCS Lite V2.5 Build 1347 and cropped with Adobe Photoshop 7.0 (no other post-processing). B) COS-7 cell expressing Willin-GFP. Maximum projection of 10 optical sections acquired as above.

4.7. Discussion

4.7.1. The effect of Willin on cultured cells

In this laboratory, it had been anecdotally observed that overexpression of Willin-GFP seemed to cause a high level of cell death after 48 hours compared to controls with transfection reagent only. A large tag such as GFP also raises concerns that the protein will not be properly targeted, a concern compounded by the problems of overexpression. To address some of these questions and to have an additional tool for the characterisation of Willin, a pWillin-FLAG construct was produced as described in section 4.2. This fusion protein, with only a very small tag, displays a comparable intracellular distribution to that of Willin-GFP (Figure 4.3), and again, casual observation of transfected cells more than 48 hours post-transfection seemed to show increased levels of cell death compared to control. This data eased fears about the effect of the GFP tag alone, but did not answer questions about overexpression, and thus an attempt was made to produce stable cell lines expressing both Willin-GFP and Willin-FLAG (section 4.3). Unfortunately, these cell lines were unsuccessful, with low transfection rates, slow recovery and most G-418-resistant cells expressing little or no detectable protein 1-2 months post-transfection. This suggests that cultured cells are not able to tolerate long-term expression of Willin, adding further evidence that Willin may be a growth suppressor. Indeed, attempts to create stable cell lines with Merlin1 have had similar outcomes due to the growth suppressive functions of that protein (Wally Ip, personal communication).

While this circumstantial evidence of Willin's function was interesting, it was necessary to quantify the effect. To that end, cell counts were performed comparing Willin-GFP with 2 related proteins: Merlin1-GFP, a known growth suppressor, and GFP-Moesin, a known growth promoter. COS-7 cells were transfected with one of

the three proteins and blind cell counts performed. Though the sample numbers are still small, these initial counts indicate a real effect of Willin overexpression increasing the rate of apoptosis in cultured cells (Figure 4.6). Further counts must be done to achieve statistical validity of these results, and a more objective test for apoptosis, such as the TUNEL assay, performed as well. It would also be worthwhile including GFP alone in the cell counts, in order to establish baseline toxicity of the tag and provide a better idea of whether Merlin1 and Willin are causing increased cell death compared to GFP; this will also address whether Moesin might have a protective role compared to GFP. It is also worth noting that an initial cell viability test using the MTT assay was performed by Jessica Davis, and showed reduced viability in cells expressing Willin-GFP compared to cells expressing Merlin1-GFP or GFP alone. Again this would need to be repeated with all proper controls in place, but provides more circumstantial evidence to support the hypothesis that Willin expression can increase levels of cell death.

4.7.2. Willin-DsRed2

A Willin construct with a red fluorescent tag was desireable for co-localisation studies with other proteins, such as Merlin1 and Ezrin, for which we have GFP-tagged versions. Such co-localisation experiments have been done for DMerlin and expanded using antibodies (McCartney et al., 2000), but as strong antibodies are not available in this case, fluorescent tags provide the most straightforward possibilities. Unfortunately, DsRed2 was not found to be an appropriate tag for this purpose, but subsequently a pWillin-mCherry construct has been produced by Andrew Robertson, and this looks more promising for co-expression experiments.

4.7.3. Willin interaction with lipid rafts

Three different methods (RIPA extraction, DRM subfractionation and Optiprep subfractionation) have shown that Willin can localise to detergent resistant membranes. Further experiments with antibodies against lipid raft-specific and caveolae-specific proteins are required to determine which DRM subtype contains Willin. The issue of overexpression must also be addressed, as it cannot be ruled out that this DRM localisation is an overexpression artifact until native protein has been tested in the same way. The lack of a strong antibody precludes this at the moment, though the weakly expressing stable cell lines may be suitable for this purpose if used at an early enough passage number. It is interesting that neurofascin155 has been found in lipid rafts, both by other groups (see section 1.2.4.2) and in our hands (data not shown), as this could provide a physiological location for the interaction of neurofascin155 and Willin.

PI(4,5)P2 has also been found in cholesterol-enriched domains (Epand et al., 2004), providing another possible lipid raft binding partner for Willin; GST-Willin had previously been shown to interact with phospholipids (Gunn-Moore et al., 2005), but it is not known how this interaction takes place. Barret et al. (2000) determined that a conserved motif in the ERMs, identified as $KK(X)_nK/RK$, was responsible for $PI(4,5)P_2$ binding. A comparable site was identified in Willin at residues 327-336: **RK**LEENEE**KK**. To determine whether this sequence was involved in lipid binding, three sequentially truncated constructs were cloned, with the digits indicating number of amino acids present: pGST-WillinΔ239, containing only the FERM domain of Willin; pGST-WillinΔ322, truncated just before the putative site; and pGST-WillinΔ356, truncated shortly after the putative site. Figure 4.15 shows the cloning

strategy adopted for these constructs. With pWillin-GFP as a template, PCR products were made using the following primers:

Forward primer for all (contains a BamHI sequence):
HGex-F: 5' CGGGATCCATGAACAAATTGAATTTTC 3'

Reverse primers (all contain EcoRI sequence and stop codon TCA):
Willin239rev: 5' CGGGAATTCTCACAGCGATGCTTCAATTTC 3'
Willin322rev: 5' CGGGAATTCTTCAGACAGGCTGCAG 3'
Willin356rev: 5' CGGGAATTCTCATTTTTCCAGCTG 3'

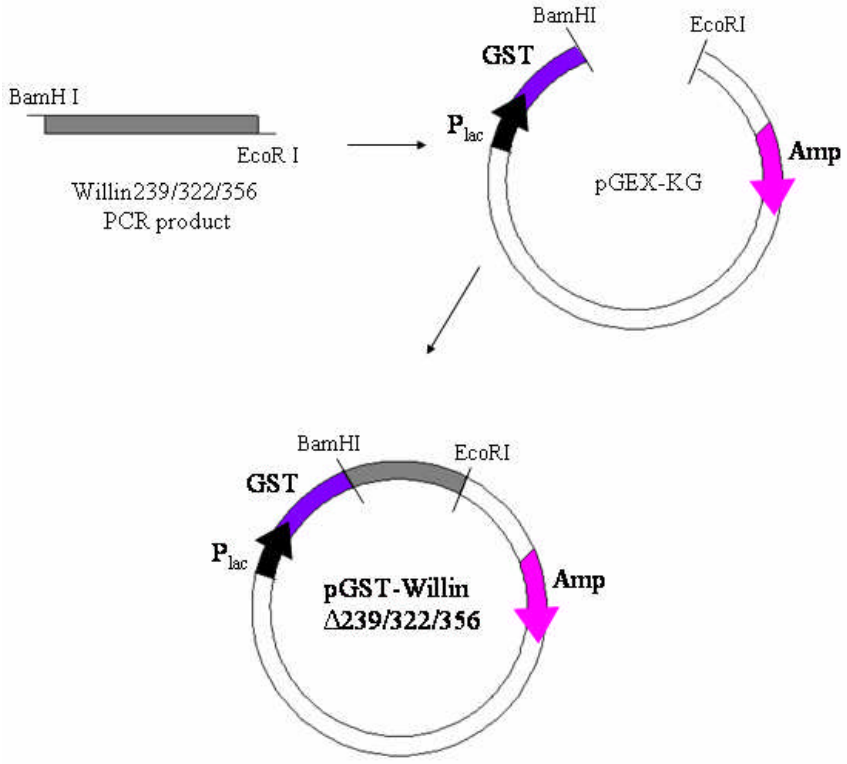

Figure 4.15. Cloning strategy for truncated pGST-Willin constructs. With pWillin-GFP as a template, three PCR products were obtained for Willin239, Willin322 and Willin356, with BamHI and EcoRI restriction sites at the 5' and 3' ends respectively. Each PCR product was ligated into a pGEX-KG vector.

Complete constructs were verified by restriction digest analysis and sequencing, then transformed into BL21/DE3 *E. coli* for expression. The final fusion proteins were predicted to have molecular weights of approximately 56kDa (GST-WillinΔ239), 66kDa (GST-WillinΔ322) and 70kDa (GST-WillinΔ356) and pI of around 9 (Expasy Compute pI/MW tool). Whole cell extracts of uninduced (U) and induced (I) BL21/DE3 were separated on a 4-12% Bis-Tris gel and detected by

Western blot as usual with the pAP913[4] antibody. Figure 4.16 shows that all three proteins (indicated by arrows) are expressed, though as with other Willin fusion proteins, have a lower observed molecular weight than predicted.

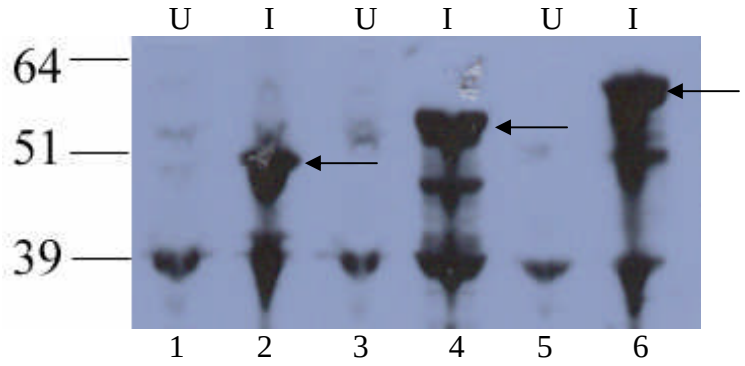

Figure 4.16. Whole cell extract from IPTG induced BL21/DE3 pGST-Willin cells was separated on a 4-12% Bis-Tris SDS-PAGE gel. The subsequent nitrocellulose membrane was probed with pAP914[3] 1:1000 and secondary anti-rabbit-HRP 1:2000 (Santa Cruz). GST-WillinΔ239 (Lanes 1 and 2), GST-WillinΔ322 (Lanes 3 and 4) and GST-WillinΔ356 (Lanes 5 and 6) samples show high expression levels when induced by IPTG.

Although the three proteins were successfully expressed, purification and storage have been more problematic, and due to time constraints, lipid binding assays have not yet been performed. However, these constructs can be used in fat blot assays (Gunn-Moore et al., 2005) and, if successful, similar constructs could be produced for use in mammalian systems to see if lipid raft association changes.

It should be noted that the lipid raft hypothesis is not without controversy due to its inconsistency of application; the localisation of some proteins to lipid rafts has been controversial because some methods have placed them within rafts while others have placed them elsewhere, there is no standard for detergent:lipid ratios or even necessarily which detergents are best suited for raft extraction, and some data even suggest that detergent extraction itself *creates* separate lipid domains that are not natively present (Edidin, 2003). Detergent-free methods (Macdonald and Pike, 2005) are available, howevever, so further investigations should also include such a method.

4.7.4. Initial characterisation of Willin2

The identification of a novel splice variant of Willin was intriguing, particularly as the octapeptide (VRQYEVTW) difference between the human forms of the two proteins is situated part way through the sequence to which the antibodies 914^3 and αWR were designed (see section 3.5.1). Unfortunately a human Image clone was not available, so a mouse clone was obtained instead. Though there are some substitutions in individual amino acids throughout the sequences, the mouse version is highly conserved compared to the human sequence (see Appendix 1), particularly in the region around the octapeptide insert. It was therefore hoped that the mouse version could give some idea as to how the octapeptide addition might affect the behaviour and distribution of the protein. Initial imaging shows that this version may have a stronger nuclear localisation than the 614 amino acid form, though why this might be the case is unknown. Quantitative analysis of cells expressing both versions must be performed to see if the localisation difference is statistically signficant. Short sequences can be very important to protein localisation, for example the RSLE motif in L1 (see section 1.2.1) found only in neurons; it is possible that in certain cell types this motif is expressed, which could explain why 914^3 and αWR have been largely unsuccessful in detecting native proteins. Difference in localisation and behaviour between human and mouse forms of Willin2 cannot be ruled out, however, so it will be desireable to obtain a human clone when one becomes available.

4.8. Conclusion

The continued study of Willin localisation and behaviour in cells has identified several interesting possibilities for further investigation. Due to technical challenges and time constraints, only initial experiments have been performed for these lines of inquiry, but with the tools produced during the course of this project it is hoped that future work will elucidate the mechanisms of action only partially revealed so far.

CHAPTER 5: INVESTIGATIONS INTO THE BINDING PARTNERS OF WILLIN

Chapter 5: Investigations into binding partners of Willin

5.1 Introduction

Proteins do not work alone to produce their effects, but are part of signalling cascades and protein complexes that are constantly adjusting to stimuli to affect cellular processes. Elucidating binding partners of a novel protein can provide clues to its function and behaviour. In the case of Willin there were two goals: first, to confirm three putative binding partners: neurofascin 155, actin and Merlin; and second, to screen for novel binding partners. As Willin was first discovered in a yeast two-hybrid screen of neurofascin 155, it was desired to confirm this reaction. Also, Willin co-localises with actin in cultured cells and the ERM proteins are known to bind actin, so this also seemed a likely interaction to study. Finally, the *Drosophila* homologue of Merlin interacts with Expanded, the putative *Drosophila* homologue of Willin; thus, it may be expected that the mammalian versions could also interact. Several biochemical methods were used to investigate these interactions, including tandem affinity purification (TAP) and co-immunoprecipitation. To screen for novel partners, two methods were to be attempted, namely yeast two-hybrid and TAP.

5.2 Confirmation of L1 family binding using the yeast two-hybrid method

The yeast two-hybrid method of detecting protein-protein interactions in yeast nucleus was first developed in 1989 by Fields and Song as an *in vivo* alternative to biochemical methods. The yeast *Saccharomyces cerevisiae* uses the transcriptional activator Gal4 to regulate expression of enzymes involved in galactose utilisation; Gal4 has two separate functional domains, one that recognises and binds to the promoter and another that activates transcription. These components, however, do not need to be

expressed on the same protein to be operative, and it is this property that is exploited by the yeast two-hybrid method. One gene of interest can be expressed in a fusion plasmid containing the DNA-binding domain, while a second gene or cDNA library can be expressed in a fusion plasmid containing the activation domain; only when both are present and interacting will the two domains be in close enough proximity to activate transcription of a reporter gene. In the case of these experiments, which are based on Clontech's MATCHMAKER Two-Hybrid system 2 (http://www.clontech.com/images/pt/PT3024-1.pdf), *lacZ* was used as the reporter gene, with its gene product, β-galactosidase, able to cleave 5-bromo-4-chloro-3-indolyl-D-galactopyranoside (x-gal) and yield a blue product when an interaction occurs (Figure 5.1).

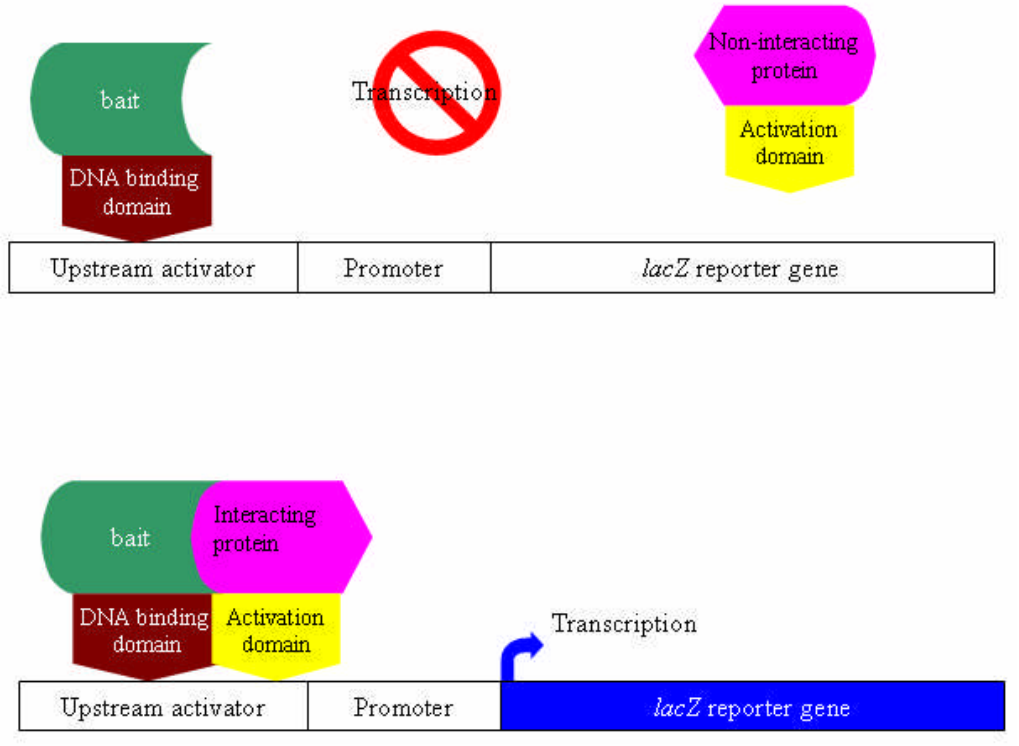

Figure 5.1. The yeast two-hybrid system. The DNA binding domain and activation domain of the Gal4 gene are expressed separately with the bait and prey proteins respectively. If the proteins interact, the two domains join to activate transcription of the lacZ reporter gene. Modified from Clontech figure found at: http://www.clontech.com/images/products/1198_fig1.gif

However, though this method has the benefit of allowing for transient and unstable interactions to be found in an *in vivo* environment (von Mering et al., 2002), it also has the drawbacks of a high proportion of false positives, perhaps as many as 50% (Deane et al., 2002), and that interactions, because they are occurring in the yeast nucleus rather than native localisations, may not have a physiological relevance (von Mering et al., 2002). While co-localisation studies can provide some support for an interaction detected by yeast two-hybrid, it is preferable to show an interaction by a biochemical method that also reflects the expression of proteins in a physiologically relevant setting.

Previous studies had indicated that the L1 family of receptors could bind, via different motifs, to the FERM domains of the ERM family of proteins (see section 1.2.6). It had been suggested that Willin could also bind to this family of receptors (Maria Hill, 2005), and so this required confirmation. In order to do this, a number of plasmids encoding for different parts of the L1 family were used. These consisted of: neurofascin155 C-terminus, L1 C-terminus, an L1 C-terminus isoform containing an RSLE motif, NrCAM C-terminus and NrCAM C-terminus isoform containing an RSLE motif. From the previous studies, it was expected that Willin would show an interaction with neurofascin and both forms of L1, but neither form of NrCAM.

The N-terminus of rat Willin (amino acids 1-341) had been previously ligated in frame into the pACT2 'prey' plasmid (Gunn-Moore et al., 2006). This construct was called '163ScII' and used in all experiments described. The cytoplasmic C-terminus of neurofascin ('NF-CT', amino acids 1065 to 1175) was ligated in frame into the pAS2-1 'bait' plasmid (Gunn-Moore et al., 2006). The cytoplasmic C-terminus of L1 ('L1-CT', amino acids 1143 to 1257) was ligated in frame into the pAS2-1 'bait' plasmid (Davey et al., 2005). Dickson et al. (2002) had previously

shown that the presence of an RSLE motif in the C-terminus of L1 allowed for Ezrin binding; this motif is spliced out of L1 in non-neuronal cells, but a naturally occurring isoform including RSLE exists and is differentially sorted to the growth cones of neurons (Kamiguchi et al., 1998). It was thought that the RSLE motif might cause a stronger interaction between L1 and Willin. A pAS2-1 'bait' plasmid encoding the L1 C-terminus with RSLE motif ('L1-RSLE', amino acids 1146-1259) was previously produced by Maria Hill. NrCAM had been found not to bind Ezrin, contrary to expectations based on co-localisation studies. This is thought to be due to an amino acid substitution in the potential FERM binding site of NrCAM, which introduces a proline and thus a cyclic pyrrolidine side group that causes a 'kink' in the structure of the protein (Hill, 2005). However, to establish whether Willin was similarly affected, the experiment was repeated using a pAS2-1 'bait' plasmid encoding the NrCAM C-terminus ('NrCAM-CT', amino acids 1102-1215), produced by Maria Hill. Like L1, NrCAM also has naturally occuring isoforms with an RSLE motif present; this exon is also usually spliced out (Dry et al., 2001), but the chick version of NrCAM preserves the RSLE motif, and was thus used to clone into a pAS2-1 'bait' plasmid by Maria Hill ('NrCAM-RSLE', amino acids 1166-1260). The C-terminus of NrCAM in pAS2-1, described above, co-transformed with full-length (amino acids 1-835) SAP102 subcloned into the pACT2 vector, was used as a positive control, as these are known interactants (Davey et al., 2005). A summary of the constructs is shown in Figure 5.2.

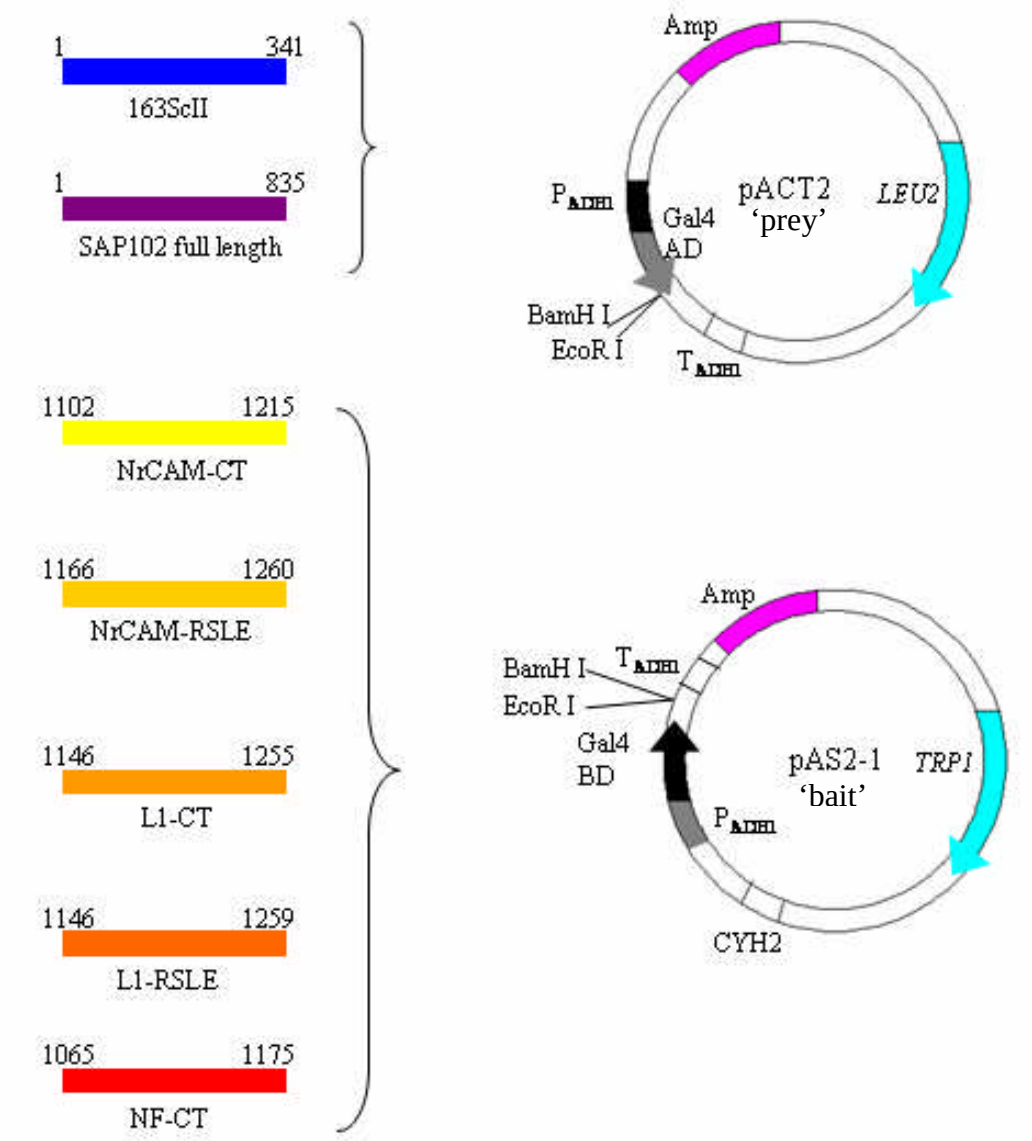

Figure 5.2. 163ScII (amino acids 1-341) and full-length SAP102 (amino acids 1-835) were subcloned in frame into the BamH I and EcoR I sites of pACT2 (Clontech) to generate GAL4 activation-domain fusion proteins. NrCAM-CT (amino acids 1102-1215), NrCAM-RSLE (amino acids 1166-1260), L1-CT (amino acids 1146-1255), L1-RSLE (amino acids 1146-1259) and NF-CT (amino acids 1065-1175) were subcloned in frame into the EcoR I and BamH I sites of pAS2-1 (Clontech) to generate GAL4 binding-domain fusion proteins.

Yeast cultures were grown as described in section 2.4.1 and transformed as described in section 2.4.2. The 163ScII construct was co-transformed with NF-CT, L1-CT, L1-RSLE, NrCAM-CT, NrCAM-RSLE or empty pAS2-1 vector (negative control). NrCAM-CT and SAP102 were co-transformed as a positive interaction control, and NF-CT and empty pACT2 vector were co-transformed as a negative

control. Transformed yeast were grown on $Trp^{-}Leu^{-}$ agar plates and left to grow for 2-5 days at 30°C; a filter lift assay positive control was also plated to ensure the X-gal was active. Once colonies were present, the filter lift assay was performed (section 2.4.3). Plates were checked at 30 minutes, 1 hour, then each subsequent hour up to 6 hours, and the appearance of blue colour noted at each time point. Table 5.1 shows a summary of the results of these experiments. The scoring system represents the time taken for the development of blue colonies in a β-galactosidase filter lift assay; ++++, < 30 min; +++, 30–60 min, ++, 1–2 h, +, 2–6 h, – > 6 h. 163ScII was found to interact strongly with NF-CT and weakly with both forms of L1. This is in contrast to Ezrin, which required the RSLE motif to bind L1, indicating that Willin probably binds to a different FERM binding motif of L1 (Cheng et al., 2005). Like Ezrin, Willin did not interact with NrCAM. Negative controls did not show colour change, but the NrCAM-SAP102 positive control showed the same level of interaction as previously reported (Davey et al., 2005).

	NF-CT (1065-1175)	L1-CT (1146-1255)	L1-RSLE (1146-1259)	NrCAM-CT (1102-1215)	NrCAM RSLE (1166-1260)	pAS2-1
163ScII	++++	++	++	-	-	-
pACT-2	-					
SAP102				++		

Table 5.1. The interaction of rat N-terminal Willin with C-terminal fragments of different members of the L1 family, based on colour change in a β-galactosidase filter lift assay. ++++, < 30 min; +++, 30–60 min, ++, 1–2 h, +, 2–6 h, – > 6 h

5.3 Confirmation of neurofascin 155 binding using the TAP method

With promising yeast two-hybrid data in hand, it was determined that further interaction studies were desirable, with two goals in mind: first, to confirm the positive interaction between Willin and neurofascin using biochemical studies in mammalian cells and co-localisation studies with fluorescent tags and immunocytochemistry; and second, potentially to screen for new binding partners. The TAP method was first developed by Rigaut, et. al. (1999) as a method of rapidly purifying protein complexes under physiological conditions as close to the native level of protein expression as possible. These complexes could then be analysed by mass spectroscopy to determine complex partners. The system began in yeast, but the principle has since been applied to mammalian cells as well (Knuesel et al., 2003; Forler et al., 2002). Unlike yeast two-hybrid, which only shows one interaction at a time, with TAP whole complexes can be identified by mass spectrometry. It was hoped that using this method, binding partners for Willin could be discovered and putative binding partners confirmed. With the TAP method a screen could occur in mammalian cell lines in a physiologically relevant setting and, if stable cell lines could be produced, an expression level closer to native than a transient transfection would allow. This method, if successful, takes less time than a yeast two-hybrid screen as well. Finally, it was hoped that by co-transfecting a TAP-tagged Willin with neurofascin 155, a pulldown experiment that was not dependant on antibodies could be performed.

5.3.1 Construction of the Willin-pIRESpuro2 CBP/TEV protein A plasmid

The pIRESpuro2 CBP/TEV protein A TAP vector was a kind gift from Professor Ron Hay. This vector has two affinity tags for purification: protein A,

which binds to IgG beads for the first purification step, followed by a tobacco etch virus (TEV) protease cleavage site to release the protein complex and then a calmodulin binding protein (CBP) sequence for the second purification (Figure 5.3). A C-terminal tag was selected to avoid any potential masking of the FERM domain, and the success of a C-terminal tag had already been shown with Willin-GFP.

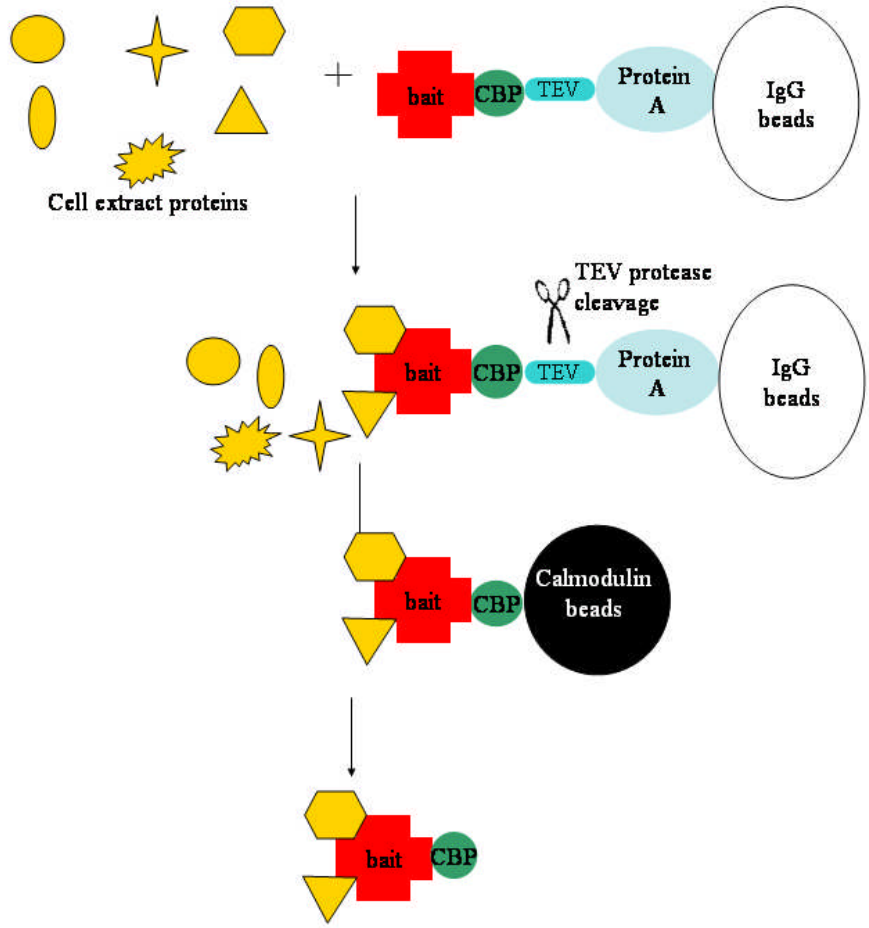

Figure 5.3. The tandem affinity purification method. Tagged bait protein is expressed in cells and the binding complex is purified in two steps; first, by Protein A binding to IgG beads, followed by TEV protease cleavage and second purification by calmodulin binding peptide binding to calmodulin beads.

To produce this DNA construct, a cloning strategy was developed and is outlined in Figure 5.4. PCR was done as described in section 2.1.1 with forward primer 5'ACCATGGACAAATTGAATTTTCATAAC 3' and reverse primer

5’TTTTCTTAAGCACAACAAACTCTGGAACTTC 3’, using the pWillin-GFP plasmid as a template. The ensuing PCR product was initially ligated into the pGEM-T vector for blue-white selection, and a plasmid containing the PCR product was identified and found to have the correct sequence. This construct was digested with SacII and blunted with DNA Polymerase I Klenow fragment as described in section 2.1.4 and the insert released by AflII digest. The TAP vector was digested with EcoRV to form a blunt end, and AflII, and the insert was to be ligated in frame into the TAP vector. Unfortunately, this final ligation step was unsuccessful, and no complete plasmid resulted.

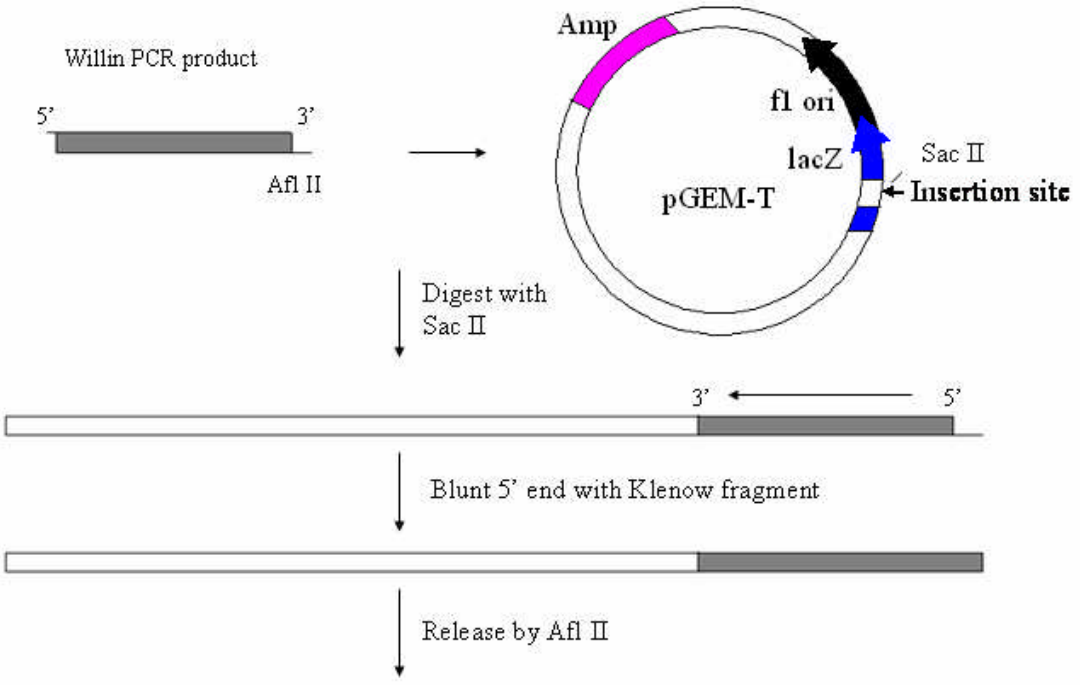

(Continued on next page)

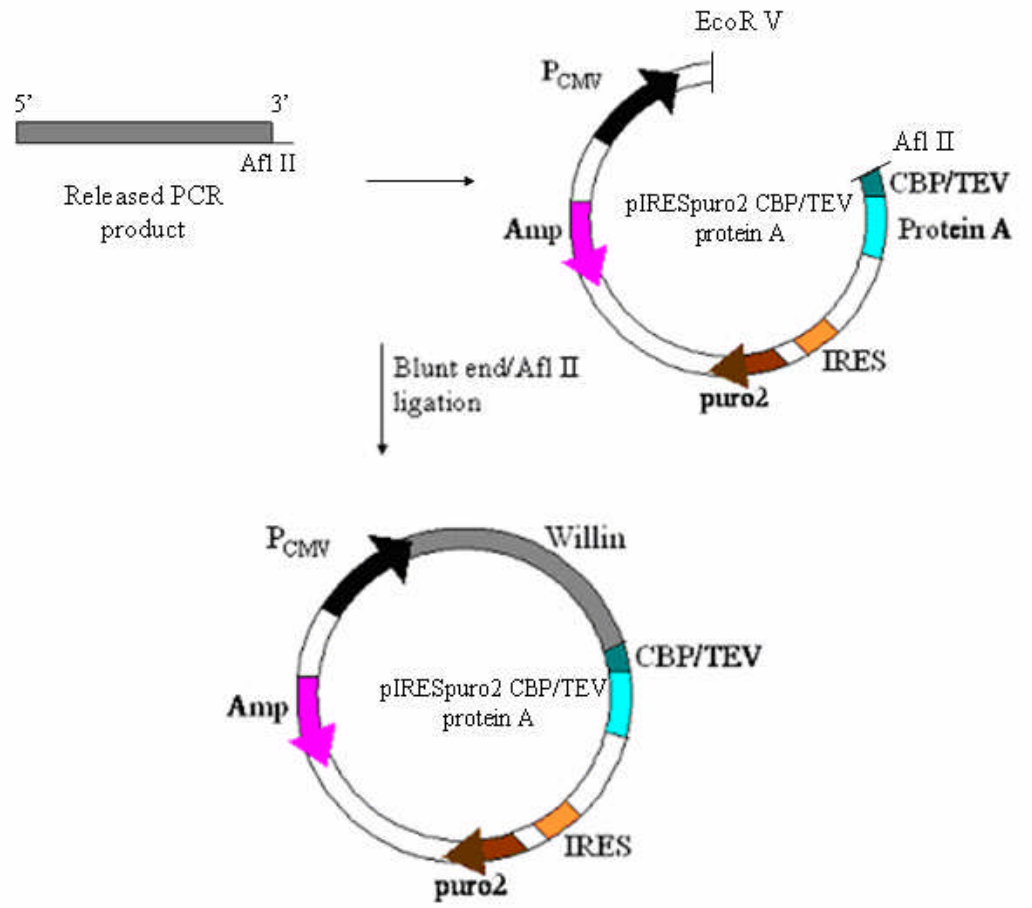

Figure 5.4. The initial cloning strategy for Willin-pIRESpuro2 CBP/TEV protein A. PCR was performed with pWillin-GFP as a template, and the ensuing PCR product was initially subcloned into the pGEM-T vector for blue-white selection. Once a plasmid was identified and found to have the correct sequence, it was digested with SacII restriction enzyme and the 5' end blunted with the DNA Polymerase I Klenow fragment. The insert was released from the plasmid by AflII digestion, and was to be ligated into the pIRESpuro2 CBP/TEV protein A TAP vector, which had been digested with EcoRV to produce a matching blunt end and AflII to produce a matching sticky end. However, this final ligation was unsuccessful.

Therefore, a new cloning strategy was developed and is outlined in Figure 5.5. Primers were designed to allow cloning with ClaI (5' CCATCGATATGGACAAATTGAATTTTCATA 3') and NheI (5' CACTCGATCGCACAACAAACTCTGGAACTT 3'). ClaI is sensitive to Dam methylation, so to use this restriction site the TAP vector had to be transformed into the dam$^-$/dcm$^-$ strain of *E. coli* (New England Biolabs) and then digested with ClaI

and NheI. It was hoped that this insert could be ligated directly into the TAP vector, but again, despite several attempts, no complete plasmid was produced.

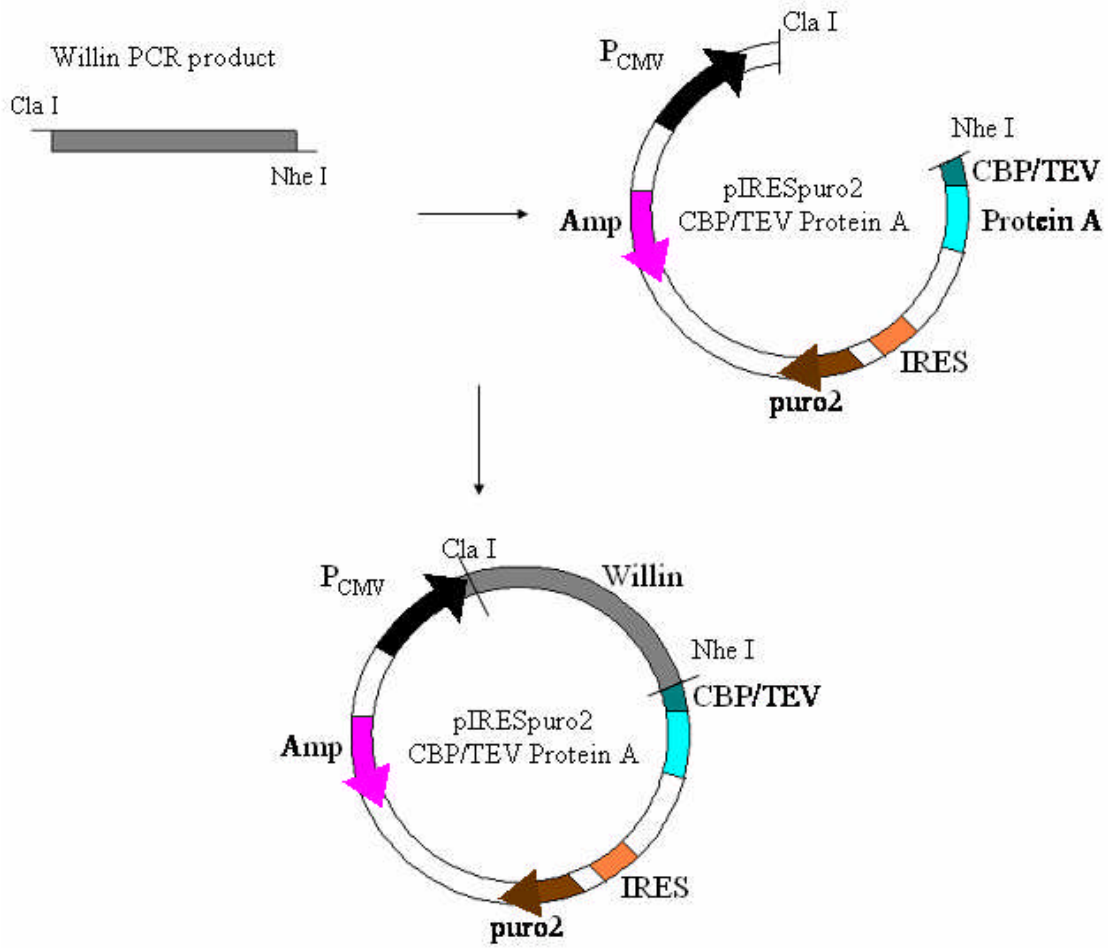

Figure 5.5. The second cloning strategy for Willin-pIRESpuro2 CBP/TEV protein A. The full-length Willin gene was to be ligated into the pIRESpuro2 CBP/TEV protein A TAP vector using the ClaI and NheI restriction sites, but the ligation was unsuccessful.

5.3.2 Construction of the Willin Stratagene CTAP A plasmid

Fortunately at this time a commercial TAP vector became available from Stratagene; this system had a more convenient multiple cloning site, allowing for easier cloning than before, and used streptavidin binding protein (SBP) and calmodulin binding protein (CBP) as the ~8kDa affinity purification tags, making a smaller tag without a cleavage step to reduce protein loss (Figure 5.6).

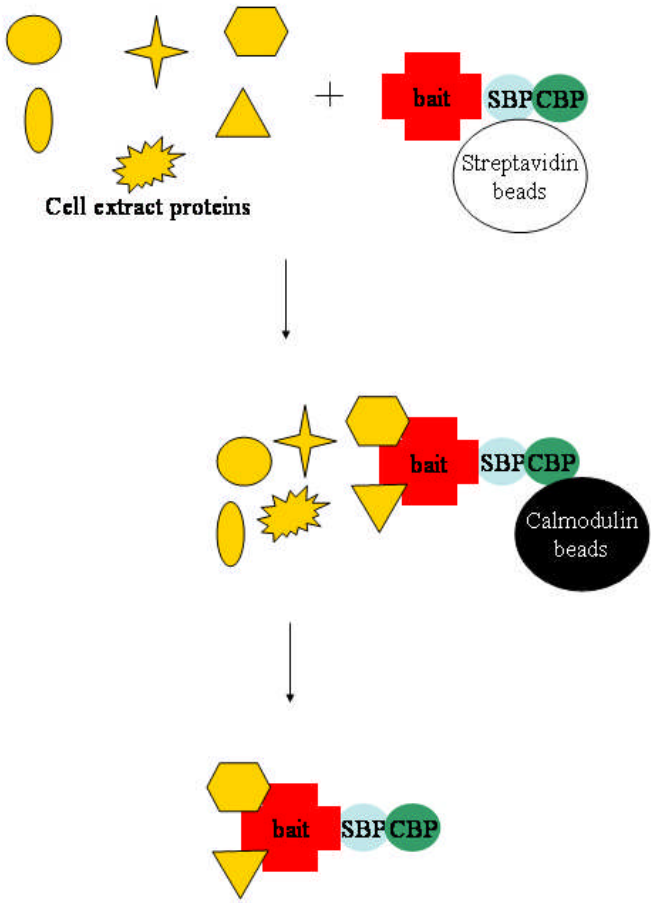

Figure 5.6. The Stratagene tandem affinity purification method. Tagged bait protein is expressed in cells and the binding complex is purified in two steps; first, by Streptavidin binding peptide binding to streptavidin beads, then by calmodulin binding peptide binding to calmodulin beads.

The multiple cloning site and frame for the pCTAP A vector is identical to that of the pCMV Tag4A vector used previously to make the pWillin-FLAG construct (see section 4.2.1); therefore the same inserts could be used to make a fusion protein with the SBP/CBP tag on the C-terminus of Willin without the need of performing PCR. First, pWillin-FLAG was digested with SacI and BamHI to release two fragments of the Willin gene. The shorter C-terminal fragment of the Willin gene was ligated into the pCTAP A vector, which had been digested with SacI and BamHI, and this partial plasmid was confirmed by restriction digest analysis. The vector was then digested again with only SacI and the longer N-terminal fragment of Willin was ligated into it.

Restriction digest analysis was used to confirm the presence of both fragments in the correct orientation, and the plasmid was also sequenced. This cloning strategy is described in Figure 5.7.

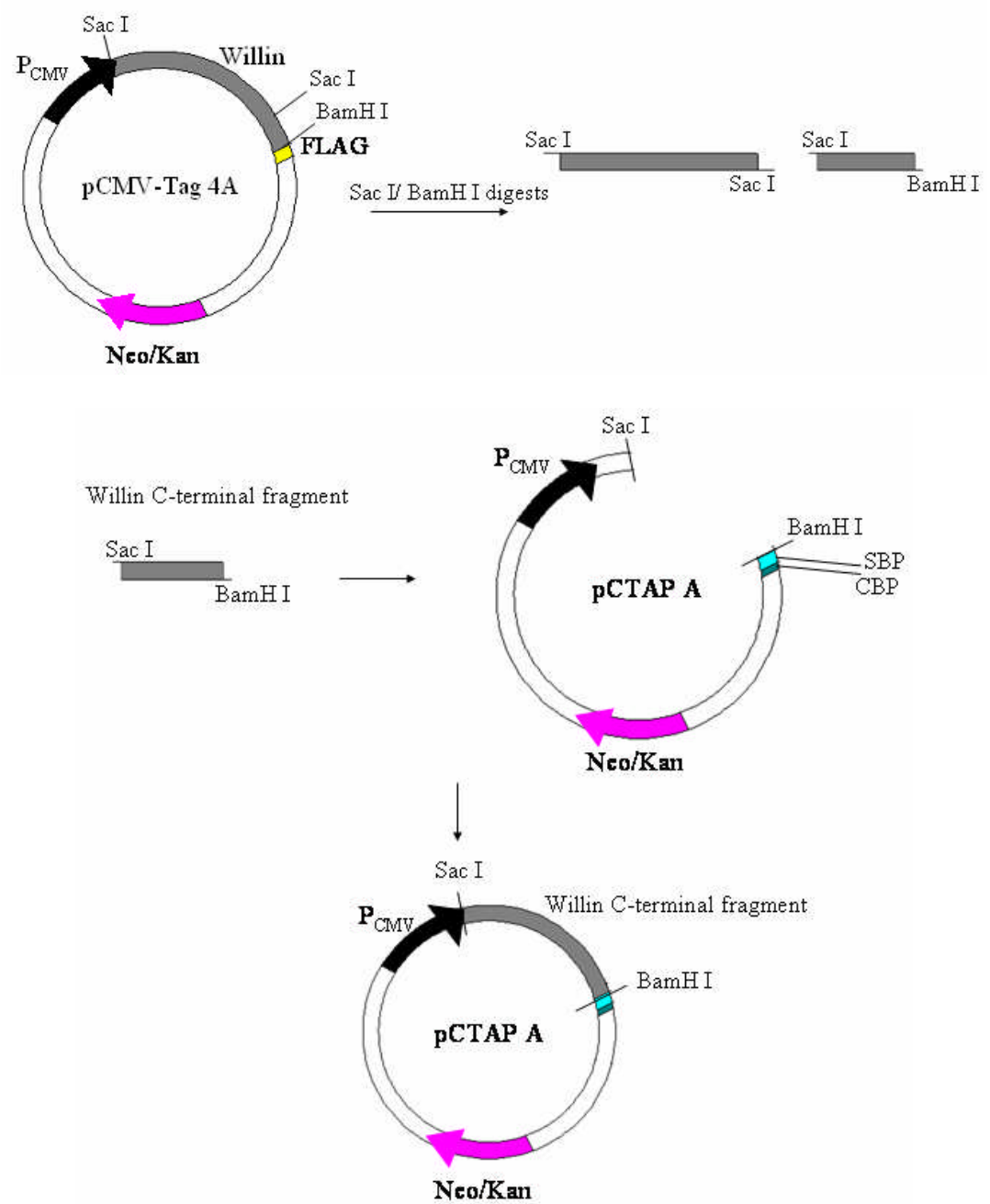

(Continued on next page)

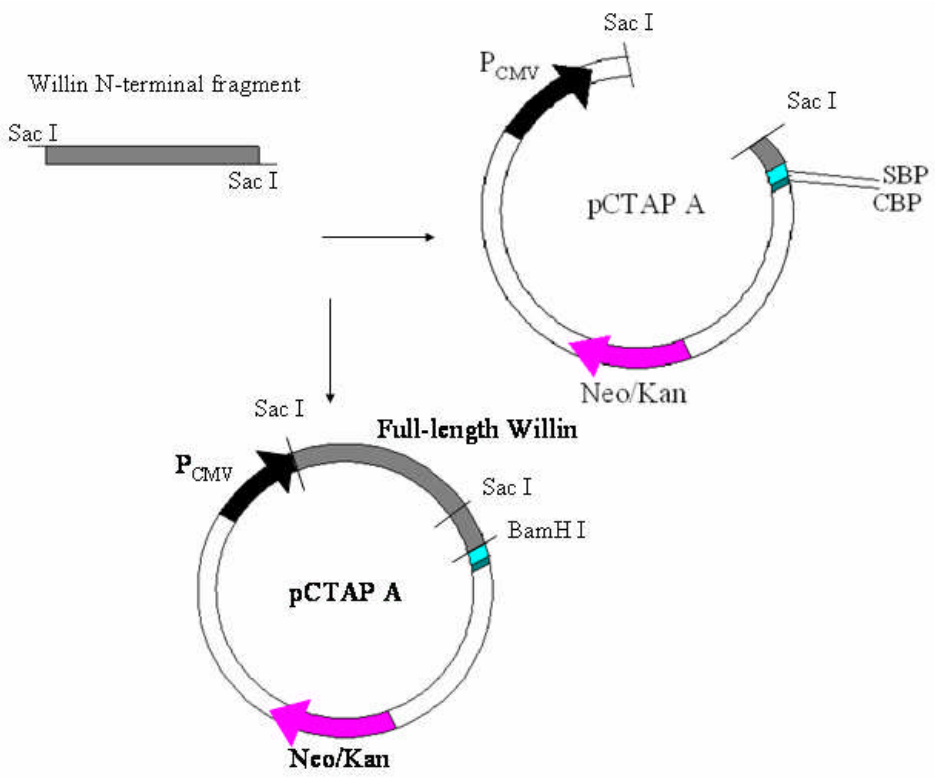

Figure 5.7. The cloning strategy for pWillin-CTAP A. pWillin-FLAG was digested with SacI and BamHI, producing 2 fragments of the Willin gene. The short C-terminal fragment was ligated first and confirmed to be present; the plasmid was then digested again with SacI and the longer N-terminal fragment ligated in. The full-length pWillin-CTAP A was confirmed by restriction digest analysis and sequencing.

Using this approach, the Willin was successfully ligated into pCTAP A. The plasmid was transfected into COS-7 cells and expression tested by Western blotting using an anti-CBP antibody (Upstate); expression was confirmed in the form of a ~60kDa band (Figure 5.8). As usual, the band is lower than the predicted ~80kDa, but is about the same size as the Willin-FLAG protein tends to be (see Figure 4.2).

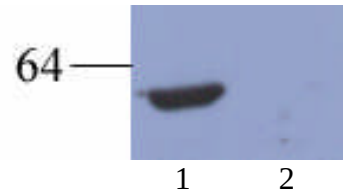

Figure 5.8. Willin-CTAP transfected (Lane 1) and untransfected (Lane 2) COS-7 whole cell extracts were separated on a 4-12% Bis-Tris gel and the subsequent nitrocellulose membrane probed with anti-CBP 1:500 and secondary anti-rabbit-HRP 1:2000.

With expression thus confirmed, a small-scale purification was then performed to test that the protein could be purified and detected by Western blot. Purification was carried out as described in section 2.3.15, with samples taken of the input lysate (A), the insoluble cell debris pellet (B), the streptavidin-unbound lysate (C), the streptavidin-purified lysate (D), the calmodulin-unbound lysate (E), the calmodulin-purified lysate (F) and the boiled calmodulin resin (G). As can be seen in Figure 5.9, expressed protein was detected in both the soluble lysate and insoluble pellet, and in the streptavidin-unbound lysate. Unfortunately, no protein was detected in any of the subsequent purification steps, implying that the protein did not bind to the streptavidin resin. Repeated attempts to bind the protein to the resin failed, and this construct was abandoned.

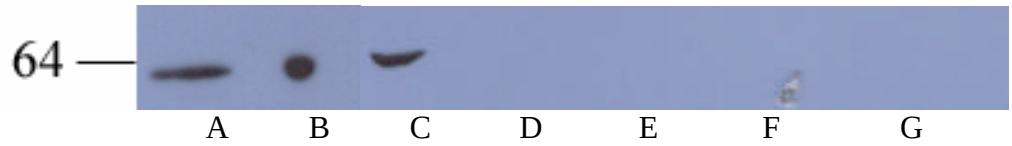

Figure 5.9. Samples A-G as described of the TAP purification were separated a 4-12% Bis-Tris gel and the subsequent nitrocellulose membrane was probed with anti-CBP 1:500 and secondary anti-rabbit-HRP 1:2000.

5.3.3 Construction of the WillinΔ239 Stratagene NTAP A plasmid

It was speculated that perhaps the majority of the Willin-CTAPA protein was insoluble, which left too little protein to carry through a full purification; that some unknown property of the full-length protein was somehow masking the SBP binding site; or that the C-terminal fusion tag was causing a problem. In the meantime, several truncated versions of Willin tagged with GST had been cloned (see section 4.6) and the truncated version found to be more soluble than the full-length version. Therefore a new construct was made to take advantage of this property, using a 239 amino acid truncated version of Willin that contained the complete FERM domain of

Willin. An insert already existed from the pGST-WillinΔ239 construct (see section 4.6) that could be ligated into the N-terminal fusion tag version of the Stratagene TAP system, thus avoiding PCR and allowing us to test whether the location of the tag made a difference. Therefore a cloning strategy was performed as described in Figure 5.10.

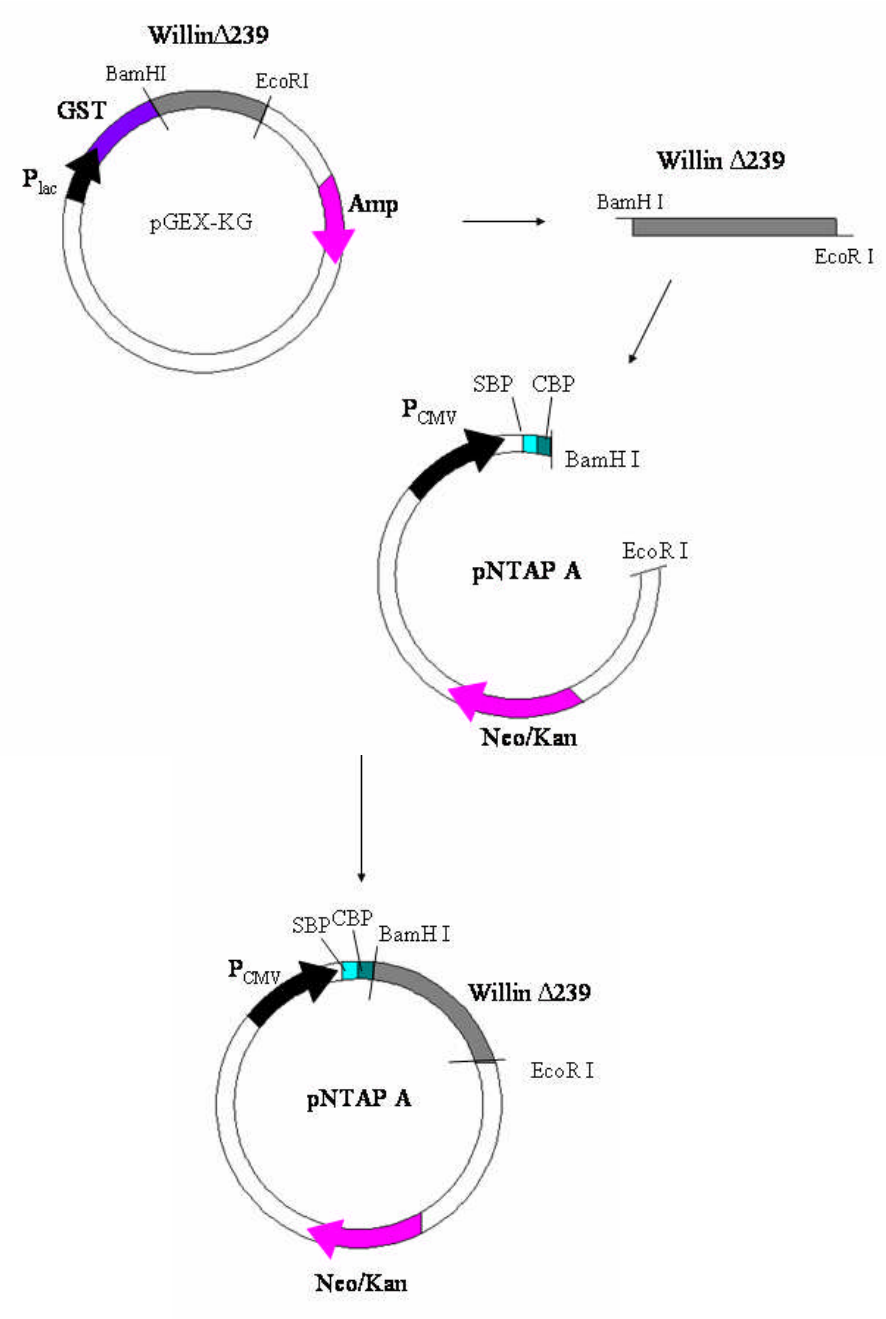

Figure 5.10. The cloning strategy for pWillinΔ239-NTAP A. WillinΔ239 was digested from pGST-WillinΔ239 with BamHI and EcoRI and ligated directly into pNTAP A.

Again a small-scale purification was carried out and protein detected by anti-CBP antibody as in section 5.3.2. Samples were taken of the whole cell extract (A), the input lysate (B), the insoluble cell debris pellet (C), the streptavidin-unbound lysate (D), the streptavidin-purified lysate (E), and the boiled streptavidin resin after elution (F). It was expected that there would be no protein in lane D and that most of the protein would carry over into lane E. Although more soluble protein appeared to be present, the expressed protein still did not bind to the streptavidin resin (Figure 5.11). Completion of remaining purification steps and a Western performed on these samples produced only a blank film (data not shown), indicating that the protein did not carry through to the last purification steps. Due to the failure of this approach as well, this method was discarded. Interestingly, the apparent molecular weight of this truncated construct is larger than the predicted ~40kDa molecular weight of the protein; this is thought to be due to the high pI of 9.2, as predicted by ExPASy theoretical pI tool (http://expasy.org/tools/pi_tool.html).

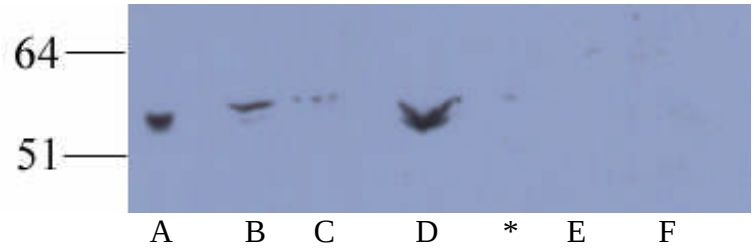

Figure 5.11. Samples A-F as described of the TAP purification were separated a 4-12% Bis-Tris gel and the subsequent nitrocellulose membrane was probed with anti-CBP 1:500 and secondary anti-rabbit-HRP 1:2000. The lane marked * was left blank due to overflow from lane D.

5.3.4 Confirmation of binding by pCMV/NTAP neurofascinCT

Despite the failure of producing a successful Willin construct for use in TAP studies, previously a TAP plasmid construct encoding the C-terminus of neurofascin155 had been successfully employed to show that it could co-purify with a

FLAG-tagged Ezrin chimeric protein when they were co-expressed in cells (Gunn-Moore et al., 2006). Therefore it was hoped that a similar experiment could be performed by co-transfecting the pCMV/NTAP neurofascinCT plasmid with pWillin-FLAG. These constructs were co-transfected into HEK-293 cells; additionally, empty pCMV/NTAP was co-transfected with pWillin-FLAG as a negative control and pFLAG-Ezrin was co-transfected with pCMV/NTAP neurofascin155 as a positive control. The shortened protocol was performed as described in section 2.3.16, with aliquots taken for analysis at the following points: input lysate, IgG-unbound supernatant, TEV cleavage supernatant and boiled rabbit IgG beads. The input protein in all of the samples is only detected in the unbound supernatant fraction, indicating that there was no binding (Figure 5.12). However, because the positive control also did not show binding, it is thought that the CMV/NTAP neurofascinCT protein probably did not bind the IgG beads. The reasons for this are unknown, but due to time constraints, further optimisation of the protocol could not be performed.

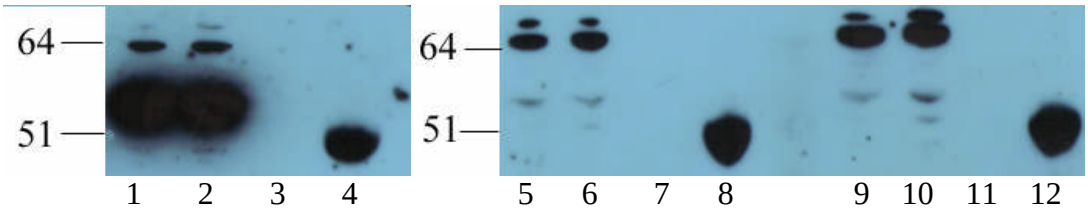

Figure 5.12. Aliquots were taken as described during the TAP purification process and separated on a 4-12% Bis-Tris gel. The subsequent nitrocellulose membrane was probed for FLAG-Ezrin and Willin-FLAG with anti-FLAG 1:500 and secondary anti-mouse HRP 1:5000. FLAG-Ezrin was detected in the input and IgG-unbound supernatant aliquots (Lanes 1 and 2) but not the TEV cleaved supernatant (Lane 3). Willin-FLAG was also detected in the input and IgG-unbound supernatant aliquots when co-transfected with either empty pCMV/NTAP (Lanes 5 and 6) or pCMV/NTAP-neurofascinCT (Lanes 9 and 10), but not the TEV cleaved supernatant in either (Lanes 7 and 11). Lanes 4, 8 and 12 show only IgG heavy chain, indicating the proteins did not remain bound to the beads after TEV cleavage.

5.4 Confirmation of neurofascin 155 binding by FLAG co-immunoprecipitation

As the TAP experiments were unsuccessful, another *in vivo* method was attempted. HEK-293 cells were co-transfected with pcDNA3 neurofascin155 and either pWillin-FLAG or empty pCMVTag4A vector. FLAG co-immunoprecipitation was carried out as described in section 2.3.18. Briefly, Protein A from *Staphylococcus aureus* immobilised on polyacrylic beads was conjugated with FLAG M2 monoclonal antibody (Sigma) and tumbled with the cell lysate at room temperature for 2 hours. The beads were then washed 2 or 3 times in 1M NaCl IP buffer (50mM NaF, 50mM TrisHCl, 1mM NaPPi, 1mM EDTA, 1mM EGTA, pH 6.8; 1mM DTT and protease inhibitors added just before use) and again 2 or 3 times in 150mM NaCl IP buffer without disturbing the pellet. The entire bead-protein complex was then resuspended in IP buffer and protein sample buffer and heated at 70^{o}C for 10 minutes, then treated as usual for SDS-PAGE and Western blotting (see sections 2.3.7, 2.3.9 and 2.3.10). The subsequent nitrocellulose membrane was then probed for neurofascin155 with the anti-neurofascin antibody.

As can be seen in Figure 5.13, when neurofascin155 and Willin-FLAG were co-expressed, they were co-immunoprecipitated. However, neurofascin155 did not co-purify with the empty FLAG vector.

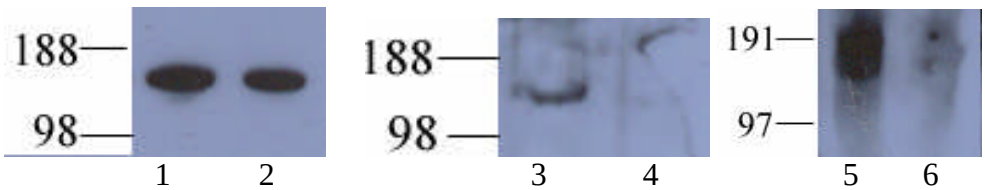

Figure 5.13. HEK-293 cells were transfected with neurofascin 155 and Willin-FLAG or neurofascin 155 and empty FLAG vector. Input lysate for neurofascin/Willin-FLAG (Lane 1) and neurofascin/FLAG (Lane 2) and co-immunoprecipitated product for neurofascin/Willin-FLAG (Lanes 3 and 5) and neurofascin/FLAG (Lanes 4 and 6) were separated on a 4-12% Bis-Tris gel. The subsequent nitrocellulose membranes were probed with anti-neurofascin 1:5000 and Santa Cruz secondary anti-rabbit-HRP 1:10,000 (A and C) or Pierce secondary anti-rabbit-HRP 1:10,000 (B).

5.5 Confirmation of neurofascin 155 binding by GST pulldown

For further biochemical confirmation of neurofascin155 binding to Willin, a GST pulldown experiment was performed as described in section 2.3.17. Briefly, HEK-293 cells were cultured on 2 X 90mm dishes and transfected with pcDNA3 neurofascin155, then harvested, lysed and sonicated in RIPA extraction buffer supplemented with protease inhibitor cocktail and PMSF. The lysate was pre-cleared by tumbling with glutathione sepharose beads and centrifuged to separate the beads. The cleared lysate was then divided into two aliquots and tumbled for 2 hours at 4^{o}C with glutathione sepharose beads conjugated with purified GST or GST-Willin. After five washes each of RIPA extraction buffer and PBS, the beads were boiled in 2X protein sample buffer and centrifuged at full speed to give the final complex. Figure 5.14 shows that neurofascin155 was present in the cell lysate input, but only bound to GST-Willin and not GST alone.

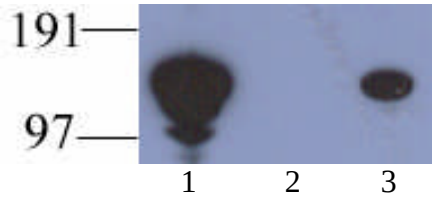

Figure 5.14. Samples of neurofascin155-transfected HEK-293 cell lysate input (Lane 1), precipitated with GST alone (Lane 2) and precipitated with GST-Willin (Lane 3) were separated on a 4-12% Bis-Tris gel. The subsequent nitrocellulose membrane was probed with anti-neurofascin 1:5000 and secondary anti-rabbit-HRP 1:10,000. To the left are shown the molecular weights (kDa).

5.6 Investigation of Merlin binding by FLAG co-immunoprecipitation

As the FLAG co-immunoprecipitation technique proved to be successful for neurofascin155, it was decided to investigate potential binding between Merlin and Willin-FLAG using this technique as well. HEK-293 cells were co-transfected with plasmids encoding for Merlin isoform 1 (pcDNA3 Merlin1) and either FLAG-tagged

Willin (pWillin-FLAG) or empty FLAG vector (pCMVTag4A). Samples were treated as above again in duplicate and probed with a polyclonal rabbit anti-Merlin primary antibody. Unfortunately, this antibody showed poor specificity and high background, as seen in Figure 5.15, and no conclusions could be drawn. A better antibody is required for further testing.

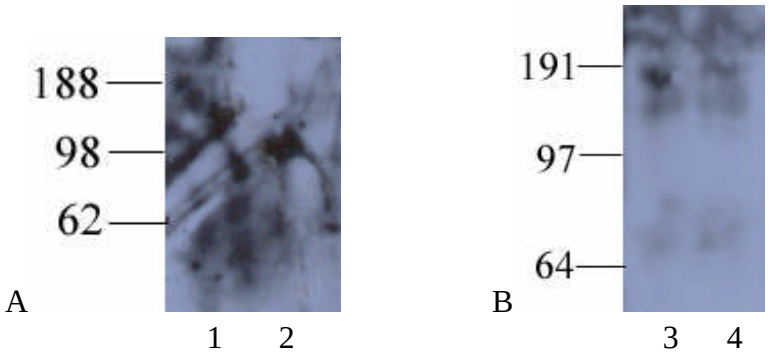

Figure 5.15. HEK-293 cells were transfected with Merlin isoform 1 and Willin-FLAG or Merlin isoform 1 and empty FLAG vector. Co-immunoprecipitated product for Merlin/Willin-FLAG (Lanes 1 and 3) and Merlin/FLAG (Lanes 2 and 4) were separated on a 4-12% Bis-Tris gel. The subsequent nitrocellulose membranes were probed with Santa Cruz anti-Merlin 1:1000 and Santa Cruz secondary anti-rabbit-HRP 1:10,000. To the left are shown the molecular weights (kDa).

5.7 The interaction of Willin with Actin

Previous studies have shown Willin to co-localise strongly with the actin cytoskeleton, but its localisation is not dependent on an intact cytoskeleton (Gunn-Moore et al., 2005). This is similar to Merlin, which retains a membrane association after cytoskeletal disruption (Stickney at al, 2004), but is different to Ezrin, which does change its localisation upon disruption of the cytoskeleton (Woodward and Crouch, 2000). Ezrin, Radixin and Moesin have a highly conserved sequence in the last 34 amino acids of their C-terminal domains which has been shown to bind actin, but other studies have also shown that actin binding can be mediated by residues 13-30 and 281-310 in the N-terminal FERM domain region (Martin et al., 1997; Roy et al., 1997); Merlin does not share the 34 amino acid ERM actin binding site, but the 281-310 amino acid region of the ERMs has homology with a sequence in Merlin at

residues 298-318, and this region has shown an actin-binding ability (Xu and Gutmann, 1998; James et al., 2001). A homologous region is not found in Willin, and the ERM C-terminal actin-binding site is also absent. Therefore, while Willin co-localises frequently with actin, it is not known whether there is a direct binding reaction *in vivo*, nor how this reaction might occur if it exists.

In order to determine whether Willin is capable of bind actin, the Actin binding protein spin-down assay for non-muscle actin by Cytoskeleton Inc. (Denver, Colorado, USA) was used as described in section 2.3.14. This kit allowed for a straightforward assay using purified GST-Willin (see sections 2.3.1-3) and interpretation by Coomassie-stained SDS-PAGE gel (see sections 2.3.7-8). Purified GST-Willin, purified GST and α-actinin were each incubated with F-actin; α-actinin is a known actin-binding protein and acted as a positive control, while GST acted as a negative control. GST-Willin was also incubated with buffer alone as another negative control. After a 1.5 hour centrifugation at 150,000*g*, the supernatants and pellets were separated and loaded onto a 4-12% Bis-Tris gel which was subsequently Coomassie stained (Figure 5.16A). Lanes B and F show GST-Willin with buffer alone; no actin was present in this mixture, and thus no protein has sedimented into the pellet fraction. Lanes C and G show GST-Willin with F-actin, lanes D and H show α-actinin with F-actin, and lanes E and I show GST with F-actin. Lane I, the negative control lane, shows a larger amount of actin (indicated by the arrowhead) in the pellet fraction than G, the GST-Willin lane. In addition GST, as indicated by the block arrows, is present in the supernatant but not the pellet, while what was thought to be GST-Willin, as indicated by arrows, is present in both the supernatant and pellet fractions. According to the interpretation instructions provided by the manufacturer, this combined evidence indicates that GST-Willin is binding to F-actin and causing

depolymerisation. However, it was noted that the size of GST-Willin is significantly lower than the expected molecular weight of 97kDa and lower than had been previously observed; this was initially thought to be due to the protein breaking down. To confirm whether GST-Willin was present, all samples containing GST-Willin or GST (lanes B, C, E, F, G and I), but not α-actinin (lanes D and H) were loaded onto a new 4-12% Bis-Tris gel and transferred to a nitrocellulose membrane for Western blot analysis using the αWR1 antibody as described in section 3.3 (Figure 5.16B). Of the supernatant fractions, only the lanes containing GST-Willin were detected by the antibody, and of the pellet fractions, only the one containing GST-Willin and F-actin was detected by the antibody.

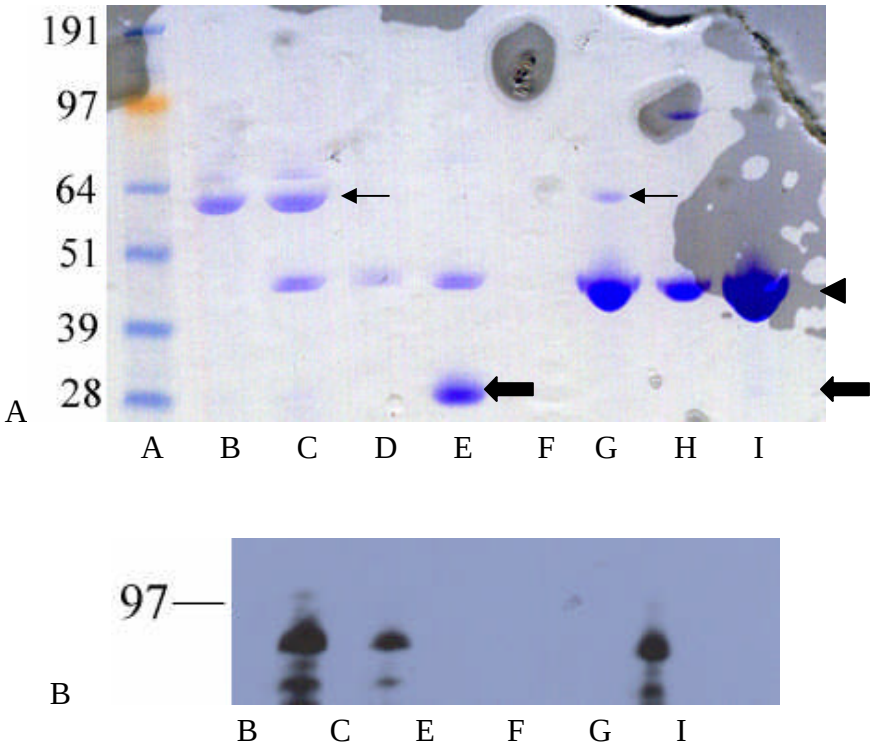

Figure 5.16. Results of the actin binding kit experiment. A) Lanes B-E are supernatant fractions and lanes F-I are pellet fractions. Lane A is the molecular weight marker. Lanes B and F show GST-Willin with buffer alone, lanes C and G show GST-Willin with F-actin, lanes D and H show α-actinin with F-actin (positive control) and lanes E and I show GST with F-actin (negative control). Block arrows indicate GST, normal arrows indicate GST-Willin and arrowhead indicates F-actin. B) Western blot of the samples containing GST-Willin and GST. The nitrocellulose membrane was probed with aWR1 1:1000 and secondary anti-rabbit-HRP (Abcam) 1:20,000. Lanes correspond to the samples in the Coomassie-stained gel.

5.8 Neurofascin 155 co-localisation studies with Willin, Ezrin and Merlin

Supporting evidence for potential interacting partners was sought by co-localisation studies. Protein interactions may be biochemically possible, but if the proteins are not in the same place at the same time in the cell, the interaction may not have physiological significance. A plasmid expressing a full-length untagged construct of neurofascin155 (pcDNA3 neurofascin155) was transfected into HEK-293 cells and probed with an anti-neurofascin antibody for these studies. A good antibody was not available for Willin and Merlin; therefore, GFP-tagged constructs of these proteins were used.

5.8.1 Willin co-localises with neurofascin 155

HEK-293 cells were grown on coverslips and co-transfected with pWillin-GFP and pcDNA3 neurofascin155 for 48 hours. Immunocytochemistry to detect neurofascin155 was then performed as described in section 2.2.8 using anti-neurofascin 1:2000 primary antibody and secondary anti-rabbit tagged with Alexa568 1:10,000. Coverslips were mounted on glass sides with Mowiol with DAPI and visualised under a Delta Vision microscope. Images were processed with Softworx (Applied Precision) software and ImageJ 1.38x.

Deconvolved fluorescence microscopy showed that Willin-GFP and neurofascin 155 partially colocalise within the membrane. Figure 5.17A shows a series of individual optical sections, with arrows pointing to regions of punctate membrane co-localisation of the two proteins; Figure 5.17B shows one optical section in closer detail, with arrows pointing to areas of co-localisation. Notably, co-localisation is not perfect, and at many points along the membrane, the two proteins appeared to be adjoining rather than overlaying (indicated by arrowheads).

A

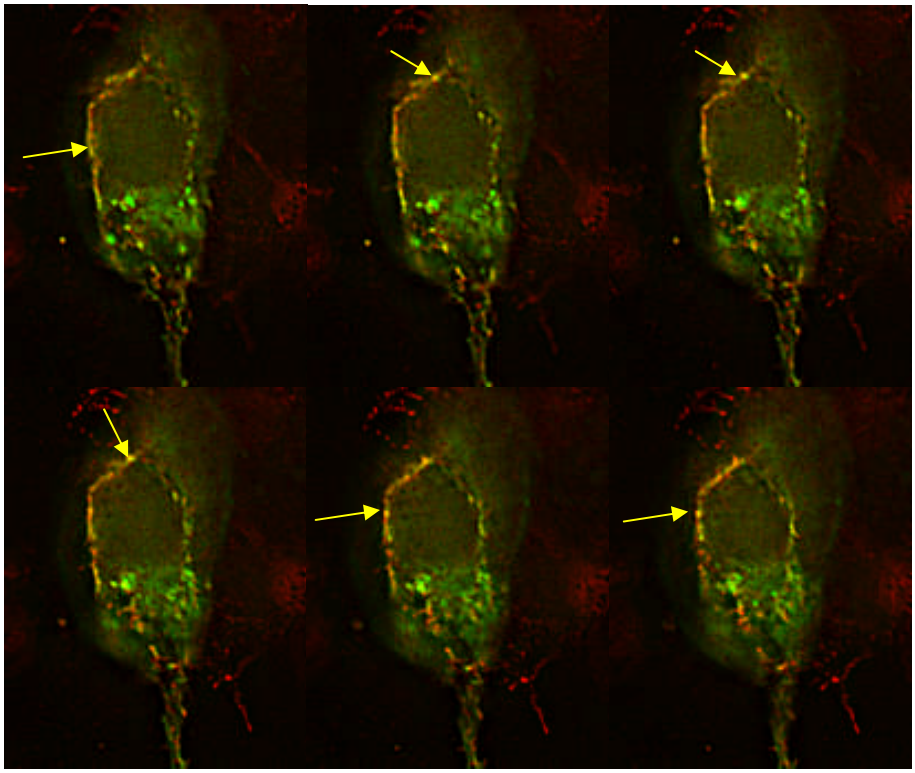

B

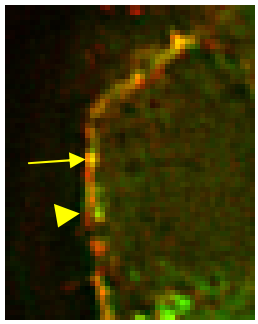

Figure 5.17. HEK-293 cells on grown coverslips were co-transfected with Willin-GFP and neurofascin 155 for 48 hours and probed with anti-neurofascin 1:2000 and secondary anti-rabbit Alexa568 1:10,000. A) A series of 0.2µm thick Z sections created using Softworx and ImageJ 1.38x, cropped with Adobe Photoshop 7.0. Arrows indicate overlay regions. B) Detail of a single Z section, with arrow indicating direct overlay and arrowhead indicating close association. Image created with Softworx and ImageJ 1.38x and cropped with Adobe Photoshop 7.0.

5.8.2 Ezrin co-localises with neurofascin 155

To support biochemical interaction evidence obtained in our lab by Dr. Fleur Davey, HEK-293 cells were also transfected with pGFP-Ezrin, pcDNA3 neurofascin155 or both. As shown in Figure 5.18, GFP-Ezrin normally localises to

the cytoplasm (A), while neurofascin155 localises to the membrane (B); however, when co-transfected, both proteins show localisation to the membrane, especially at sites of cell-cell contact (C). Images A and B were obtained with a Leica TCS4D confocal microscope (Gunn-Moore et al., 2006), but to avoid bleed-through problems associated with strong neurofascin155 expression, the co-transfected cells (C) were observed on the Delta Vision system.

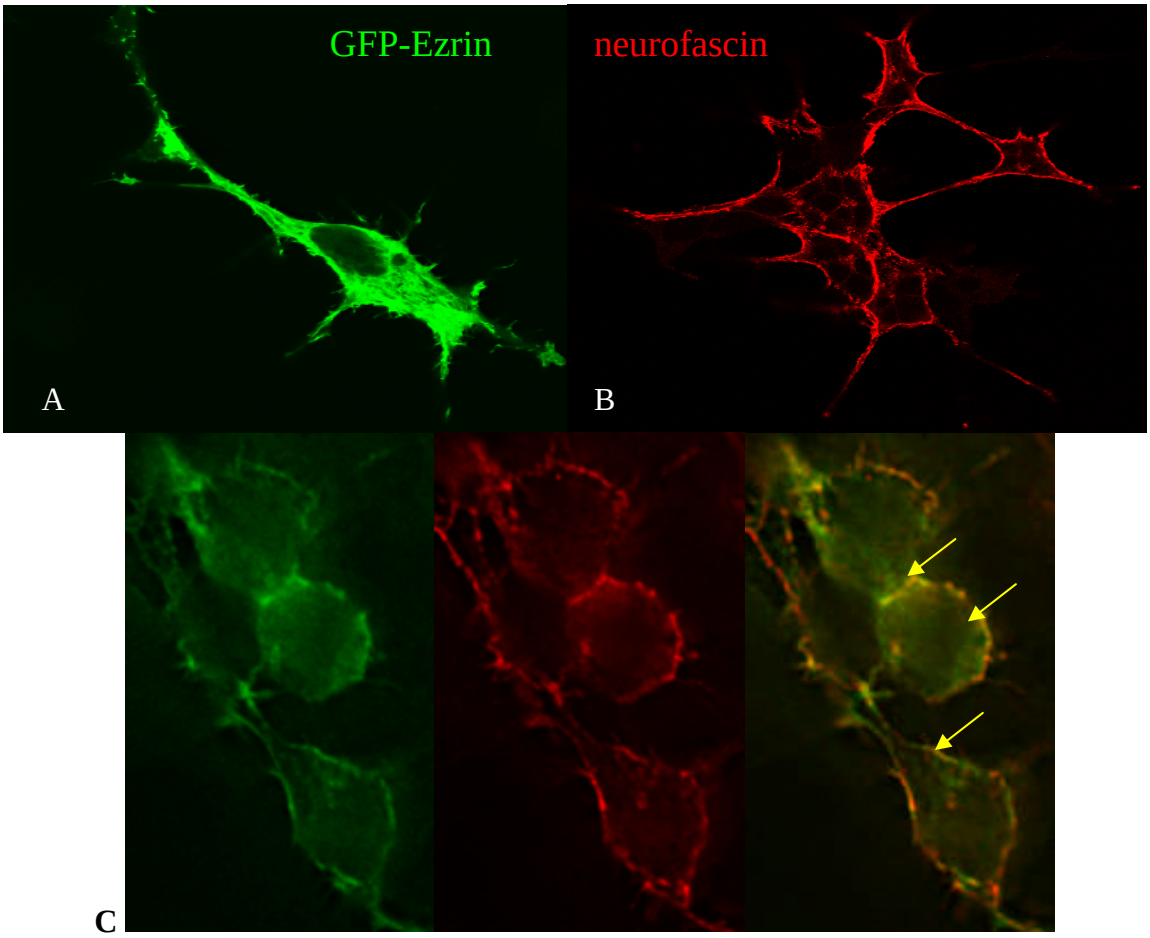

Figure 5.18. HEK293 cells were transfected with (A) GFP-Ezrin, (B) neurofascin155 or both (C) for 48 hours and probed with anti-neurofascin 1:2000 and secondary anti-rabbit Alexa568 1:10,000. For A and B, a single Z section acquired on a Leica TCS4D confocal microscope are shown. (Modified from Gunn-Moore et al., 2006) For C, images are single Z sections obtained on the Delta Vision system and processed with Softworx, ImageJ 1.38x and Adobe Photoshop 7.0. Arrows indicate sites of co-localisation.

5.8.3 Merlin co-localises with neurofascin 155

Previous work from other groups indicated that both Merlin and neurofascin 155 localise to paranodes of Schwann cells and to lipid rafts (Chang et al., 2000; Schafer et al., 2004; Scherer and Gutmann, 1996; Stickney et al., 2004), and our group had previously shown that neurofascin155 can bind to FERM containing proteins. Merlin-mutant Schwann cells show abnormal myelination; are unable to redifferentiate to myelinating cells in culture; and express developmental molecules such as L1 rather than pro-myelination proteins (Hung et al., 2002). Additionally, at least some of the prototypic Merlin mutations in NF2 patients have been shown to be soluble in Triton X-100 (Deguen et al., 1998), indicating that raft localisation is an important physiological aspect of its function (Stickney et al., 2004). Neurofascin 155, meanwhile, is essential to paranode formation prior to myelination (Sherman et al., 2005), and loss of lipid raft association causes disassembly of the paranodal junction in multiple sclerosis (Maier et al., 2007). Therefore, it seems possible that Merlin and neurofascin could interact, and that this interaction may have ramifications for paranodal development, myelination and schwannoma oncogenesis.

To study this potential interation, HEK-293 cells were transfected with pMerlin1-GFP and pcDNA3 neurofascin155. Anti-neurofascin and secondary anti-rabbit Alexa568 were used to probe for neurofascin. The proteins show co-localisation at several punctate membrane points (figure 5.19A), particularly at membrane projections (5.19B).

A

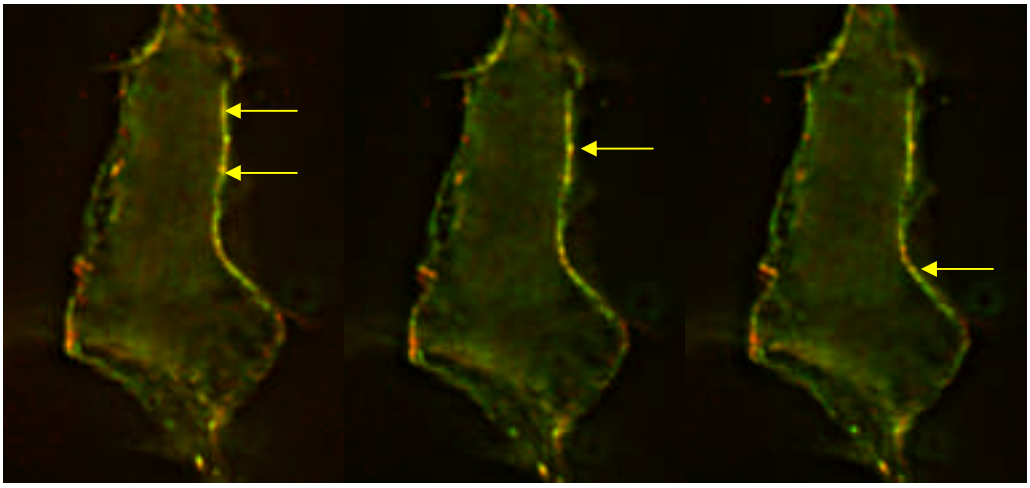

B

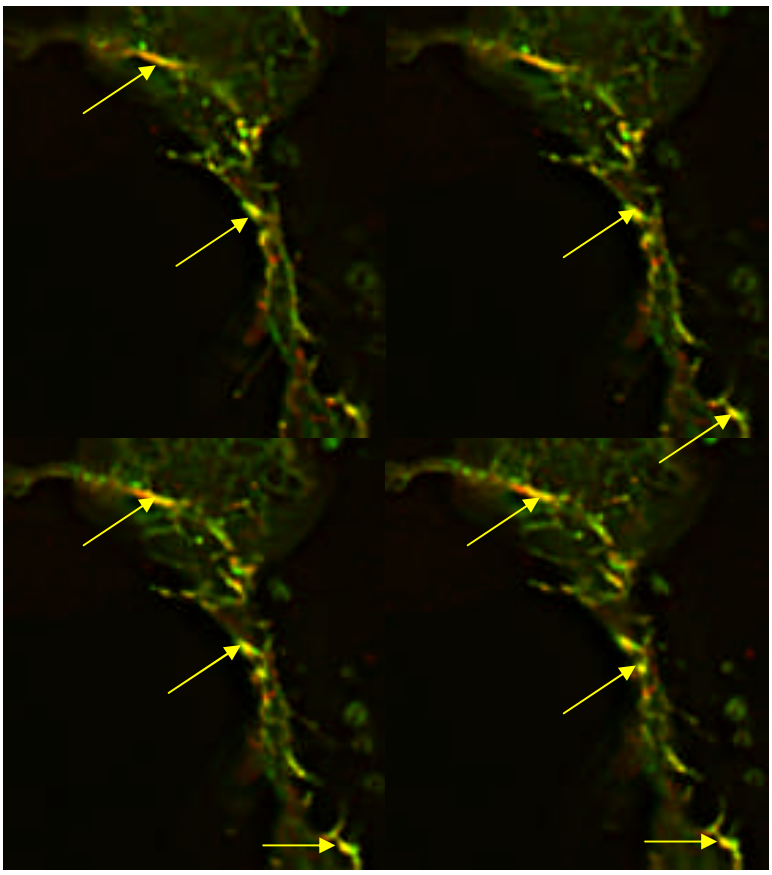

Figure 5.19. HEK-293 cells on grown coverslips were co-transfected with Merlin1-GFP and neurofascin 155 for 48 hours and probed with anti-neurofascin 1:2000 and secondary anti-rabbit Alexa568 1:10,000. A) A series of 0.2µm thick Z sections showing punctate membrane localisation of Merlin1-GFP and neurofascin155. B) A series of 0.2µm thick Z sections showing localisation of Merlin1-GFP and neurofascin155 to membrane projections. Arrows indicate points of co-localisation. Images acquired on the Delta Vision system and processed with Softworx and Adobe Photoshop 7.0.

Further characterisation of this potential interaction was outwith the scope of this project; however, it is worth noting that Willin has also been observed in lipid rafts (see section 4.5.2.4, Figure 4.10), providing added support to its interaction with neurofascin 155 and potential interaction with Merlin.

5.9 Discussion

The identification of binding partners is a key step in the characterisation of a novel protein. In the case of Willin, several potential binding partners were identified based on how the protein was discovered, its relationship to other members of the FERM protein family and its localisation as determined in previous studies. In addition to confirming or refuting these putative interactions, it was also desirable to screen for new potential partners that might give further insight into the function of Willin. To these ends, several techniques were attempted with mixed success, and the results obtained have raised interesting new possibilities for future work.

5.9.1 Yeast two-hybrid studies

The yeast two-hybrid results discussed in section 5.2 confirmed the previous observations of the ability of Willin to interact with L1 members of the L1 family. Like Ezrin, Willin does not seem capable of binding NrCAM, regardless of whether an RSLE motif is present, though the two proteins do co-localise (Maria Hill, Ph.D. thesis). It is interesting that Willin seems able to bind L1 regardless of the RSLE motif, unlike Ezrin which seems only to bind via the RSLE motif. It is possible that the relative weakness of the Willin-L1 interaction indicates a false positive, but if it is a true interaction, it indicates a different mechanism to that which Ezrin employs to bind L1, leading to the conclusion that different physiological roles are assigned to these interactions. Ezrin is important in L1-mediated branching of neurites (Cheng et al., 2005); could Willin counter this action to control how much branching occurs, possibly even binding at the same time as Ezrin to a different FERM-binding site? Further work must be done to verify this interaction and its physiological impact.

Ideally, a screen of a cDNA library using Willin as ‘bait’ would have been desirable; however, previously constructed plasmids with Willin cloned in frame in

the pAS2-1 'bait' plasmid showed both low expression and auto-activation (Brannigan, 2006). Cloning of new yeast two-hybrid constructs and the subsequent screening procedures were outwith the scope of this project.

5.9.2. Tandem affinity purification

Unfortunately, the various TAP methods attempted were unsuccessful. In the case of the Willin-TAP systems, cloning difficulties gave way to insolubility issues, leading to insufficient protein being available for the purification steps. Using a sonicated whole cell lysate, where insoluble proteins are kept, may yield better results. It is also possible that the protein did not bind to the purification resins, though why this is the case is unknown.

It is not known why the TAP- neurofascin155 system was unsuccessful. It is possible that full-length neurofascin is required for interaction with Willin in mammalian cells, perhaps due to their localisation to lipid rafts. Even if this is not the case, the method is techinically challenging, and the TAP protein was not tested directly to confirm its expression levels in this study. Further optimisation may be required and can be performed at a later date.

5.9.3 Co-immunoprecipitation assays

Thankfully, the FLAG co-immunoprecipitation method did provide a successful means of confirming the Willin-neurofascin155 interaction. This time the full-length neurofascin protein was expressed instead of only the C-terminus, which may have improved the chance of interaction. Also, sonicated whole cell lysates were used, preventing any loss of insoluble proteins. The method needs to be repeated for Willin-Merlin due to the poor quality of the Merlin antibody.

The GST pulldown experiment with GST-Willin and neurofascin155 was also successful, as again a sonicated whole cell lysate was used. As will be discussed in section 5.9.4, however, the GST-Willin protein was contaminated by a bacterial chaperone protein, and so this experiment should be repeated to ensure that it is not a false positive.

5.9.4. The actin binding assay

The interaction of Willin and actin is still unconfirmed, though preliminary data is promising. Without any of the conserved actin-binding regions of the other ERM proteins present in Willin, it is difficult to predict how this interaction might take place. The difficulties of producing and purifying GST-Willin, and the impossibility of preventing its apparent breakdown, make the actin-binding experiment challenging; the results presented here should be seen only as an initial step in confirming this reaction, and an assay more comparable with those performed on other ERM proteins should be the next step in this investigation.

If the interpretation provided by the manufacturer of the protocol is accurate, i.e., Willin depolymerises F-actin, this would prove to be quite different from Merlin, which has been shown to stabilise F-actin filaments and slow disassembly (James et al., 2001); the ERMs have also been shown to promote filamentation (Defacque et al., 2000). The significance of this is unclear, but F-actin disruption can be a trigger for apoptosis (White et al., 2001), and could thus be a mechanism for how Willin kills cells.

It would be premature, however, to ascribe such a function before a Willin-actin interaction can be confirmed, and unfortunately, the result shown in section 5.7 is likely not be that straightforward. The approximately 60kDa band present in the purified GST-Willin lanes may not be a breakdown product. A previous GST-Willin

preparation had produced a large amount of a protein of this size, and upon mass spectrometry analysis, this band was shown to be the bacterial chaperone protein GroEL. GroEL and its partner GroES direct ATP-dependant folding of proteins in prokaryotes (Hartl, 1996). GroEL is not always present in GST-Willin purifications, but it does appear to be present in this sample. This is problematic because GroEL is known to bind actin, having an important role in its correct folding in bacteria (Siegers et al., 1999). Although GST-Willin is also present, this confounding factor cannot be ignored, and so this result cannot be trusted. Fortunately, it is possible to remove GroEL from the GST-Willin preparation; as GroEL is ATP-dependant, a high-volume ATP wash can be used to separate it (Thain et al., 1996). Also, denatured bacterial proteins can be added to the GST-Willin lysates to compete for GroEL binding (Rohman and Harrison-Lavoie, 2000). These methods will need to be tested for their usefulness with the GST-Willin preparation, and used to in future to ensure a pure product for the actin binding experiment.

This contamination is not thought to be a problem for the pulldown data presented in section 5.5, as there is no reason to believe that GroEL will bind neurofascin. Of course the experiment should be repeated with a decontaminated GST-Willin sample, but as the FLAG pulldown experiment gave the same result without any confounding factors involved, the level of confidence in that experiment is significantly higher than for the actin binding assay..

5.9.5. Co-localisation studies

The Delta Vision deconvolved fluorescence microscopy of cells expressing neurofascin155 and either Willin-GFP, Merlin1-GFP or GFP-Ezrin shows punctate co-localisation of the FERM-containing proteins with the receptor. In the case of

Willin and Ezrin, this supports biochemical data, and in the case of Merlin, provides further impetus to investigate the potential interaction biochemically. It will now be important to determine the physiological significance of these interactions; the use of transgenic animals will be essential for this, especially in the case of Willin where nothing is known about its native physiological action.

Figure 5.20 summarises the findings of this chapter. Willin has been confirmed to bind neurofascin155 by several methods and two splice variants of L1 by yeast two-hybrid, but it is unable to bind either variant of NrCAM, while interactions with Merlin and actin are still inconclusive.

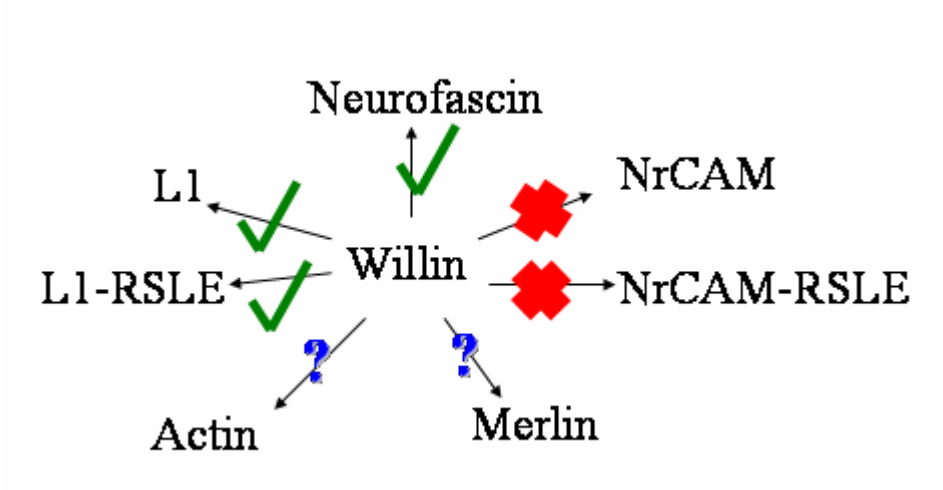

Figure 5.20. A summary of results for putative Willin binding partners. Willin has shown the ability to bind neurofascin, L1 and L1-RSLE, but not NrCAM or NrCAM RSLE, and its ability to bind actin and Merlin is still inconclusive.

CHAPTER 6: DISCUSSION

Chapter 6: Discussion

The overall aim of this project was to increase the body of knowledge of the novel FERM-containing protein Willin, with a specific interest in binding partners and subcellular localisation. As with other FERM-containing proteins, the study of Willin is fraught with technical challenges, some of which have not yet been overcome, and which have slowed the progress of these aims. However, neurofascin155 has been confirmed as a binding partner by yeast two-hybrid and two biochemical methods in addition to co-localisation under fluorescence microscopy (Chapter 5), and a potential cellular location, the lipid raft, proposed for this interaction (Chapter 4). Several tagged constructs with different versions of Willin have been produced for use in various assays (Chapters 4 and 5), and both custom and commercial antibodies tested (and unfortunately largely ruled out) for suitability (Chapter 3). A potential relationship with the tumour suppressor Merlin is being investigated, as well as the hypothesis that Willin may be a homologue of *Drosophila* expanded (Chapters 4 and 5). From this new knowledge, some speculation can be made about a possible physiological role for Willin.

6.1. Junctions, FERM proteins and the L1 family

Yeast two-hybrid, biochemical and co-localisation experiments show that Willin is able to bind neurofascin 155. Previous work in this laboratory has shown that Ezrin and neurofascin 155 interact (Gunn-Moore et al., 2006), and work is ongoing to determine whether Merlin interacts with neurofascin 155. In addition, it is known that Merlin and Ezrin interact (Nguyen et al., 2001), and the *Drosophila* homologues of Merlin and Willin interact (McCartney et al., 2000). The added

knowledge that all of these proteins are found in Schwann cells, with all but (thus far) Willin confirmed to be at the paranode (Scherer et al., 2001; Tait et al., 2000), leads to the tantalising idea of a regulatory signalling complex guiding Schwann cell differentiation, growth and myelination activity. This possibility is bolstered by what is known of Drosophila homologues of these proteins and the parallel nature of the invertebrate septate junction (SJ) and the paranodal septate-like junction (PSJ).

As discussed in sections 4.3 and 4.4, Willin has been observed to slow growth and cause cell death when overexpressed in cell lines. This correlates with the function of its proposed *Drosophila* homologue, expanded, which regulates growth and apoptosis in disc development (Boedigheimer and Laughon, 1993; Blaumueller and Mlodzik, 2000). The L1 family also has a *Drosophila* homologue, neuroglian (Hortsch, 1996), and the ERM proteins are represented only by Moesin (McCartney and Fehon, 1996). All are present at epithelial membranes, but from there the situation becomes murkier.

The literature is unclear about the exact locations of these proteins. Luque and Milán (2007) refer to neuroglian as being a component of adherens junctions, while others place it at the septate junctions (Genova and Fehon, 2003). Expanded, meanwhile, is said to be 'at or very near' adherens junctions (Boedigheimer et al., 1997); interestingly, a later paper states simply that expanded is found at adherens junctions (Blaumueller and Mlodzik, 2000), apparently based on this reference. Hamaratoglu et al. (2006) mention Merlin and expanded together as being at adherens junctions in Drosophila epithelium, and three references are cited for this. However, the first paper was concerned with mammalian cells, not Drosophila (Lallemand et al., 2003); the second (McCartney et al., 2000) refers to an older publication that stated 'at least **part** [emphasis added] of the detected DMerlin … protein was associated

with the adherens junction', but the data was not shown (McCartney and Fehon, 1996); and the third, refering to expanded, stated 'Ex protein is close to or in adherens junctions' (Boedigheimer et al., 1997). Other papers are more cautious and state that Merlin and/or expanded are adjacent to adherens junctions without stating whether they are apical or basal to them (Edgar, 2006) or avoid specificity altogether, referring only to 'apical junctions' as the localisation of Merlin and expanded (Maitra et al., 2006). Another FERM containing protein, coracle, is found at septate junctions, and appears to be required for SJ integrity as well as embryonic and larval development (Ward et al., 2001).

It is apparent that much clarification is required in this field. However, some information can be gleaned from the chaos. In Drosophila, neuroglian, moesin, merlin, expanded and another FERM protein, coracle, are all found at signalling junctions of the epithelium, potentially at structures that are homologous to mammalian paranodes, where neurofascin 155, Ezrin, and Merlin are found. Willin has also been seen in Schwann cells (Figure 4.6), and thus may also turn out to localise at the paranode. It is not yet known what role the FERM proteins may play at the paranode, but neurofascin is required for its formation and proper recruitment of many of its proteins (Sherman et al., 2005). It is also known that merlin defects can lead to abnormal myelination (Giovannini et al., 2000) and to dedifferentiation of Schwann cells from a myelinating stage to a growth stage (Hung et al., 2002). Of course, merlin defects are also the chief cause of Schwann cell tumours (Giovannini et al., 2000). Clearly, proliferative and developmental processes are at work, and the nature of these proteins makes it likely that they are being put together in a molecular architecture that allows for the complex signalling required of such a tightly-regulated system as myelination. One model for explaining the potential interactions and

physiological functions of this complex arrangement is shown in Figure 6.1 and is as follows: in development of the peripheral nervous system, neurofascin 155 and Ezrin interact to promote growth and axoglial contact. Merlin and Willin then join the complex, perhaps by one binding to Ezrin to oppose its action, while the other binds to neurofascin 155 to stabilise the paranode. A loss of Merlin leads to a loss of compact myelin and, possibly by the continued action of Ezrin, Schwann cells develop into schwannomas. The action of Willin alone may be enough to slow, but not prevent, proliferation, leading to the known slow growth phenotype of these tumours (Propp et al., 2006). It is certain that this is far too simplistic an explanation; it does not explain how Caspr, a known interactant of merlin (Denisenko-Nehrbass et al., 2003) and neurofascin (Charles et al., 2002), nor how the various potential signalling pathways known to affect and be affected by the ERMs, merlin and neurofascin are involved. However, it does provide a basic set of interactions for future study, able to be done in either *Drosophila* or mammalian systems, which may lead to greater insights into this complex field.

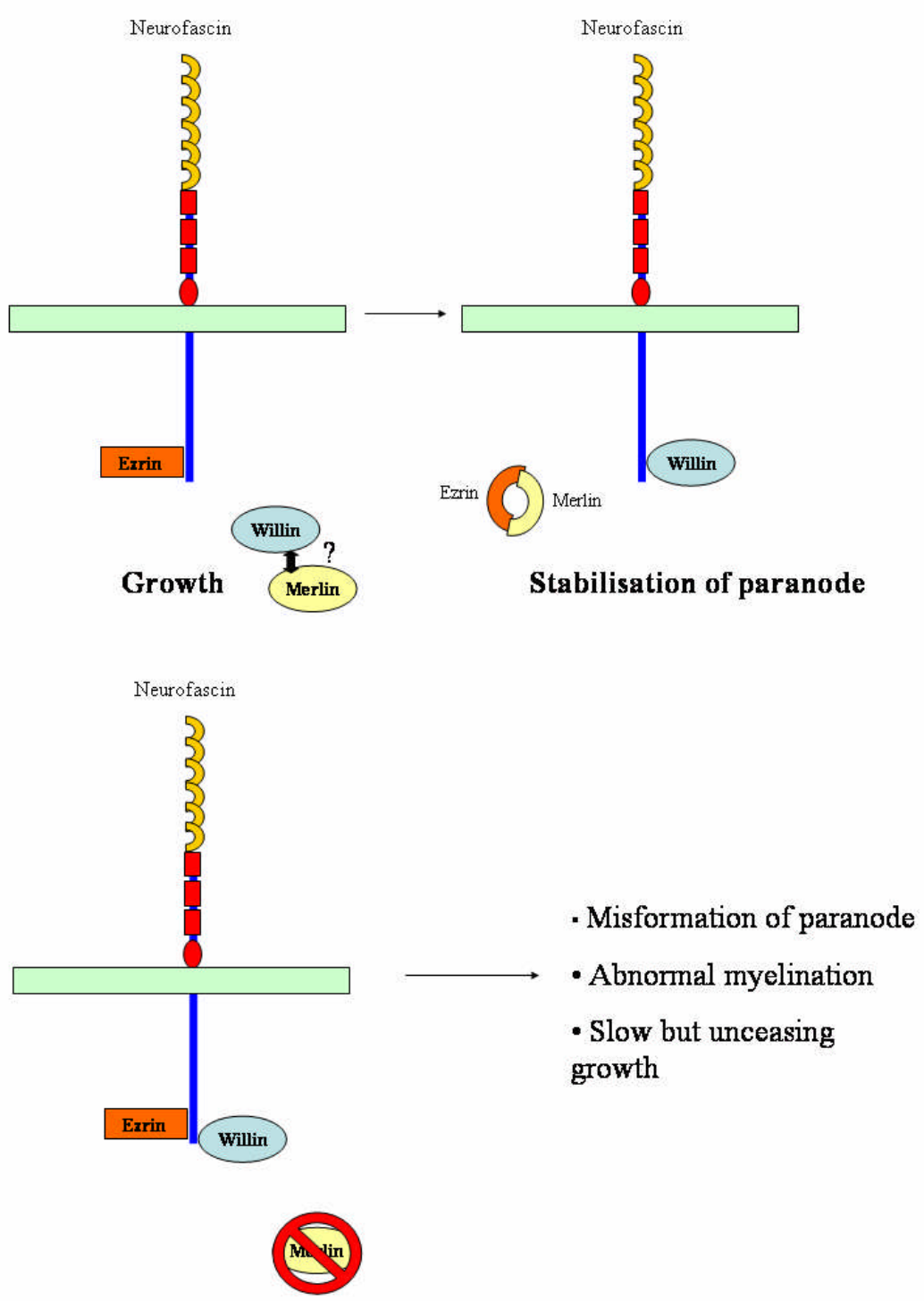

Figure 6.1. A proposed mechanism for FERM protein action in paranode development. During Schwann cell growth and proliferation, Ezrin is bound to neurofascin to promote growth. During formation and stabilisation of the paranode, Merlin binds to Ezrin to stop this action and willin binds neurofascin to stabilise the paranode. When Merlin is lost, Willin can still bind neurofascin and control proliferation to some extent, but Ezrin stays bound, leading to misformation of the paranode, abnormal myelination and slow but unceasing growth.

6.2. Future work

There is still a great deal to be discovered about Willin. Which signalling pathways are involved in the Willin translocation observed in PC12 cells stimulated by growth factors? Does Willin bind the cytoskeleton and phospholipids *in vivo*? Does Willin associate with the ERMs and Merlin, other L1 family members and other receptors? Does Willin self-associate like the ERMs and Merlin, and does it exist in both active and inactive forms; if so, what triggers the change between these two forms? Are the two splice variants of Willin significantly different from each other in their behaviour and distribution? Perhaps most importantly, what role does Willin play in the body?

It will be essential in the future, particularly to answer the final question, to knock out Willin expression and observe the effects. In cell culture, this can be done with RNA interference (RNAi), in which short fragments, known as short interference RNA (siRNA), bind to mRNA and knock down expression of a gene (Bass, 2000). Specific siRNAs to Willin have been designed, and will first be tested against cells expressing Willin-GFP to ensure that the GFP signal is reduced. As the lack of a strong antibody would make it difficult to detect native protein expression levels, Northern blots to detect mRNA may be the best alternative for monitoring gene expression. The second avenue, which would follow successful RNAi experiments, would be to produce a transgenic Willin knockout animal. This should preferably be an inducible, conditional knockout that can be 'switched on' in specific tissues of interest in order to avoid problems such as embryonic lethals and potentially confounding problems from other tissues. An inducible Cre-lox recombination system (Brocard et al., 1997) would be ideal for this, and an obvious place to start would be in Schwann cells. One could predict that deleting Willin in Schwann cells

could lead to defects in myelination and overgrowth, and perhaps disruption of paranodes and neurofascin155 localisation. Structural defects could be monitored by electron microscopy, and to overcome antibody issues, a GFP or lacZ labelled system with Northern blot confirmation could be used to monitor gene expression and subsequent gene silencing. However, it is also important to produce a good antibody able to detect both splice variants so the native protein, whatever it may be, can be studied, thus eliminating concerns about overexpression and the effect of tags. This would also allow for closer study within tissues and better information for interpreting function.

Efforts should also be continued to confirm putative and discover novel binding partners for Willin. Once technical challenges are overcome, a screen should be performed for potential new partners. More evidence is also required to support or disprove the hypothesis that Willin a potential homologue of Expanded, possibly by testing whether Willin expression can rescue Expanded mutants. This could be done by expressing a human Willin gene in a *Drosophila* system, as has been performed successfully with human Merlin and lethal *Drosophila* Merlin mutants (LaJeunesse et al., 1998). The pWillin-mCherry construct that has been recently produced can be used to study the potential interaction between Willin and Merlin as well, as these two proteins could be expected to behave similarly to their *Drosophila* counterparts if indeed Willin is expanded. Co-localisation studies with Merlin1-GFP should be performed in future.

As a FERM protein, it is likely that Willin is involved in a multitude of signalling pathways, and certainly this possibility is strengthened by its suggested localisation to lipid rafts and translocation under growth factor stimulation. Expanded is also involved in signalling, most clearly through the Hippo pathway, where it

interacts with Merlin and regulates transcriptions factors such as Cyclin E (Edgar, 2006). Cyclins, and indeed most of the Hippo pathway proteins, have mammalian homologues (Xiao et al., 2005; Chan et al., 2005; Tamaskovic et al., 2003), and could thus be a good starting point for investigation of Willin's role in signalling. Cyclin D, which is affected by human Merlin (Xiao et al., 2005) and Cyclin E are studied by Prof. CS Herrington, our collaborator in the Bute Medical School, and would thus be ideal markers to observe in knockdown and knockout experiments as well. If Willin acts like expanded, the observed levels of at least one of the Cyclins could be expected to increase concomitant cell proliferation (Edgar, 2006), and this could be detected by Cyclin staining and cell counting without the need for a Willin antibody. In addition, the role of Rho family small GTPases should also be investigated as potential effectors of Willin translocation as observed in PC12 cells.

References

Ahronowitz, I., Xin, W., Kiely, R., Sims, K., MacCollin, M., and Nunes, F. P. (2007). Mutational spectrum of the NF2 gene: A meta-analyslis of 12 years of research and diagnostic laboratory findings. Human Mutation *28*, 1-12.

Amieva, M. R., Wilgenbus, K. K., and Furthmayr, H. (1994). Radixin Is a Component of Hepatocyte Microvilli in-Situ. Experimental Cell Research *210*, 140-144.

Amieva, M. R., and Furthmayr, H. (1995). Subcellular-Localization of Moesin in Dynamic Filopodia, Retraction Fibers, and Other Structures Involved in Substrate Exploration, Attachment, and Cell-Cell Contacts. Experimental Cell Research *219*, 180-196.

Ashburner, M., and Bergman, C. M. (2005). Drosophila melanogaster: A case study of a model genomic sequence and its consequences. Genome Research *15*, 1661-1667.

Auvinen, E., Kivi, N., and Vaheri, A. (2007). Regulation of ezrin localization by Rac1 and PIPK in human epithelial cells. Experimental Cell Research *313*, 824-833.

Banerjee, S., Pillai, A. M., Paik, R., Li, J. J., and Bhat, M. A. (2006). Axonal ensheathment and septate junction formation in the peripheral nervous system of Drosophila. Journal of Neuroscience *26*, 3319-3329.

Barret, C., Roy, C., Montcourrier, P., Mangeat, P., and Niggli, V. (2000). Mutagenesis of the phosphatidylinositol 4,5-bisphosphate (PIP2) binding site in the NH2-terminal domain of ezrin correlates with its altered cellular distribution. Journal of Cell Biology *151*, 1067-1079.

Bashour, A. M., Meng, J. J., Ip, W., MacCollin, M., and Ratner, N. (2002). The Neurofibromatosis Type 2 Gene Product, merlin, Reverses the F-Actin Cytoskeletal Defects in Primary Human Schwannoma Cells. Molecular and Cellular Biology *22*, 1150-1157.

Bass, B. L. (2000). Double-stranded RNA as a template for gene silencing. Cell *101*, 235-238.

Baumgartner, S., Littleton, J. T., Broadie, K., Bhat, M. A., Harbecke, R., Lengyel, J. A., ChiquetEhrismann, R., Prokop, A., and Bellen, H. J. (1996). A Drosophila neurexin is required for septate junction and blood-nerve barrier formation and function. Cell *87*, 1059-1068.

Berryman, M., Franck, Z., and Bretscher, A. (1993). Ezrin Is Concentrated in the Apical Microvilli of a Wide Variety of Epithelial-Cells Whereas Moesin Is Found Primarily in Endothelial-Cells. Journal of Cell Science *105*, 1025-1043.

Blaumueller, C. M., Mlodzik, Marek (2000). The Drosophila tumor suppressor expanded regulates growth, apoptosis, and patterning during development. Mechanisms of Development *92*, 251-262.

Boedigheimer, M., and Laughon, A. (1993). Expanded - a Gene Involved in the Control of Cell-Proliferation in Imaginal Disks. Development *118*, 1291-1301.

Boedigheimer, M. J., Nguyen, K. P., and Bryant, P. J. (1997). expanded functions in the apical cell domain to regulate the growth rate of imaginal discs. Developmental Genetics *20*, 103-110.

Bonilha, V. L., Finnemann, S. C., and Rodriguez-Boulan, E. (1999). Ezrin promotes morphogenesis of apical microvilli and basal infoldings in retinal pigment epithelium. Journal of Cell Biology *147*, 1533-1547.

Brault, E., Gautreau, A., Lamarine, M., Callebaut, I., Thomas, G., and Goutebroze, L. (2001). Normal membrane localization and actin association of the NF2 tumor suppressor protein are dependent on folding of its N-terminal domain. J Cell Sci *114*, 1901-1912.

Bretscher, A., Reczek, D., and Berryman, M. (1997). Ezrin: a protein requiring conformational activation to link microfilaments to the plasma membrane in the assembly of cell surface structures. Journal of Cell Science *110*, 3011-3018.

Bretscher, A., Chambers, D., Nguyen, R., and Reczek, D. (2000). ERM-Merlin and EBP50 protein families in plasma membrane organization and function. Annu Rev Cell Dev Biol *16*, 113-143.

Bretscher, A., Edwards, K., and Fehon, R. G. (2002). ERM proteins and merlin: integrators at the cell cortex. Nat Rev Mol Cell Biol *3*, 586-599.

Brocard, J., Warot, X., Wendling, O., Messaddeq, N., Vonesch, J. L., Chambon, P., and Metzger, D. (1997). Spatio-temporally controlled site-specific somatic mutagenesis in the mouse. Proceedings of the National Academy of Sciences of the United States of America *94*, 14559-14563.

Buhusi, M., Midkiff, B. R., Gates, A. M., Richter, M., Schachner, M., and Maness, P. F. (2003). Close homolog of L1 is an enhancer of integrin-mediated cell migration. Journal of Biological Chemistry *278*, 25024-25031.

Cao, T. T., Deacon, H. W., Reczek, D., Bretscher, A., and von Zastrow, M. (1999). A kinase-regulated PDZ-domain interaction controls endocytic sorting of the beta 2-adrenergic receptor. Nature *401*, 286-290.

Chan, E. H., Nousiainen, M., Chalamalasetty, R. B., Schafer, A., Nigg, E. A., and Sillie, H. H. (2005). The Ste20-like kinase Mst2 activates the human large tumor suppressor kinase Lats1. Oncogene *24*, 2076-2086.

Chang, B. J., Cho, I. J., and Brophy, P. J. (2000). A study on the immunocytochemical localization of neurofascin in rat sciatic nerve. J Vet Sci *1*, 67-71.

Charles, P., Tait, S., Faivre-Sarrailh, C., Barbin, G., Gunn-Moore, F., Denisenko-Nehrbass, N., Guennoc, A. M., Girault, J. A., Brophy, P. J., and Lubetzki, C. (2002). Neurofascin is a glial receptor for the paranodin/Caspr-contactin axonal complex at the axoglial junction. Current Biology *12*, 217-220.

Chen, J., and Mandel, L. J. (1997). Unopposed phosphatase action initiates ezrin dysfunction: a potential mechanism for anoxic injury. American Journal of Physiology-Cell Physiology *42*, C710-C716.

Chen, S., Mantei, N., Dong, L., and Schachner, M. (1999). Prevention of neuronal cell death by neural adhesion molecules L1 and CHL1. Journal of Neurobiology *38*, 428-439.

Cheng, L., Itoh, K., and Lemmon, V. (2005). L1-mediated branching is regulated by two ezrin-radixin-moesin (ERM)-binding sites, the RSLE region and a novel juxtamembrane ERM-binding region. J Neurosci *25*, 395-403.

Chishti, A. H., Kim, A. C., Marfatia, S. M., Lutchman, M., Hanspal, M., Jindal, H., Liu, S. C., Low, P. S., Rouleau, G. A., Mohandas, N., *et al.* (1998). The FERM domain: a unique module involved in the linkage of cytoplasmic proteins to the membrane. Trends Biochem Sci *23*, 281-282.

Cho, E., Feng, Y., Rauskolb, C., Maitra, S., Fehon, R., and Irvine, K. D. (2006). Delineation of a Fat tumor suppressor pathway. Nat Genet.

Conacci-Sorrell, M. E., Ben-Yedidia, T., Shtutman, M., Feinstein, E., Einat, P., and Ben-Ze'ev, A. (2002). Nr-CAM is a target gene of the beta-catenin/LEF-1 in melanoma and colon cancer and its expression enhances motility and confers tumorigenesis. Genes & Development *16*, 2058-2072.

Conboy, J. G. (1986). Molecular-Cloning and Characterization of the Gene Coding for Red-Cell Membrane Skeletal Protein-4.1. Biorheology *23*, 218-218.

Correas, I. (1991). Characterization of Isoforms of Protein-4.1 Present in the Nucleus. Biochemical Journal *279*, 581-585.

Crawford, R. M., Treharne, K. J., Best, O. G., Muimo, R., Riemen, C. E., and Mehta, A. (2005). A novel physical and functional association between nucleoside diphosphate kinase A and AMP-activated protein kinase alpha1 in liver and lung. Biochem J *392*, 201-209.

Crepaldi, T., Gautreau, A., Comoglio, P. M., Louvard, D., and Arpin, M. (1997). Ezrin is an effector of hepatocyte growth factor-mediated migration and morphogenesis in epithelial cells. Journal of Cell Biology *138*, 423-434.
Curto, M., and McClatchey, A. I. (2004). Ezrin...a metastatic detERMinant? Cancer Cell *5*, 113-114.

Davey, F., Hill, M., Falk, J., Sans, N., and Gunn-Moore, F. J. (2005). Synapse associated protein 102 is a novel binding partner to the cytoplasmic terminus of neurone-glial related cell adhesion molecule. Journal of Neurochemistry *94*, 1243-1253.

Davis, J. Q., Mclaughlin, T., and Bennett, V. (1993). Ankyrin-Binding Proteins Related to Nervous-System Cell-Adhesion Molecules - Candidates to Provide Transmembrane and Intercellular Connections in Adult Brain. Journal of Cell Biology *121*, 121-133.

Davis, J. Q., and Bennett, V. (1994). Ankyrin Binding-Activity Shared by the Neurofascin/L1/Nrcam Family of Nervous-System Cell-Adhesion Molecules. Journal of Biological Chemistry *269*, 27163-27166.

Davis, J. Q., Lambert, S., and Bennett, V. (1996). Molecular composition of the node of Ranvier: Identification of ankyrin-binding cell adhesion molecules neurofascin (Mucin+ third FNIII domain-) and NrCAM at nodal axon segments. Journal of Cell Biology *135*, 1355-1367.

Decker, L., and ffrench-Constant, C. (2004). Lipid rafts and integrin activation regulate oligodendrocyte survival. Journal of Neuroscience *24*, 3816-3825.

Defacque, H., Egeberg, M., Habermann, A., Diakonova, M., Roy, C., Mangeat, P., Voelter, W., Marriott, G., Pfannstiel, J., Faulstich, H., and Griffiths, G. (2000). Involvement of ezrin/moesin in de novo actin assembly on phagosomal membranes. Embo Journal *19*, 199-212.

Deguen, B., Merel, P., Goutebroze, L., Giovannini, M., Reggio, H., Arpin, M., and Thomas, G. (1998). Impaired interaction of naturally occurring mutant NF2 protein with actin-based cytoskeleton and membrane. Hum Mol Genet *7*, 217-226.

Demyanenko, G. P., Tsai, A. Y., and Maness, P. F. (1999). Abnormalities in neuronal process extension, hippocampal development, and the ventricular system of L1 knockout mice. Journal of Neuroscience *19*, 4907-4920.

Denisenko-Nehrbass, N., Goutebroze, L., Galvez, T., Bonnon, C., Stankoff, B., Ezan, P., Giovannini, M., Faivre-Sarrailh, C., and Girault, J. A. (2003). Association of Caspr/paranodin with tumour suppressor schwannomin/merlin and beta1 integrin in the central nervous system. J Neurochem *84*, 209-221.

Dhodapkar, K. M., Friedlander, D., Scholes, J., and Grumet, M. (2001). Differential expression of the cell-adhesion molecule Nr-CAM in hyperplastic and neoplastic human pancreatic tissue. Human Pathology *32*, 396-400.

Dichamp, C., Taillibert, S., Aguirre-Cruz, L., Lejeune, J., Marie, Y., Kujas, M. E., Delattre, J. Y., Hoang-Xuan, K., and Sanson, M. (2004). Loss of 14q chromosome in oligodendroglial and astrocytic tumors. Journal of Neuro-Oncology *67*, 281-285.

Dickson, T. C., Mintz, C. D., Benson, D. L., and Salton, S. R. (2002). Functional binding interaction identified between the axonal CAM L1 and members of the ERM family. J Cell Biol *157*, 1105-1112.

Dihne, M., Bernreuther, C., Sibbe, M., Paulus, W., and Schachner, M. (2003). A new role for the cell adhesion molecule L1 in neural precursor cell proliferation, differentiation, and transmitter-specific subtype generation. Journal of Neuroscience *23*, 6638-6650.

Dirks, P., Thomas, U., and Montag, D. (2006). The cytoplasmic domain of NrCAM binds to PDZ domains of synapse-associated proteins SAP90/PSD95 and SAP97. European Journal of Neuroscience *24*, 25-31.

Doi, Y., Itoh, M., Yonemura, S., Ishihara, S., Takano, H., Noda, T., Tsukita, S., and Tsukita, S. (1999). Normal development of mice and unimpaired cell adhesion cell motility actin-based cytoskeleton without compensatory up-regulation of ezrin or radixin in moesin gene knockout. Journal of Biological Chemistry *274*, 2315-2321.

Dubreuil, R. R., MacVicar, G., Dissanayake, S., Liu, C. H., Homer, D., and Hortsch, M. (1996). Neuroglian-mediated cell adhesion induces assembly of the membrane skeleton at cell contact sites. Journal of Cell Biology *133*, 647-655.

Edgar, B. A. (2006). From cell structure to transcription: Hippo forges a new path. Cell *124*, 267-273.

Edidin, M. (2003). The state of lipid rafts: from model membranes to cells. Annu Rev Biophys Biomol Struct *32*, 257-283.

Einheber, S., Zanazzi, G., Ching, W., Scherer, S., Milner, T. A., Peles, E., and Salzer, J. L. (1997). The axonal membrane protein Caspr, a homologue of neurexin IV, is a component of the septate-like paranodal junctions that assemble during myelination. Journal of Cell Biology *139*, 1495-1506.

Evans, D. G. R., Huson, S. M., Donnai, D., Neary, W., Blair, V., Newton, V., and Harris, R. (1992). A Clinical-Study of Type-2 Neurofibromatosis. Quarterly Journal of Medicine *84*, 603-618.

Faivre-Sarrailh, C., Banerjee, S., Li, J. J., Hortsch, M., Laval, M., and Bhat, M. A. (2004). Drosophila contactin, a homolog of vertebrate contactin, is required for septate junction organization and paracellular barrier function. Development *131*, 4931-4942.

Fehon, R. G., Dawson, I. A., and Artavanistsakonas, S. (1994). A Drosophila Homolog of Membrane-Skeleton Protein-4.1 Is Associated with Septate Junctions and Is Encoded by the Coracle Gene. Development *120*, 545-557.

Franck, Z., Gary, R., and Bretscher, A. (1993). Moesin, Like Ezrin, Colocalizes with Actin in the Cortical Cytoskeleton in Cultured-Cells, but Its Expression Is More Variable. Journal of Cell Science *105*, 219-231.

Fukasawa, T., Chono, J. M., Sakurai, S., Koshiishi, N., Ikeno, R., Tanaka, A., Matsumoto, Y., Hayashi, Y., Koike, M., and Fukayama, M. (2000). Allelic loss of 14q and 22q, NF2 mutation, and genetic instability occur independently of c-kit mutation in gastrointestinal stromal tumor. Japanese Journal of Cancer Research *91*, 1241-1249.

Garcia-Alonso, L., Romani, S., and Jimenez, F. (2000). The EGF and FGF receptors mediate neuroglian function to control growth cone decisions during sensory axon guidance in Drosophila. Neuron *28*, 741-752.

Gatto, C. L., Walker, B. J., and Lambert, S. (2003). Local ERM activation and dynamic growth cones at Schwann cell tips implicated in efficient formation of nodes of Ranvier. J Cell Biol *162*, 489-498.

Gautreau, A., Poullet, P. R., Louvard, D., and Arpin, M. (1999). Ezrin, a plasma membrane-microfilament linker, signals cell survival through the phosphatidylinositol 3-kinase/Akt pathway. Proceedings of the National Academy of Sciences of the United States of America *96*, 7300-7305.

Gautreau, A., Louvard, D., and Arpin, M. (2002). ERM proteins and NF2 tumor suppressor: the Yin and Yang of cortical actin organization and cell growth signaling. Curr Opin Cell Biol *14*, 104-109.

Genova, J. L., and Fehon, R. G. (2003). Neuroglian, Gliotactin, and the Na+/K+ ATPase are essential for septate junction function in Drosophila. Journal of Cell Biology *161*, 979-989.

Giovannini, M., Robanus-Maandag, E., van der Valk, M., Niwa-Kawakita, M., Abramowski, V., Goutebroze, L., Woodruff, J. M., Berns, A., and Thomas, G. (2000). Conditional biallelic Nf2 mutation in the mouse promotes manifestations of human neurofibromatosis type 2. Genes & Development *14*, 1617-1630.

Gronholm, M., Sainio, M., Zhao, F., Heiska, L., Vaheri, A., and Carpen, O. (1999). Homotypic and heterotypic interaction of the neurofibromatosis 2 tumor suppressor protein merlin and the ERM protein ezrin. J Cell Sci *112 (Pt 6)*, 895-904.

Gronholm, M., Muranen, T., Toby, G. G., Utermark, T., Hanemann, C. O., Golemis, E. A., and Carpen, O. (2006). A functional association between merlin and HEI10, a cell cycle regulator. Oncogene *25*, 4389-4398.

Gunn-Moore, F. J., Welsh, G. I., Herron, L. R., Brannigan, F., Venkateswarlu, K., Gillespie, S., Brandwein-Gensler, M., Madan, R., Tavare, J. M., Brophy, P. J., *et al.* (2005). A novel 4.1 ezrin radixin moesin (FERM)-containing protein, 'Willin'. FEBS Lett *579*, 5089-5094.

Gunn-Moore, F. J., Hill, M., Davey, F., Herron, L. R., Tait, S., Sherman, D., and Brophy, P. J. (2006). A functional FERM domain binding motif in neurofascin. Molecular and Cellular Neuroscience *33*, 441-446.

Gutmann, D. H. (2001). The neurofibromatoses: when less is more. Hum Mol Genet *10*, 747-755.

Haas, M. A., Vickers, J. C., and Dickson, T. C. (2004). Binding partners L1 cell adhesion molecule and the ezrin-radixin-moesin (ERM) proteins are involved in development and the regenerative response to injury of hippocampal and cortical neurons. Eur J Neurosci *20*, 1436-1444.

Haas, M. A., Vickers, J. C., and Dickson, T. C. (2007). Rho kinase activates ezrin-radixin-moesin (ERM) proteins and mediates their function in cortical neuron growth, morphology and motility in vitro. Journal of Neuroscience Research *85*, 34-46.

Hall, S. G., and Bieber, A. J. (1997). Mutations in the Drosophila neuroglian cell adhesion molecule affect motor neuron pathfinding and peripheral nervous system patterning. Journal of Neurobiology *32*, 325-340.

Hamada, K., Shimizu, T., Matsui, T., Tsukita, S., and Hakoshima, T. (2000). Structural basis of the membrane-targeting and unmasking mechanisms of the radixin FERM domain. Embo J *19*, 4449-4462.

Hamada, K., Shimizu, T., Yonemura, S., Tsukita, S., and Hakoshima, T. (2003). Structural basis of adhesion-molecule recognition by ERM proteins revealed by the crystal structure of the radixin-ICAM-2 complex. Embo J *22*, 502-514.

Hamaratoglu, F., Willecke, M., Kango-Singh, M., Nolo, R., Hyun, E., Tao, C., Jafar-Nejad, H., and Halder, G. (2006). The tumour-suppressor genes NF2/Merlin and Expanded act through Hippo signalling to regulate cell proliferation and apoptosis. Nat Cell Biol *8*, 27-36.

Harrison, G. M., Davies, G., Martin, T. A., Jiang, W. G., and Mason, M. D. (2002). Distribution and expression of CD44 isoforms and Ezrin during prostate cancer-endothelium interaction. International Journal of Oncology *21*, 935-940.

Hassel, B., Rathjen, F. G., and Volkmer, H. (1997). Organization of the neurofascin gene and analysis of developmentally regulated alternative splicing. Journal of Biological Chemistry *272*, 28742-28749.

Hemming, N. J., Anstee, D. J., Mawby, W. J., Reid, M. E., and Tanner, M. J. A. (1994). Localization of the Protein 4.1-Binding Site on Human Erythrocyte Glycophorin-C and Glycophorin-D. Biochemical Journal *299*, 191-196.

Henry, M. D., Agosti, C. G., and Solomon, F. (1995). Molecular Dissection of Radixin - Distinct and Interdependent Functions of the Amino-Terminal and Carboxy-Terminal Domains. Journal of Cell Biology *129*, 1007-1022.

Hillenbrand, R., Molthagen, M., Montag, D., and Schachner, M. (1999). The close homologue of the neural adhesion molecule L1 (CHL1): patterns of expression and promotion of neurite outgrowth by heterophilic interactions. European Journal of Neuroscience *11*, 813-826.

Hortsch, M. (2000). Structural and functional evolution of the L1 family: Are four adhesion molecules better than one? Molecular and Cellular Neuroscience *15*, 1-10.

Howell, O. W., Palser, A., Polito, A., Melrose, S., Zonta, B., Scheiermann, C., Vora, A. J., Brophy, P. J., and Reynolds, R. (2006). Disruption of neurofascin localization reveals early changes preceding demyelination and remyelination in multiple sclerosis. Brain *129*, 3173-3185.

Huang, J. B., Wu, S., Barrera, J., Matthews, K., and Pan, D. J. (2005). The Hippo signaling pathway coordinately regulates cell proliferation and apoptosis by inactivating Yorkie, the Drosophila homolog of YAP. Cell *122*, 421-434.

Hung, G., Colton, J., Fisher, L., Oppenheimer, M., Faudoa, R., Slattery, W., and Linthicum, F. (2002). Immunohistochemistry study of human vestibular nerve schwannoma differentiation. Glia *38*, 363-370.

Ishibashi, T., Dupree, J. L., Ikenaka, K., Hirahara, Y., Honke, K., Peles, E., Popko, B., Suzuki, K., Nishino, H., and Baba, H. (2002). A myelin galactolipid, sulfatide, is essential for maintenance of ion channels on myelinated axon but not essential for initial cluster formation. Journal of Neuroscience *22*, 6507-6514.

Ishiguro, H., Liu, Q. R., Gong, J. P., Hall, F. S., Ujike, H., Morales, M., Sakurai, T., Grumet, M., and Uhl, G. R. (2006). NrCAM in addiction vulnerability: Positional cloning, drug-regulation, haplotype-specific expression, and altered drug reward in knockout mice. Neuropsychopharmacology *31*, 572-584.

Itoh, K., Fushiki, S., Kamiguchi, H., Arnold, B., Altevogt, P., and Lemmon, V. (2005). Disrupted Schwann cell-axon interactions in peripheral nerves of mice with altered L1-integrin interactions. Molecular and Cellular Neuroscience *30*, 131-136.

Kahya, N., Brown, D. A., and Schwille, P. (2005). Raft partitioning and dynamic behavior of human placental alkaline phosphatase in giant unilamellar vesicles. Biochemistry *44*, 7479-7489.
Kamiguchi, H., and Lemmon, V. (1998). A neuronal form of the cell adhesion molecule L1 contains a tyrosine-based signal required for sorting to the axonal growth cone. Journal of Neuroscience *18*, 3749-3756.

Kaul, S. C., Mitsui, Y., Komatsu, Y., Reddel, R. R., and Wadhwa, R. (1996). A highly expressed 81 kDa protein in immortalized mouse fibroblasts: Its proliferative function and identity with ezrin. Oncogene *13*, 1231-1237.

Kissil, J. L., Wilker, E. W., Johnson, K. C., Eckman, M. S., Yaffe, M. B., and Jacks, T. (2003). Merlin, the product of the Nf2 tumor suppressor gene, is an inhibitor of the p21-activated kinase, Pak1. Mol Cell *12*, 841-849.

Krieg, J., and Hunter, T. (1992). Identification of the 2 Major Epidermal Growth Factor-Induced Tyrosine Phosphorylation Sites in the Microvillar Core Protein Ezrin. Journal of Biological Chemistry *267*, 19258-19265.

LaJeunesse, D. R., McCartney, B. M., and Fehon, R. G. (1998). Structural analysis of Drosophila merlin reveals functional domains important for growth control and subcellular localization. J Cell Biol *141*, 1589-1599.

Lallemand, D., Curto, M., Saotome, I., Giovannini, M., and McClatchey, A. I. (2003). NF2 deficiency promotes tumorigenesis and metastasis by destabilizing adherens junctions. Genes Dev *17*, 1090-1100.

Lamb, R. F., Ozanne, B. W., Roy, C., McGarry, L., Stipp, C., Mangeat, P., and Jay, D. G. (1997). Essential functions of ezrin in maintenance of cell shape and lamellipodial extension in normal and transformed fibroblasts. Current Biology *7*, 682-688.

Lamb, R. S., Ward, R. E., Schweizer, L., and Fehon, R. G. (1998). Drosophila coracle, a member of the protein 4.1 superfamily, has essential structural functions in the septate junctions and developmental functions in embryonic and adult epithelial cells. Molecular Biology of the Cell *9*, 3505-3519.

Lane, R. P., Chen, X. N., Yamakawa, K., Vielmetter, J., Korenberg, J. R., and Dreyer, W. J. (1996). Characterization of a highly conserved human homolog to the chicken neural cell surface protein Bravo/Nr-CAM that maps to chromosome band 7q31. Genomics *35*, 456-465.

Lankes, W., Griesmacher, A., Grunwald, J., Schwartzalbiez, R., and Keller, R. (1988). A Heparin-Binding Protein Involved in Inhibition of Smooth-Muscle Cell-Proliferation. Biochemical Journal *251*, 831-842.

Lankes, W. T., and Furthmayr, H. (1991). Moesin - a Member of the Protein-4.1 Talin Ezrin Family of Proteins. Proceedings of the National Academy of Sciences of the United States of America *88*, 8297-8301.

Leone, P. E., Bello, M. J., de Campos, J. M., Vaquero, J., Sarasa, J. L., Pestana, A., and Rey, J. A. (1999). NF2 gene mutations and allelic status of 1p, 14q and 22q in sporadic meningiomas. Oncogene *18*, 2231-2239.

Levy, B., Mukherjee, T., and Hirschhorn, K. (2000). Molecular cytogenetic analysis of uterine leiomyoma and leiomyosarcoma by comparative genomic hybridization. Cancer Genetics and Cytogenetics *121*, 1-8.

Li, Q. Z., Nance, M. R., Kulikauskas, R., Nyberg, K., Fehon, R., Karplus, P. A., Bretscher, A., and Tesmer, J. J. G. (2007). Self-masking in an intact ERM-merlin protein: An active role for the central alpha-helical domain. Journal of Molecular Biology *365*, 1446-1459.

Li, W., and Crouch, D. H. (2000). Cloning and expression profile of chicken radixin. Biochimica Et Biophysica Acta-Gene Structure and Expression *1491*, 327-332.

Liu, H. S., Jan, M. S., Chou, C. K., Chen, P. H., and Ke, N. J. (1999). Is green fluorescent protein toxic to the living cells? Biochemical and Biophysical Research Communications *260*, 712-717.

Luque, C. M., and Milan, M. (2007). Growth control in the proliferative region of the Drosophila eye-head primordium: the elbow-noc gene complex. Dev Biol *301*, 327-339.

Macdonald, J. L., and Pike, L. J. (2005). A simplified method for the preparation of detergent-free lipid rafts. J Lipid Res *46*, 1061-1067.

Madan, R., Brandwein-Gensler, M., Schlecht, N. F., Elias, K., Gorbovitsky, E., Belbin, T. J., Mahmood, R., Breining, D., Qian, H., Childs, G., *et al.* (2006). Differential tissue and subcellular expression of ERM proteins in normal and malignant tissues: Cytoplasmic ezrin expression has prognostic signficance for head and neck squamous cell carcinoma. Head and Neck-Journal for the Sciences and Specialties of the Head and Neck *28*, 1018-1027.

Maddala, R., Reddy, V. N., Epstein, D. L., and Rao, V. (2003). Growth factor induced activation of Rho and Rac GTPases and actin cytoskeletal reorganization in human lens epithelial cells. Molecular Vision *9*, 329-336.

Maier, O., Baron, W., and Hoekstra, D. (2007). Reduced raft-association of NF155 in active MS-lesions is accompanied by the disruption of the paranodal junction. Glia *55*, 885-895.

Maitra, S., Kulikauskas, R. M., Gavilan, H., and Fehon, R. G. (2006). The tumor suppressors Merlin and Expanded function cooperatively to modulate receptor endocytosis and signaling. Curr Biol *16*, 702-709.

Mangeat, P., Roy, C., and Martin, M. (1999). ERM proteins in cell adhesion and membrane dynamics. Trends Cell Biol *9*, 187-192.

Marshall, C. J. (1995). Specificity of Receptor Tyrosine Kinase Signaling - Transient Versus Sustained Extracellular Signal-Regulated Kinase Activation. Cell *80*, 179-185.

Martin, M., Andreoli, C., Sahuquet, A., Montcourrier, P., Algrain, M., and Mangeat, P. (1995). Ezrin Nh2-Terminal Domain Inhibits the Cell Extension Activity of the Cooh-Terminal Domain. Journal of Cell Biology *128*, 1081-1093.

Martin, M., Roy, C., Montcourrier, P., Sahuquet, A., and Mangeat, P. (1997). Three determinants in ezrin are responsible for cell extension activity. Molecular Biology of the Cell *8*, 1543-1557.

McCartney, B. M., and Fehon, R. G. (1996). Distinct cellular and subcellular patterns of expression imply distinct functions for the Drosophila homologues of moesin and the neurofibromatosis 2 tumor suppressor, merlin. J Cell Biol *133*, 843-852.

McCartney, B. M., Kulikauskas, R. M., LaJeunesse, D. R., and Fehon, R. G. (2000). The neurofibromatosis-2 homologue, Merlin, and the tumor suppressor expanded function together in Drosophila to regulate cell proliferation and differentiation. Development *127*, 1315-1324.

McClatchey, A. I., and Giovannini, M. (2005). Membrane organization and tumorigenesis--the NF2 tumor suppressor, Merlin. Genes Dev *19*, 2265-2277.

McLaughlin, M. E., Kruger, G. M., Slocum, K. L., Crowley, D., Michaud, N. A., Huang, J., Magendantz, M., and Jacks, T. (2007). The Nf2 tumor suppressor reulates cell-cell adhesion during tissue fusion. Proceedings of the National Academy of Sciences of the United States of America *104*, 3261-3266.

Menegoz, M., Gaspar, P., LeBert, M., Galvez, T., Burgaya, F., Palfrey, C., Ezan, P., Amos, F., and Girault, J. A. (1997). Paranodin, a glycoprotein of neuronal paranodal membranes. Neuron *19*, 319-331.

Meng, J. J., Lowrie, D. J., Sun, H., Dorsey, E., Pelton, P. D., Bashour, A. M., Groden, J., Ratner, N., and Ip, W. (2000). Interaction Between Two Isoforms of the NF2 Tumor Suppressor Protein, Merlin, and Between Merlin and Ezrin, Suggests Modulation of ERM Proteins by Merlin. Journal of Neuroscience Research *62*, 491-502.

Muranen, T., Gronholm, M., Renkema, G. H., and Carpen, O. (2005). Cell cycle-dependent nucleocytoplasmic shuttling of the neurofibromatosis 2 tumour suppressor merlin. Oncogene *24*, 1150-1158.

Ng, T., Parsons, M., Hughes, W. E., Monypenny, J., Zicha, D., Gautreau, A., Arpin, M., Gschmeissner, S., Verveer, P. J., Bastiaens, P. I. H., and Parker, P. J. (2001). Ezrin is a downstream effector of trafficking PKC-integrin complexes involved in the control of cell motility. Embo Journal *20*, 2723-2741.

Nguyen, R., Reczek, D., and Bretscher, A. (2001). Hierarchy of merlin and ezrin N- and C-terminal domain interactions in homo- and heterotypic associations and their relationship to binding of scaffolding proteins EBP50 and E3KARP. J Biol Chem *276*, 7621-7629.

Niggli, V., Andreoli, C., Roy, C., and Mangeat, P. (1995). Identification of a Phosphatidylinositol-4,5-Bisphosphate-Binding Domain in the N-Terminal Region of Ezrin. Febs Letters *376*, 172-176.

Obremski, V. J., Hall, A. M., and Fernandez-Valle, C. (1998). Merlin, the neurofibromatosis type 2 gene product, and beta1 integrin associate in isolated and differentiating Schwann cells. J Neurobiol *37*, 487-501.

Okada, T., Lopez-Lago, M., and Giancotti, F. G. (2005). Merlin/NF-2 mediates contact inhibition of growth by suppressing recruitment of Rac to the plasma membrane. J Cell Biol *171*, 361-371.

Pasternack, G. R., Anderson, R. A., Leto, T. L., and Marchesi, V. T. (1985). Interactions between Protein-4.1 and Band-3 - an Alternative Binding-Site for an Element of the Membrane Skeleton. Journal of Biological Chemistry *260*, 3676-3683.

Pearson, M. A., Reczek, D., Bretscher, A., and Karplus, P. A. (2000). Structure of the ERM protein moesin reveals the FERM domain fold masked by an extended actin binding tail domain. Cell *101*, 259-270.

Pellock, B. J., Buff, E., White, K., and Hariharan, I. K. (2007). The Drosophila tumor suppressors Expanded and Merlin differentially regulate cell cycle exit, apoptosis, and Wingless signaling. Developmental Biology *304*, 102-115.

Pelton, P. D., Sherman, L. S., Rizvi, T. A., Marchionni, M. A., Wood, P., Friedman, R. A., and Ratner, N. (1998). Ruffling membrane, stress fiber, cell spreading and proliferation abnormalities in human Schwannoma cells. Oncogene *17*, 2195-2209.

Pietromonaco, S. F., Simons, P. C., Altman, A., and Elias, L. (1998). Protein kinase C-theta phosphorylation of moesin in the actin-binding sequence. Journal of Biological Chemistry *273*, 7594-7603.

Polesello, C., and Payre, F. (2004). Small is beautiful: what flies tell us about ERM protein function in development. Trends Cell Biol *14*, 294-302.

Pujuguet, P., Del Maestro, L., Gautreau, A., Louvard, D., and Arpin, M. (2003). Ezrin regulates E-cadherin-dependent adherens junction assembly through Rac1 activation. Molecular Biology of the Cell *14*, 2181-2191.

Rathjen, F. G., and Schachner, M. (1984). Immunocytological and Biochemical-Characterization of a New Neuronal Cell-Surface Component (L1-Antigen) Which Is Involved in Cell-Adhesion. Embo Journal *3*, 1-10.

Reed, J. A., Lin, Q. H., Chen, D. H., Mian, I. S., and Medrano, E. E. (2005). SKI pathways inducing progression of human melanoma. Cancer and Metastasis Reviews *24*, 265-272.

Richardson, H., Okeefe, L. V., Marty, T., and Saint, R. (1995). Ectopic Cyclin-E Expression Induces Premature Entry into S Phase and Disrupts Pattern-Formation in the Drosophila Eye Imaginal Disc. Development *121*, 3371-3379.

Roy, C., Martin, M., and Mangeat, P. (1997). A dual involvement of the amino-terminal domain of ezrin in F- and G-actin binding. Journal of Biological Chemistry *272*, 20088-20095.

Sakurai, T., Ramoz, N., Reichert, J. G., Corwin, T. E., Kryzak, L., Smith, C. J., Silverman, J. M., Hollander, E., and Buxbaum, J. D. (2006). Association analysis of the NrCAM gene in autism and in subsets of families with severe obsessive-compulsive or self-stimulatory behaviors. Psychiatric Genetics *16*, 251-257.

Sato, N., Yonemura, S., Obinata, T., Tsukita, S., and Tsukita, S. (1991). Radixin, a Barbed End-Capping Actin-Modulating Protein, Is Concentrated at the Cleavage Furrow During Cytokinesis. Journal of Cell Biology *113*, 321-330.

Sato, N., Funayama, N., Nagafuchi, A., Yonemura, S., Tsukita, S., and Tsukita, S. (1992). A Gene Family Consisting of Ezrin, Radixin and Moesin - Its Specific Localization at Actin Filament Plasma-Membrane Association Sites. Journal of Cell Science *103*, 131-143.

Schafer, D. P., Bansal, R., Hedstrom, K. L., Pfeiffer, S. E., and Rasband, M. N. (2004). Does paranode formation and maintenance require partitioning of neurofascin 155 into lipid rafts? Journal of Neuroscience *24*, 3176-3185.

Scherer, S. S., and Gutmann, D. H. (1996). Expression of the neurofibromatosis 2 tumor suppressor gene product, merlin, in Schwann cells. J Neurosci Res *46*, 595-605.

Shaw, R. J., Henry, M., Solomon, F., and Jacks, T. (1998a). RhoA-dependent phosphorylation and relocalization of ERM proteins into apical membrane/actin protrusions in fibroblasts. Mol Biol Cell *9*, 403-419.

Shaw, R. J., McClatchey, A. I., and Jacks, T. (1998b). Localization and functional domains of the neurofibromatosis type II tumor suppressor, merlin. Cell Growth Differ *9*, 287-296.

Shaw, R. J., Paez, J. G., Curto, M., Yaktine, A., Pruitt, W. M., Saotome, I., O'Bryan, J. P., Gupta, V., Ratner, N., Der, C. J., *et al.* (2001). The Nf2 tumor suppressor, merlin, functions in Rac-dependent signaling. Dev Cell *1*, 63-72.

Sherman, D. L., Tait, S., Melrose, S., Johnson, R., Zonta, B., Court, F. A., Macklin, W. B., Meek, S., Smith, A. J. H., Cottrell, D. F., and Brophy, P. J. (2005). Neurofascins are required to establish axonal domains for saltatory conduction. Neuron *48*, 737-742.

Sherman, L., Xu, H. M., Geist, R. T., Saporito-Irwin, S., Howells, N., Ponta, H., Herrlich, P., and Gutmann, D. H. (1997). Interdomain binding mediates tumor growth suppression by the NF2 gene product. Oncogene *15*, 2505-2509.

Silva, E., Tsatskis, Y., Gardano, L., Tapon, N., and McNeill, H. (2006). The Tumor-Suppressor Gene fat Controls Tissue Growth Upstream of Expanded in the Hippo Signaling Pathway. Curr Biol.

Simons, K., and Ehehalt, R. (2002). Cholesterol, lipid rafts, and disease. Journal of Clinical Investigation *110*, 597-603.

Smith, W. J., Nassar, N., Bretscher, A., Cerione, R. A., and Karplus, P. A. (2003). Structure of the active N-terminal domain of Ezrin. Conformational and mobility changes identify keystone interactions. J Biol Chem *278*, 4949-4956.

Speck, O., Hughes, S. C., Noren, N. K., Kulikauskas, R. M., and Fehon, R. G. (2003). Moesin functions antagonistically to the Rho pathway to maintain epithelial integrity. Nature *421*, 83-87.

Stickney, J. T., Bacon, W. C., Rojas, M., Ratner, N., and Ip, W. (2004). Activation of the tumor suppressor merlin modulates its interaction with lipid rafts. Cancer Res *64*, 2717-2724.

Stokowski, R. P., and Cox, D. R. (2000). Functional analysis of the neurofibromatosis type 2 protein by means of disease-causing point mutations. Am J Hum Genet *66*, 873-891.

Sun, C. X., Robb, V. A., and Gutmann, D. H. (2002). Protein 4.1 tumor suppressors: getting a FERM grip on growth regulation. J Cell Sci *115*, 3991-4000.

Tait, S., Gunn-Moore, F., Collinson, J. M., Huang, J., Lubetzki, C., Pedraza, L., Sherman, D. L., Colman, D. R., and Brophy, P. J. (2000). An oligodendrocyte cell adhesion molecule at the site of assembly of the paranodal axo-glial junction. Journal of Cell Biology *150*, 657-666.

Takahashi, K., Sasaki, T., Mammoto, A., Takaishi, K., Kameyama, T., Tsukita, S., Tsukita, S., and Takai, Y. (1997). Direct interaction of the Rho GDP dissociation inhibitor with ezrin/radixin/moesin initiates the activation of the Rho small G protein. Journal of Biological Chemistry *272*, 23371-23375.

Takahashi, K., Sasaki, T., Mammoto, A., Hotta, I., Takaishi, K., Imamura, H., Nakano, K., Kodama, A., and Takai, Y. (1998). Interaction of radixin with Rho small G protein GDP/GTP exchange protein Dbl. Oncogene *16*, 3279-3284.

Takeuchi, K., Kawashima, A., Nagafuchi, A., and Tsukita, S. (1994a). Structural diversity of band 4.1 superfamily members. J Cell Sci *107 (Pt 7)*, 1921-1928.

Takeuchi, K., Sato, N., Kasahara, H., Funayama, N., Nagafuchi, A., Yonemura, S., and Tsukita, S. (1994b). Perturbation of cell adhesion and microvilli formation by antisense oligonucleotides to ERM family members. J Cell Biol *125*, 1371-1384.

Tamaskovic, R., Bichsel, S. J., and Hemmings, B. A. (2003). NDR family of AGC kinases - essential regulators of the cell cycle and morphogenesis. Febs Letters *546*, 73-80.

Tepass, U., and Tanentzapf, G. (2001). Epithelial cell polarity and cell junctions in Drosophila. Annual Review of Genetics *35*, 747-784.

Terawaki, S., Maesaki, R., and Hakoshima, T. (2006). Structural basis for NHERF recognition by ERM proteins. Structure *14*, 777-789.

Theobald, M., Christiansen, H., Schmidt, A., Melekian, B., Wolkewitz, N., Christiansen, N. M., Brinkschmidt, C., Berthold, F., and Lampert, F. (1999). Sublocalization of putative tumor suppressor gene loci on chromosome arm 14q in neuroblastoma. Genes Chromosomes & Cancer *26*, 40-46.

Trofatter, J. A., Maccollin, M. M., Rutter, J. L., Murrell, J. R., Duyao, M. P., Parry, D. M., Eldridge, R., Kley, N., Menon, A. G., Pulaski, K., *et al.* (1993). A Novel Moesin-

Like, Ezrin-Like, Radixin-Like Gene Is a Candidate for the Neurofibromatosis-2 Tumor Suppressor. Cell *72*, 791-800.

Tse, J. Y. M., Ng, H. K., Lau, K. M., Lo, K. W., Poon, W. S., and Huang, D. P. (1997). Loss of heterozygosity of chromosome 14q in low- and high-grade meningiomas. Human Pathology *28*, 779-785.

Tsukita, S., Hieda, Y., and Tsukita, S. (1989). A New 82-Kd Barbed End-Capping Protein (Radixin) Localized in the Cell-to-Cell Adherens Junction - Purification and Characterization. Journal of Cell Biology *108*, 2369-2382.

Tsukita, S., Oishi, K., Sato, N., Sagara, J., and Kawai, A. (1994). ERM family members as molecular linkers between the cell surface glycoprotein CD44 and actin-based cytoskeletons. J Cell Biol *126*, 391-401.

Turunen, O., Sainio, M., Jaaskelainen, J., Carpen, O., and Vaheri, A. (1998). Structure-function relationships in the ezrin family and the effect of tumor-associated point mutations in neurofibromatosis 2 protein. Biochim Biophys Acta *1387*, 1-16.

Turunen, O., Wahlstrom, T., and Vaheri, A. (1994). Ezrin has a COOH-terminal actin-binding site that is conserved in the ezrin protein family. J Cell Biol *126*, 1445-1453.

Ussar, S., Wang, H. V., Linder, S., Fassler, R., and Moser, M. (2006). The Kindlins: Subcellular localization and expression during murine development. Experimental Cell Research *312*, 3142-3151.

Venkateswarlu, K., Gunn-Moore, F., Tavare, J. M., and Cullen, P. J. (1999). EGF- and NGF-stimulated translocation of cytohesin-1 to the plasma membrane of PC12 cells requires PI 3-kinase activation and a functional cytohesin-1 PH domain. Journal of Cell Science *112*, 1957-1965.

Volkmer, H., Hassel, B., Wolff, J. M., Frank, R., and Rathjen, F. G. (1992). Structure of the Axonal Surface Recognition Molecule Neurofascin and Its Relationship to a Neural Subgroup of the Immunoglobulin Superfamily. Journal of Cell Biology *118*, 149-161.

Walensky, L. D., Shi, Z. T., Blackshaw, S., DeVries, A. C., Demas, G. E., Gascard, P., Nelson, R. J., Conboy, J. G., Rubin, E. M., Snyder, S. H., and Mohandas, N. (1998). Neurobehavioral deficits in mice lacking the erythrocyte membrane cytoskeletal protein 4.1. Current Biology *8*, 1269-1272.

Wang, S. L., Hawkins, C. J., Yoo, S. J., Muller, H. A. J., and Hay, B. A. (1999). The Drosophila caspase inhibitor DIAP1 is essential for cell survival and is negatively regulated by HID. Cell *98*, 453-463.

Ward, R. E. t., Schweizer, L., Lamb, R. S., and Fehon, R. G. (2001). The protein 4.1, ezrin, radixin, moesin (FERM) domain of Drosophila Coracle, a cytoplasmic component of the septate junction, provides functions essential for embryonic development and imaginal cell proliferation. Genetics *159*, 219-228.

Wei, J., Hortsch, M., and Goode, S. (2004). Neuroglian stabilizes epithelial structure during Drosophila oogenesis. Developmental Dynamics *230*, 800-808.

Wick, W., Grimmel, C., Wild-Bode, C., Platten, M., Arpin, M., and Weller, M. (2001). Ezrin-dependent promotion of glioma cell clonogenicity, motility, and invasion mediated by BCL-2 and transforming growth factor-beta 2. Journal of Neuroscience *21*, 3360-3368.

Wu, K. L., Khan, S., Lakhe-Reddy, S., Jarad, G., Mukherjee, A., Obejero-Paz, C. A., Konieczkowski, M., Sedor, J. R., and Schelling, J. R. (2004). The NHE1 Na+/H+ exchanger recruits ezrin/radixin/moesin proteins to regulate Akt-dependent cell survival. Journal of Biological Chemistry *279*, 26280-26286.

Xiao, G. H., Gallagher, R., Shetler, J., Skele, K., Altomare, D. A., Pestell, R. G., Jhanwar, S., and Testa, J. R. (2005). The NF2 tumor suppressor gene product, merlin, inhibits cell proliferation and cell cycle progression by repressing cyclin D1 expression. Molecular and Cellular Biology *25*, 2384-2394.

Xu, H. M., and Gutmann, D. H. (1998). Merlin differentially associates with the microtubule and actin cytoskeleton. J Neurosci Res *51*, 403-415.

Yamasaki, M., Thompson, P., and Lemmon, V. (1997). CRASH syndrome: Mutations in L1CAM correlate with severity of the disease. Neuropediatrics *28*, 175-178.

Yawata, A., Kanzaki, A., Gilsanz, F., Delaunay, J., and Yawata, Y. (1997). A markedly disrupted skeletal network with abnormally distributed intramembrane particles in complete protein 4.1-deficient red blood cells (allele 4.1 Madrid): Implications regarding a critical role of protein 4.1 in maintenance of the integrity of the red blood cell membrane. Blood *90*, 2471-2481.

Yonemura, S., Hirao, M., Doi, Y., Takahashi, N., Kondo, T., and Tsukita, S. (1998). Ezrin/radixin/moesin (ERM) proteins bind to a positively charged amino acid cluster in the juxta-membrane cytoplasmic domain of CD44, CD43, and ICAM-2. J Cell Biol *140*, 885-895.

Yonemura, S., and Tsukita, S. (1999). Direct involvement of ezrin/radixin/moesin (ERM)-binding membrane proteins in the organization of microvilli in collaboration with activated ERM proteins. J Cell Biol *145*, 1497-1509.

Yonemura, S., Matsui, T., Tsukita, S., and Tsukita, S. (2002). Rho-dependent and -independent activation mechanisms of ezrin/radixin/moesin proteins: an essential role for polyphosphoinositides in vivo. Journal of Cell Science *115*, 2569-2580.

Zelina, P., Avci, H. X., Thelen, K., and Pollerberg, G. E. (2005). The cell adhesion molecule NrCAM is crucial for growth cone behaviour and pathfinding of retinal ganglion cell axons. Development *132*, 3609-3618.

Zhou, R. H., Zhu, L. X., Kodani, A., Hauser, P., Yao, X. B., and Forte, J. G. (2005). Phosphorylation of ezrin on threonine 567 produces a change in secretory phenotype and repolarizes the gastric parietal cell. Journal of Cell Science *118*, 4381-4391.

Appendix 1: Accession numbers, DNA and Protein sequences

Human Willin DNA sequence, accession number BC020521

ATGAACAAATTGAATTTTCATAACAACAGAGTCATGCAAGACCGCCGCAG
TGTGTGCATTTTCCTTCCCAACGATGAATCTCTGAACATCATCATAAATGT
TAAGATTCTGTGTCACCAGTTGCTGGTCCAGGTTTGTGACCTGCTCAGGCT
AAAGGACTGCCACCTCTTTGGACTCAGTGTTATACAAAATAATGAACATG
TGTATATGGAGTTGTCACAAAAGCTTTACAAATATTGTCCAAAAGAATGG
AAGAAAGAGGCCAGCAAGGGTATCGACCAATTTGGGCCTCCTATGATCAT
CCACTTCCGTGTGCAGTACTATGTGGAAAATGGCAGATTGATCAGTGACA
GAGCAGCAAGATACTATTATTACTGGCACCTGAGAAAACAAGTTCTTCAT
TCTCAGTGTGTGCTCCGAGAGGAGGCCTACTTCCTGCTGGCAGCCTTTGCC
CTGCAGGCTGATCTTGGGAACTTCAAAAGGAATAAGCACTATGGAAAATA
CTTCGAGCCAGAGGCTTACTTCCCATCTTGGGTTGTTTCCAAGAGGGGGAA
GGACTACATCCTGAAGCACATTCCAAACATGCACAAAGATCAGTTTGCAC
TAACAGCTTCCGAAGCTCATCTTAAATATATCAAAGAGGCTGTCCGACTG
GATGACGTCGCTGTTCATTACTACAGATTGTATAAGGATAAAAGGGAAAT
TGAAGCATCGCTGACTCTTGGATTGACCATGAGGGGAATACAGATTTTTC
AGAATTTAGATGAAGAGAAACAATTACTTTATGATTTCCCCTGGACAAAT
GTTGGAAAATTGGTGTTTGTGGGTAAGAAATTTGAGATTTTGCCAGATGG
CTTGCCTTCTGCCCGGAAGCTCATATACTACACGGGGTGCCCCATGCGCTC
CAGACACCTCCTGCAACTTCTGAGCAACAGCCACCGCCTCTATATGAATCT
GCAGCCTGTCCTGCGCCATATCCGGAAGCTGGAGGAAAACGAAGAGAAG
AAGCAGTACCGGGAATCTTACATCAGTGACAACCTGGACCTCGACATGGA
CCAGCTGGAAAAACGGTCGCGGGCCAGCGGGAGCAGTGCGGGCAGCATG
AAACACAAGCGCCTGTCCCGTCATTCCACCGCCAGCCACAGCAGTTCCCA
CACCTCGGGCATTGAGGCAGACACCAAGCCCCGGGACACGGGGCCAGAA
GACAGCTACTCCAGCAGTGCCATCCACCGCAAGCTGAAAACCTGCAGCTC
AATGACCAGTCATGGCAGCTCCCACACCTCAGGGGTGGAGAGTGGCGGCA
AAGACCGGCTGGAAGAGGACTTACAGGACGATGAAATAGAGATGTTGGT
TGATGACCCCCGGGATCTGGAGCAGATGAATGAAGAGTCTCTGGAAGTCA
GCCCAGACATGTGCATCTACATCACAGAGGACATGCTCATGTCGCGGAAG
CTGAATGGACACTCTGGGTTGATTGTGAAAGAAATTGGGTCTTCCACCTCG
AGCTCTTCAGAAACAGTTGTTAAGCTTCGTGGCCAGAGTACTGATTCTCTT
CCACAGACTATATGTCGGAAACCAAAGACCTCCACTGATCGACACAGCTT
GAGCCTCGATGACATCAGACTTTACCAGAAAGACTTCCTGCGCATTGCAG
GTCTGTGTCAGGACACTGCTCAGAGTTACACCTTTGGATGTGGCCATGAAC
TGGATGAGGAAGGCCTCTATTGCAACAGTTGCTTGGCCCAGCAGTGCATC
AACATCCAAGATGCTTTTCCAGTCAAAAGAACCAGCAAATACTTTTCTCTG
GATCTCACTCATGATGAAGTTCCAGAGTTTGTTGTGTAA

Human Willin2 DNA sequence, accession number AK055545

ATGAACAAATTGAATTTTCATAACAACAGAGTCATGCAAGACCGCCGCAG
TGTGTGCATTTTCCTTCCCAACGATGAATCTCTGAACATCATCATAAATGT
TAAGATTCTGTGTCACCAGTTGCTGGTCCAGGTTTGTGACCTGCTCAGGCT
AAAGGACTGCCACCTCTTTGGACTCAGTGTTATACAAAATAATGAACATG
TGTATATGGAGTTGTCACAAAAGCTTTACAAATATTGTCCAAAAGAATGG
AAGAAAGAGGCCAGCAAGGTACGACAATACGAAGTCACTTGGGGTATCG
ACCAATTTGGGCCTCCTATGATCATCCACTTCCGTGTGCAGTACTATGTGG
AAAATGGCAGATTGATCAGTGACAGAGCAGCAAGATACTATTATTACTGG
CACCTGAGAAAACAAGTTCTTCATTCTCAGTGTGTGCTCCGAGAGGAGGC
CTACTTCCTGCTGGCAGCCTTTGCCCTGCAGGCTGATCTTGGGAACTTCAA
AAGGAATAAGCACTATGGAAAATACTTCGAGCCAGAGGCTTACTTCCCAT
CTTGGGTTGTTTCCAAGAGGGGGAAGGACTACATCCTGAAGCACATTCCA
AACATGCACAAAGATCAGTTTGCACTAACAGCTTCCGAAGCTCATCTTAA
ATATATCAAAGAGGCTGTCCGACTGGATGACGTCGCTGTTCATTACTACA
GATTGTATAAGGATAAAAGGGAAATTGAAGCATCGCTGACTCTTGGATTG
ACCATGAGGGGAATACAGATTTTTCAGAATTTAGATGAAGAGAAACAATT
ACTTTATGATTTCCCCTGGACAAATGTTGGAAAATTGGTGTTTGTGGGTAA
GAAATTTGAGATTTTGCCAGATGGCTTGCCTTCTGCCCGGAAGCTCATATA
CTACACGGGGTGCCCCATGCGCTCCAGACACCTCCTGCAACTTCTGAGCA
ACAGCCACCGCCTCTATATGAATCTGCAGCCTGTCCTGCGCCATATCCGGA
AGCTGGAGGAAAACGAAGAGAAGAAGCAGTACCGGGAATCTTACATCAG
TGACAACCTGGACCTCGACATGGACCAGCTGGAAAAACGGTCGCGGGCCA
GCGGGAGCAGTGCGGGCAGCATGAAACACAAGCGCCTGTCCCGTCATTCC
ACCGCCAGCCACAGCAGTTCCCACACCTCGGGCATTGAGGCAGACACCAA
GCCCCGGGACACGGGGCCAGAAGACAGCTACTCCAGCAGTGCCATCCACC
GCAAGCTGAAAACCTGCAGCTCAATGACCAGTCATGGCAGCTCCCACACC
TCAGGGGTGGAGAGTGGCGGCAAAGACCGGCTGGAAGAGGACTTACAGG
ACGATGAAATAGAGATGTTGGTTGATGACCCCCGGGATCTGGAGCAGATG
AATGAAGAGTCTCTGGAAGTCAGCCCAGACATGTGCATCTACATCACAGA
GGACATGCTCATGTCGCGGAAGCTGAATGGACACTCTGGGTTGATTGTGA
AAGAAATTGGGTCTTCCACCTCGAGCTCTTCAGAAACAGTTGTTAAGCTTC
GTGGCCAGAGTACTGATTCTCTTCCACAGACTATATGTCGGAAACCAAAG
ACCTCCACTGATCGACACAGCTTGAGCCTCGATGACATCAGACTTTACCA
GAAAGACTTCCTGCGCATTGCAGGTCTGTGTCAGGACACTGCTCAGAGTT
ACACCTTTGGATGTGGCCATGAACTGGATGAGGAAGGCCTCTATTGCAAC
AGTTGCTTGGCCCAGCAGTGCATCAACATCCAAGATGCTTTTCCAGTCAAA
AGAACCAGCAAATACTTTTCTCTGGATCTCACTCATGATGAAGTTCCAGAG
TTTGTTGTGTAA

Mouse Willin2 DNA sequence, accession number BC053929

ATGAACAAACTGACCTTCCATAACAACAAAGCCATGCAGGACCGTCGCAG
AGTGTGTATTTTCCTCCCCAATGACAAGTCCGTGAGCATCATCATAAATGT
TAAAATTCTGTGTCACCAGTTGCTGGTCCAGGTGTGTGACCTGCTCAGGTT
AAAGGACAGTCACCTCTTTGGTCTCAGTGTTATACAAAATAATGAACATG
TATATATGGAATTGTCACAAAAGCTTTATAAGTATTGTCCAAAAGAATGG
AAAAAGGAGGCCAGCAAGGTACGGCAATACGAAGTCACTTGGGGCATCG
ACCAGTTTGGGCCCCCCATGATCATCCACTTCCGGGTGCAGTACTACGTGG
AGAATGGGAAGCTGATCAGTGACCGAATTGCAAGATACTATTATTACTGG
CACCTACGGAAACAGGTGCTGCACTCCCAGTGTGTGCTCAGAGAGGAGGC
CTACTTCCTGCTGGCAGCCTTTGCACTGCAAGCTGACCTCGGCAACTTCAA
AAGGAAACTGCACCACGGAGACTACTTTGAGCCAGAGGCTTACTTCCCGG
CATGGGTTGTTTCCAAGCGGGGGAAGGACTACATCCTGAAACACATCCCA
AACATGCACAAGGACCAGTTTGCCCTGACGGCCTCCGAGGCCTACCTAAA
GTACATCAAAGAAGCCGTCCGACTGGACGACGTCGCCATCCATTACTACA
GACTGTACAAGGATAAAAGGGAGGCTGAAGGCTCACTGACCCTAGGACT
GACCATGCGAGGAATACAGATTTTTCAGAATCTAGAAGAAGAGAAACAAT
TGCTCTATGATTTCCCCTGGACAAATGTTGGGAAGTTGGTGTTTGTGGGCA
AGAAGTTTGAGATTTTGCCAGATGGCCTTCCCTCCGCCAGGAAGCTGGTCT
ACTACACAGGGTGTCCCACGCGCTCCCGGCATCTCCTGCAGCTCCTGAGC
AACAGCCACCGCCTCTACATGAACCTGCAGCCCGTCCTGCGCCACCTCCG
CAAGCAGGAGGAGAATGAAGAGAAAAAGCAGTACCGGGAATCCTACATC
AGCGACAACCTGGACCTTGACATGGACCCGCTGGAAAAGCGGTCCCGAGC
CAGTGGGAGCAGCGCTGGCAGCGTGAAGCATAAGCGCCTGTCCCGCCACT
CCACGGCCAGCCACAGCAGCTCCCACACCTCCGGCATCGAGGCAGACACC
AAGCCCCGGGACCCAGGGCCGGAAGACAGCTGTTCAGGCAGCGCCATGC
ACCGGAAGCTGAAGACCTGCAGCTCCATGACCAGCCACGGCAGCTCCCAC
ACCTCTGGGGTTGAGAGTGGAGGCAAAGACCGCCTGGAAGAGGACTCGC
AAGATGAGGAAATCGAGATGCTGGTGGATGACCCCAGGGACCTGGAGCC
GATGCCTGAAGAGTCGCTGGAAGTCAGCCCAGAGATGTGTATCTACATCA
CGGAAGATATGCTCCTGTCGAGGAAGCTGAACGGACACTCAGGGTTAATT
GTGAAAGAAATCGGCTCCTCCACCTCCAGCTCTTCGGAAACGGTTGTCAG
GCTGCGTGGACAGAGCACCGACTCCCTTCCACAGACGATATGTCGAAAAC
CAAAGACTTCCACCGATCGCCATAGCCTGAGCCTTGACGACATCAGACTG
TACCAGAAAGACTTCCTGCGCATCGCGGGCCTGTGTCAGGACACTGCTCA
GAGCTACACGTTTGGGTGTGGCCATGAACTGGATGAGAGCGGTCTCTACT
GCAACAGCTGCCTGGCTCAGCAGTGTGTCAACATACAGGACGCATTCCCA
GTGAAAAGAGCCAGCAAGTACTTTTCTCTGGACCTTACTCACGACGAAGT
CCCAGAGTTCGTCGTCTGA

Human Willin protein sequence
FERM domain is underlined. Antibody sequences (αWR/914[3], αFRMD6 and CK2 respectively) are italicised.

MNKLNFHNNRVMQDRRSVCIFLPNDESLNIIIINVKILCHQLLVQVCDLLRLKD
CHLFGLSVIQNNEHVYMELSQKLYKYCPKEWK*KEASKGIDQFGPPMIIH*FRVQ
YYVENGRLISDRAARYYYYWHLRKQVLHSQCVLREEAYFLLAAFALQADLG
NFKRNKHYGKYFEPEAYFPSWVVSKRGKDYILKHIPNMHKDQFALTASEAHL
KYIKEAVRLDDVAVHYYRLYKDKREIEASLTLGLTMRGIQIFQNLDEEKQLL
YDFPWTNVGKLVFVGKKFEILPDGLPSARKLIYYTGCPMRSRHLLQLLSNSHR
LYMNLQPVLRHIRKLEENEEKKQYRESYISDNLDLDMDQLEKRSRASGSSAG
SMKHKRLSRHSTASHSSSHTSGIEADTKPRDTGPEDSYSSSAIHRKLKTCSSMT
SHGSSHTSGVESGGKDRL*EEDLQDDEIEMLVDDPRDLEQMNEESLEVSPDMCIY*
ITEDMLMSRKLNGHSGLIVKEIGSSTSSSSETVVKLRGQSTDSLPQTICRKPKTSTDR
*HSLSLDDIRLYQKDFLRIAGLCQDTAQSYTFGCGHELDEE*GLYCNSCLAQQCINI
QDAFPVKRTS*KYFSLDLTHDEVPEFVV*

Human Willin2 protein sequence, accession number Q96NE9
Extra octapeptide is underlined.

MNKLNFHNNRVMQDRRSVCIFLPNDESLNIIIINVKILCHQLLVQVCDLLRLKD
CHLFGLSVIQNNEHVYMELSQKLYKYCPKEWKKEASKVRQYEVTWGIDQFG
PPMIIHFRVQYYVENGRLISDRAARYYYYWHLRKQVLHSQCVLREEAYFLLA
AFALQADLGNFKRNKHYGKYFEPEAYFPSWVVSKRGKDYILKHIPNMHKDQ
FALTASEAHLKYIKEAVRLDDVAVHYYRLYKDKREIEASLTLGLTMRGIQIFQ
NLDEEKQLLYDFPWTNVGKLVFVGKKFEILPDGLPSARKLIYYTGCPMRSRH
LLQLLSNSHRLYMNLQPVLRHIRKLEENEEKKQYRESYISDNLDLDMDQLEK
RSRASGSSAGSMKHKRLSRHSTASHSSSHTSGIEADTKPRDTGPEDSYSSSAIH
RKLKTCSSMTSHGSSHTSGVESGGKDRLEEDLQDDEIEMLVDDPRDLEQMNE
ESLEVSPDMCIYITEDMLMSRKLNGHSGLIVKEIGSSTSSSSETVVKLRGQSTD
SLPQTICRKPKTSTDRHSLSLDDIRLYQKDFLRIAGLCQDTAQSYTFGCGHELD
EEGLYCNSCLAQQCINIQDAFPVKRTSKYFSLDLTHDEVPEFVV

Mouse Willin2 protein sequence

MNKLTFHNNKAMQDRRRVCIFLPNDKSVSIIIINVKILCHQLLVQVCDLLRLKD
SHLFGLSVIQNNEHVYMELSQKLYKYCPKEWKKEASKVRQYEVTWGIDQFG
PPMIIHFRVQYYVENGKLISDRIARYYYYWHLRKQVLHSQCVLREEAYFLLA
AFALQADLGNFKRKLHHGDYFEPEAYFPAWVVSKRGKDYILKHIPNMHKDQ
FALTASEAYLKYIKEAVRLDDVAIHYVGKLVFVGKKFEILPDGLPSARKLVYY
TGCPTRSRHLLQLLSNSHRLYMNLQPVLRHLRKQEENEEKKQYRESYISDNL
DLDMDPLEKRSRASGSSAGSVKHKRLSRHSTASHSSSHTSGIEADTKPRDPGP
EDSCSGSAMHRKLKTCSSMTSHGSSHTSGVESGGKDRLEEDSQDEEIEMLVD
DPRDLEPMPEESLEVSPEMCIYITEDMLLSRKLNGHSGLIVKEIGSSTSSSSETV
VRLRGQSTDSLPQTICRKPKTSTDRHSLSLDDIRLYQKDFLRIAGLCQDTAQSY
TFGCGHELDESGLYCNSCLAQQCVNIQDAFPVKRASKYFSLDLTHDEVPEFV
V

Appendix 2: Sequences of primers used

All primers are written 5' to 3', with restriction digest sequences underlined

Primer name	Primer sequence	Restriction site
WFLAG forward	CCACCTCGAGCTCTTCAG	SacI
WFLAG reverse	CGGGATCCCACAACAAACTCTGGAAC	BamHI
HGex F	CGGGATCCATGAACAAATTGAATTTTC	BamHI
Willin239rev	CGGGAATTCTCACAGCGATGCTTCAATTTC	EcoRI
Willin322rev	CGGGAATTCTTCAGACAGGCTGCAG	EcoRI
Willin356rev	CGGGAATTCTCATTTTTCCAGCTG	EcoRI
WillinCTAPF	ACCATGGACAAATTGAATTTTCATAAC	none
WillinCTAPR	TTTTCTTAAGCACAACAAACTCTGGAACTTC	AflII
WillinClaI	CCATCGATATGGACAAATTGAATTTTCATA	ClaI
WillinNheI	CACTCGATCGCACAACAAACTCTGGAACTT	NheI
Willin2forward	GGAATTCGCCATGAACAAACTGACCTTCC	EcoRI
Willin2reverse	CGGGATCCGACGACGAACTCTGGGAC	BamHI

Appendix 3: Antibody specific protocols

Primary antibody: pAP914[3] 1:1000
Secondary antibody: Upstate or Santa Cruz anti-rabbit-HRP 1:5000
Protocol: As described in section 2.3.10

Primary antibody: APHen2 1:1000
Secondary antibody: Sigma anti-chicken-HRP 1:10,000
Protocol: As described in section 2.3.10

Primary antibody: αWR1 1:1000
Secondary antibody: Santa Cruz anti-rabbit-HRP 1:10,000
Protocol: As described in section 2.3.10

Primary antibody: Sigma anti-FLAG M2 1:500
Secondary antibody: Santa Cruz anti-mouse-HRP 1:10,000
Protocol: Block at room temperature 30 minutes 3% milk-TBS
Wash 1x TBS
Primary antibody 1:500 3% milk-TBS 30 minutes
Wash 1x TBS 10 minutes
Secondary antibody 1:10,000 3% milk-TBS 30 minutes
Wash 8x 3minutes TBS

Primary antibody: anti-neurofascin 1:2000
Secondary antibody: Santa Cruz anti-rabbit-HRP 1:10,000
Protocol: As desccribed in section 2.3.10

Primary antibody: Santa Cruz anti-Merlin 1:1000
Secondary antibody: Santa Cruz anti-rabbit-HRP 1:10,000
Protocol: As described in section 2.3.10

Primary antibody: anti-GFP 1:1000
Secondary antibody: Santa Cruz anti-mouse-HRP 1:10,000
Protocol: As described in section 2.3.10

Primary antibody: RAD4 pan-ERM 1:5000
Secondary antibody: Santa Cruz anti-rabbit-HRP 1:10,000
Protocol: As described in section 2.3.10

Primary antibody: anti-CBP 1:500
Secondary antibody: Santa Cruz anti-rabbit 1:2000
Protocol: Block overnight 4^{o}C 5% milk TBS-T
Wash 2x with distilled water
Primary antibody 1:500 5% milk-TBS 2 hours
Wash 2x with distilled water
Secondary antibody 1:2000 5% milk-TBS 1.5 hours
Wash 2x with distilled water
Wash 1x TBS-0.05% Tween
Rinse 5 times with distilled water

Appendix 4: List of Suppliers

Supplier	Address
Abcam	Cambridge, UK
Atlas Antibodies	Stockholm, Sweden
BD Biosciences/Clontech	Oxford, UK
Biometra	Goettingen, Germany
Cell Lines Service	Eppelheim, Germany
Cytoskeleton	Denver, USA
Davids Biotechnologie	Regensburg, Germany
Fisher Scientific	Loughborough, UK
Genovac	Freiburg, Germany
Globepharm	Essex, UK
Invitrogen/Gibco	Paisley, UK
Millipore	Watford, UK
New England Biolabs	Hertfordshire, UK
Nunc/VWR	Leicestershire, UK
Pierce	Tattenhall, UK
Promega	Southampton, UK
Qiagen	Crawley, UK
Roche	East Sussex, UK
Rovalab	Teltow, Germany
Santa Cruz	Calne, UK
Sigma-Aldrich	Dorset, UK
Stratagene	Cambridge, UK
Thistle Scientific	Glasgow, UK